REPORT DOCUMENTATION PAGE

Form Approved
OMB NO. 0704-0188

Public Reporting burden for this collection of information is estimated to average 1 hour per response, including the time for reviewing instructions, searching existing data sources, gathering and maintaining the data needed, and completing and reviewing the collection of information. Send comment regarding this burden estimates or any other aspect of this collection of information, including suggestions for reducing this burden, to Washington Headquarters Services, Directorate for information Operations and Reports, 1215 Jefferson Davis Highway, Suite 1204, Arlington, VA 22202-4302, and to the Office of Management and Budget, Paperwork Reduction Project (0704-0188,) Washington, DC 20503.

1. AGENCY USE ONLY (Leave Blank)

2. REPORT DATE 16 March 2004

3. REPORT TYPE AND DATES COVERED
Final Technical Report 27-November-2000 -> 26 June 2003

4. TITLE AND SUBTITLE
Sensor Modeling and 3D Visualization

5. FUNDING NUMBERS
~~Contract~~ DAAD 19-01-1-0002

6. AUTHOR(S)
James Bethel and Joseph Spann

7. PERFORMING ORGANIZATION NAME(S) AND ADDRESS(ES)
Purdue University, School of Civil Engineering, West Lafayette, IN and BAE Systems – Mission Solutions, San Diego, CA (subcontractor)

8. PERFORMING ORGANIZATION REPORT NUMBER ARO-004

9. SPONSORING / MONITORING AGENCY NAME(S) AND ADDRESS(ES)

U. S. Army Research Office
P.O. Box 12211
Research Triangle Park, NC 27709-2211

10. SPONSORING / MONITORING AGENCY REPORT NUMBER
41876.1-EV

11. SUPPLEMENTARY NOTES
The views, opinions and/or findings contained in this report are those of the author(s) and should not be construed as an official Department of the Army position, policy or decision, unless so designated by other documentation.

12 a. DISTRIBUTION / AVAILABILITY STATEMENT

Approved for public release; distribution unlimited.

12 b. DISTRIBUTION CODE

13. ABSTRACT (Maximum 200 words)

Two related, but independent investigations were carried out under this project. The first related to sensor (camera) modeling as needed for the photogrammetric exploitation of imagery for mapping and geopositioning purposes. This task was further subdivided into two subtasks. The first of these involved performing a geometric camera calibration for a set of 4 co-boresighted video cameras (called CAMIS) used by TEC (Topographic Engineering Center) for remote sensing and mapping purposes. This involved setting up a laboratory calibration facility, collecting system imagery in that facility, developing software and algorithms to align the fixtures in the facility, and developing software and algorithms to perform the camera calibration. The second subtask was to investigate the detection of errors in aerial triangulation, motivated by recurrent problems using the SOCET SET triangulation module for large blocks of images. The approach here was to implement and test two algorithms for such error detection in a prototype MATLAB GUI (graphical user interface). Testing showed that both algorithms had merit for the error/blunder detection problem.

The second task in the project was the further development of Vesper for the Battlespace (VFB) product. The goals here were to develop and demonstrate advanced sensor data fusion, 2D and 3D visualization capabilities, combine the visualization environment with precise geo-registration, creating a single, end-to-end data visualization system. This system enhances time critical operations such as intelligence gathering, mission planning and rehearsal, and operational command and control. Specific modules within VFB include auto geo-registration of EO,SAR,IR,HSI, and SIG data, sensor model update, sensor projectors, object models (DTED, etc.), and interactive 2D/3D visualization.

14. SUBJECT TERMS
Sensor model, camera, calibration, CAMIS, aerial triangulation, blunder detection, robust estimation, visualization, registration, fusion, graphics

15. NUMBER OF PAGES
112

16. PRICE CODE

17. SECURITY CLASSIFICATION OR REPORT UNCLASSIFIED	18. SECURITY CLASSIFICATION ON THIS PAGE UNCLASSIFIED	19. SECURITY CLASSIFICATION OF ABSTRACT UNCLASSIFIED	20. LIMITATION OF ABSTRACT UL

SENSOR MODELING AND 3D VISUALIZATION
FINAL TECHNICAL REPORT

Foreward

Note that this actual report is very brief, with the bulk of the technical material located in previously produced papers, reports, and presentations, that are attached as appendices.

Appendices

A. Paper describing the CAMIS calibration project.
B. Technical Report describing the CAMIS calibration project
C. Presentation slides giving and overview of the CAMIS calibration project.
D. Report describing the work done for the aerial triangulation blunder detection project
E. Presentation slides for VESPER, VFB (1)
F. Presentation slides for VESPER, VFB (2)
G. Presentation slides for VESPER, VFB (3)

Statement of the Problem Studied

There were several related but independent problems that were studied for this project. The three principal ones were: (1) Determine a practical laboratory calibration procedure for small format aerial camera systems such as the CAMIS system, (2) Determine a practical algorithm for blunder detection in the processing of aerial photogrammetric blocks, and (3) Develop and enhance a visualization environment where new imagery can be imported, registered, and viewed in a 3D multi-modal setting.

Publications (peer reviewed conference proceedings)

1. Alharthy, A., and Bethel, J., 2002, “Geometric Calibration of the CAMIS Sensor”, presented at the FIG/ACSM/ASPRS Conference, April 25, 2002, Washington DC
2. Alharthy, A. and Bethel, J., 2002, “Laboratory Calibration of a Multiband Sensor”, presented at ISPRS Commission III conference, Sept. 2002, Graz, Austria

Personnel

1. James Bethel co-PI
2. Joseph Spann co-PI
3. Abdullatif Alharthy, PhD received, August 2003
4. Ade Mulyana, PhD expected, August 2004
5. Junhee Youn, PhD expected, May 2005
6. Karen Kaufman

Inventions

None. (See earlier form DOD822**)**

Bibliography

See individual papers and reports for bibliography sections.

GEOMETRIC CALIBRATION OF THE CAMIS SENSOR

Abdullatif Alharthy, James Bethel
School of Civil Engineering, Purdue University
1284 Civil Engineering Building
West Lafayette, IN 47907
alharthy@ecn.purdue.edu
bethel@ecn.purdue.edu

ABSTRACT:

CAMIS is a system for airborne remote sensing and is designed to utilize modern solid-state imaging and data acquisition technology. It is composed of four CCD cameras with band pass optical filters to obtain four band images. In this paper, we summarize the work that has been done during the geometric calibration of the CAMIS sensor. We modified the conventional calibration procedure especially for this sensor and we modified and used a matching technique to make the process more efficient. A network bundle adjustment program was developed and used to adjust the laboratory measurements and locate the targets. Images of the target field were then taken by each of the four cameras of the CAMIS sensor. Two matching techniques were used to determine and refine the target locations in the image space. We modified the matching algorithm to overcome certain radiometric effects and thereby found the location of the target centers in image space.

To recover the most significant camera parameters, a full math model was used. The unified least squares approach was used iteratively to solve this nonlinear overdetermined system. In order to determine the lens distortion behavior, the radial and decentering components were estimated. Then the radial distortion curve was equalized and the corresponding changes to the sensor parameters were recorded. Finally, we present four sets of adjusted parameters, one per camera.

1. INTRODUCTION

The CAMIS sensor consists of four co-boresighted area-CCD cameras with band pass filters: blue, green, red, and near infrared. In this paper, we summarize the work that has been done during the geometric calibration of the CAMIS sensor. The procedure required many preliminary steps such as preparing the calibration site which involved target layout, setting up the coordinate system and locating fiducial monuments within that system. Three arc-second theodolites and a steel tape were used to measure the angles and distances in the network of calibration targets. In order to adjust those measurements and to get the target coordinates into the reference coordinate system, we developed a network bundle adjustment program. Images of the target field were then taken by each of the four cameras of the CAMIS sensor. The coordinates of the targets in both the object and the image system were used as observations for estimating the sensor parameters in a second bundle program configured for self-calibration.

After planning the data flow, the images were taken and the calibration procedure was started. To cover the most significant parameters, a full math model was used (Samtaney, 1999). A description of this model and its use are outlined in this paper. The unified least square approach was used iteratively to solve this nonlinear overdetermined system since we have some prior knowledge about a number of the sensor parameters (Mikhail and Ackerman, 1976). Moreover, in order to see the distortion behavior, the radial and decentering distortions were calculated and plotted separately. Afterward, the radial distortion curve was equalized and the corresponding changes to the sensor parameters were recorded. We repeated the procedure for each camera individually and consequently our results have four sets of adjusted parameters, one per camera. The basic steps and algorithms that were used during the calibration process are outlined below. In the actual use of this imaging system, often three of the bands are registered and resampled to a reference band. In that case, only the calibration of that reference band would be used.

2. CALIBRATION

The aim of this work was to make a laboratory calibration for the geometric parameters of the CAMIS sensor. CAMIS stands for Computerized Airborne Multicamera Imaging System. It is designed to utilize modern solid-state imaging and data acquisition technology. It is composed of four CCD cameras with band pass optical filters to obtain four band images. The center wavelength of those bands is as follows: 450, 550, 650 and 800 nm. However, each sensor has its own optics and obtains its own image independently from the others at the same time. Those four images can be integrated into a composite image or viewed individually. The CAMIS sensor has been used in multispectral imaging and mapping purposes by mounting it in an airplane with GPS and INS systems. These auxiliary sensors provide very good position and attitude data for stabilizing the subsequent bundle block adjustment. The calibration procedure required a number of steps and they are summarized below.

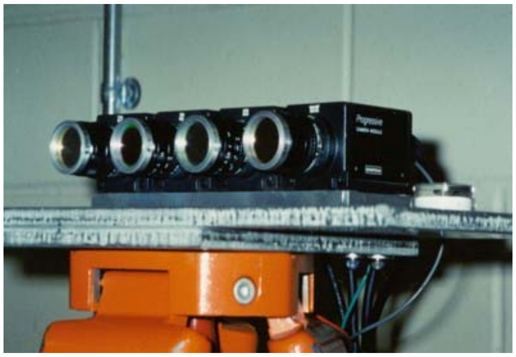
Figure 1: the four cameras

2.1 SITE PREPARATION

The idea of the calibration was to layout some targets in the object space, locate them accurately, and acquire an image of those targets by the sensor. Then, we relate the coordinates of the targets in both systems, image and object space, in order to obtain the camera parameters. So, the procedure starts by setting up the calibration site. First, we designed the targets to be cross shapes so their center positions will be obtained very easily. Then they have been laid out in an "X" pattern that allows us to recover the needed geometric parameters and systematic errors as shown in figure 3. Those targets were placed on an almost flat service wall and the sensor position was located around 8 meters away from that wall. In order to register the objects in the scene, an object space coordinate system was established at the site and two other instrument stations were marked to use in the measurements.

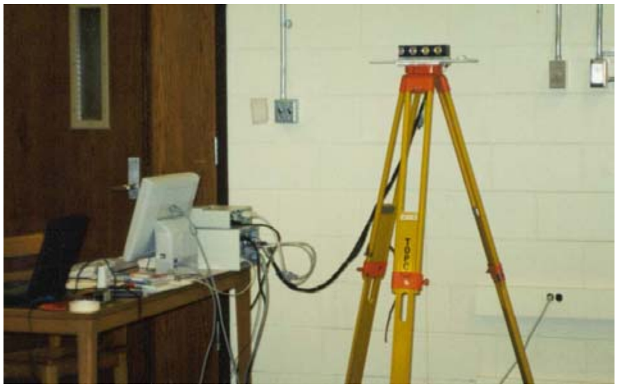
Figure 2: sensor setup for calibration

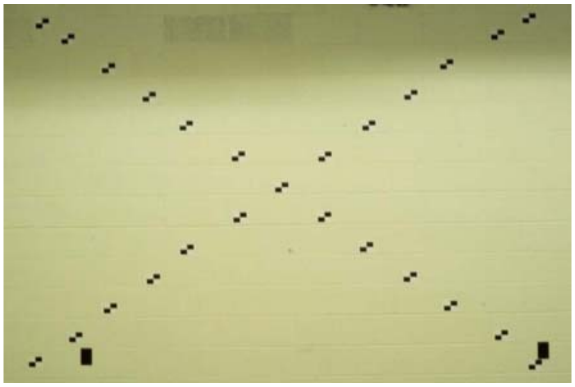
Figure 3: target layout

2.2 MEASUREMENTS AND ADJUSTMENT IN OBJECT SPACE

Two three arc-second theodolites were mounted at the referenced stations and were used to measure directions to all relevant objects of the network: target centers, theodolite locations, and camera case monuments. The origin of the object space was chosen to be theodolite one at station one at the right of the sensor position. Many manual measurements were made of the camera physical layout, using machinist calipers. The lenses were also placed on an optical bench for determining the locations of the nodal points. A cross section of one camera is shown in figure 4. This was needed to locate the camera front nodal point with respect to the camera body, which would be located in the network by theodolite observations. The spacings between the wall targets were measured with a steel tape. Having all these observations, we end up with an overdetermined system of equations. We developed a bundle program to simultaneously adjust the theodolite and distance observations. As a result of that, we determined all of our targets and camera stations in the referenced coordinate system. The next step was capturing images by the sensor(s).

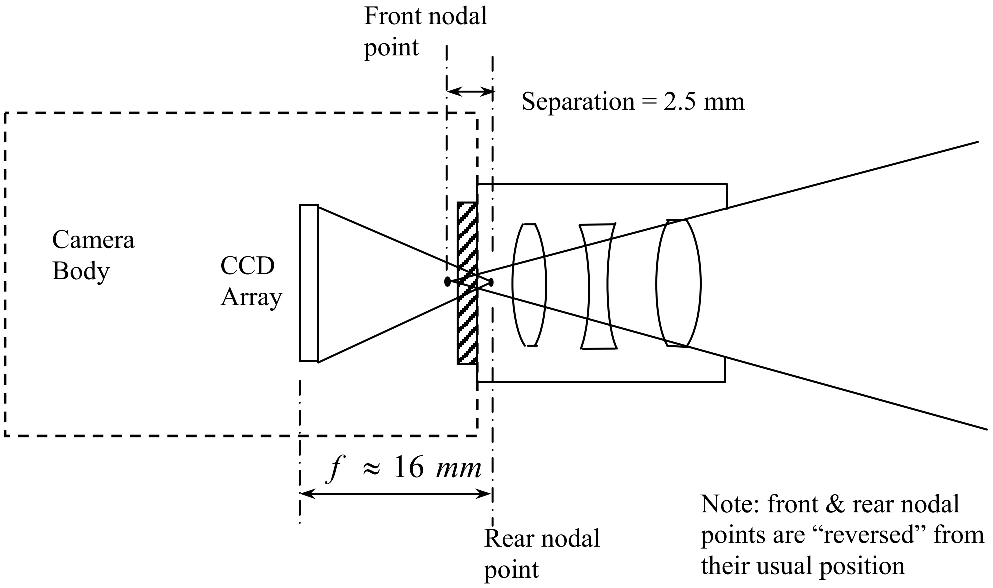

Figure 4: cross section of one camera showing the lenses, rear and front nodal points.

2.3 CAPTURING IMAGES AND OBTAINING IMAGE SPACE COORDINATES

Before the measurements, the sensor was mounted on a leveled plate fixed on a survey tripod. In this sense, the exposure stations were fixed and predetermined to an accuracy of a few millimeters. In this step we tried to simulate the real working conditions by setting the lenses to the "working" infinity focus position. Images were viewed after captured to verify acceptable radiometry. With the band pass filters our illumination setup was just sufficient to produce acceptable image definition for the targets. In the future, stronger light sources would be used to allow more flexibility. After this step, the laboratory work ended and the processing procedure started.

2.4 IMAGE SPACE CALCULATIONS

Once the images were captured, we ran a cross correlation matching program to get rough approximation of target positions in the image space to within a pixel. The cross correlation matching function works by computing the similarity between two same sized widows (Mikhail, bethel and McGlone, 2001; Mikhail and Ackerman, 1976). One window patch contains the ideal target and the other contains a window from the image. In general, a matching problem is a key algorithm for other applications and image analysis. Despite the fact that, the cross correlation matching results showed that we are only away from the exact position by a pixel or less, we needed more accurate and precise methods to guarantee the sub-pixel precision. This level of precision is necessary for a camera calibration problem. Least squares matching (LSQM) is very adequate technique for this purpose. LSQM utilizes the first derivative (gradient) of the intensity in both x and y directions to obtain the best correspondence and the exact matching can be reached by moving one window with respect to the other one (Atkinson, 1996). Some obstacles, such as radiometric effects, were faced and solved by modifying the algorithm. As a result of this step, the image space coordinates for the targets have been obtained. Results using both techniques are shown in figure 5.

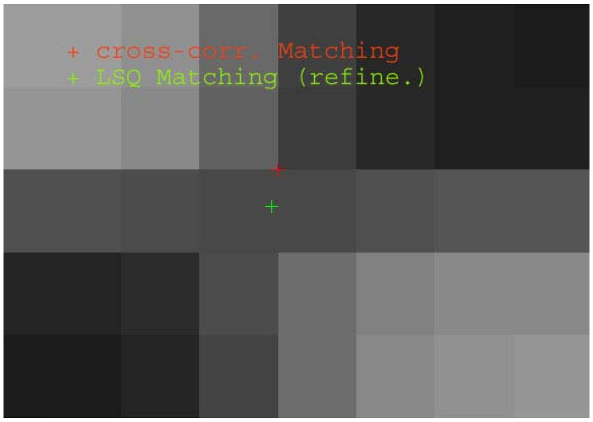

Figure 5: Target center determination using two matching algorithms.

2.5 CAMERA PARAMETER ESTIMATION

First, a full math model was chosen to perform the geometric calibration and estimate the sensor parameters. In this math model, Ravi Samtaney (1999) tried to cover the significant factors that might occur in geometric calibration. This model is explored more below. The model relates the target coordinates in object space and image space through the camera parameters. This overdetermined and nonlinear system needs an optimization criterion to be solved. Since we have some initial values for a number of the camera parameters and their uncertainty, we decided to use the unified least squares algorithm to solve the system. Using the resulting distortion parameters, plots were drawn to describe the radial and decentering distortion behavior. Finally, the radial distortion curve was equalized by small changes in corresponding parameters. The results of the process for each sensor are tabulated in the results section.

3. TARGET LOCATIONS IN IMAGE SPACE (MATCHING)

3.1 INTRODUCTION

In order to find the target locations in the image, two matching approaches were used. First, the approximate locations are obtained using the cross correlation matching. Second, we refine the results of the first algorithm using least squares matching.

3.2 CROSS-CORRELATION MATCHING

Cross-correlation determines the similarity between two corresponding patches. The conventional cross-correlation approach cannot give the precise location of an object due to many factors. Differences in attitude, distortion, and signal noise are some examples that affect the correspondence in geometry and radiometry (Mikhail, bethel and McGlone, 2001; Atkinson 1996). However, this algorithm usually gives an approximate location of the correspondence within a few pixels.

The ideal template will be passed through the image and the matching function will be computed and recorded at the center pixel of the patch. The match function, the normalized cross correlation coefficient, ranges between +1 and -1. The maximum value equals +1, which means there is a full match between the two windows or, in other words, they are identical. Usually a threshold will be used to distinguish between matches and non-matches. Then the pixels with a cross correlation above the threshold will be considered candidates for the match. Some individual correlation results, as shown in figure 3, are off from the center of the target only by a pixel or less. These results enable us to use the least squares refining technique directly.

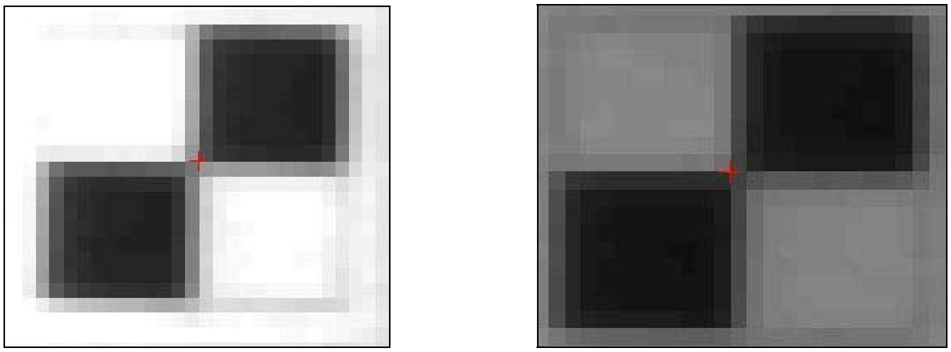

Figure 3: two cross correlation match results.

3.3 LEAST SQUARES MATCHING (LSQM)

Least squares matching works as a powerful and an accurate technique to refine an object's coordinates in the image space based on the correspondence between a image chip and a reference or template chip (Mikhail, Moffitt and Francis, 1980; Atkinson, 1996). This technique utilizes the gradient in the x and y directions in order to move the two patches with respect to each other in order to get the best match. The match precision that we are looking for with this technique is within a hundredth of a pixel or so. The similarity between the two targets was only geometrically modeled for this specific problem since the radiometric differences were eliminated through some preprocessing steps, as we will see below. The problem is to match an ideal shape of the target with a small window from the image containing the imaged target. The following steps describe the automated procedure that was used for setting up the two windows for matching:

1) Obtain the approximate location of the imaged target using the first matching approach (cross correlation) as described above. Those locations should be within a few pixels of the exact location in order to make the geometric model in LSQM converge and to produce accurate results.

2) Having the rough estimated location, a window around that location from the image with adequate size will be extracted for matching purposes. This is all done systematically inside the code.

3) The ideal or template target is retrieved at this point. Similarity in the intensity is enforced between the two windows.

After specifying the two windows with the same size for matching, the LSQM procedure takes place. Requiring similarity in intensity between each of the two corresponding pixels from the two windows is the basic condition for this procedure. Since the two patches do not have the same coordinate system, a 6-parameter geometric transformation is used to relate them in the matching procedure (Atkinson, 1996). Those parameters will be corrected iteratively and will be used to calculate the new coordinates x', y' in order to use them in resampling the grid for the template window. We used bilinear interpolation to resample the intensity values during this procedure.

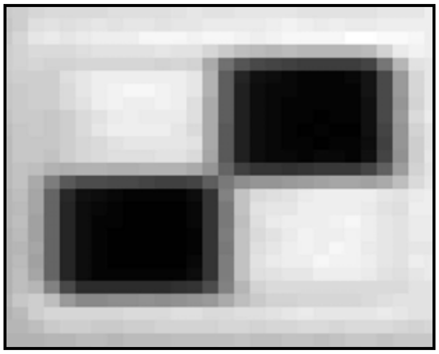

Figure 4a: the target in image patch

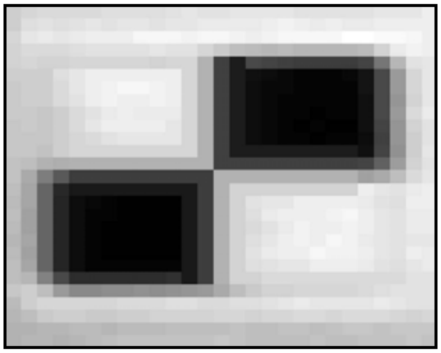

Figure 4b: the ideal or template target

The whole procedure will be repeated as needed but using the new template window with the new intensity values every time and the parameters will be updated. The match will be achieved when the system converges and those 6-parameters do not change any further. The system might diverge if there is no similarity between the two patches or the approximate location of the match far off from the real one by more than several pixels (Mikhail, Moffitt and Francis, 1980; Atkinson, 1996).

4. MATHEMATICAL MODEL FOR SELF-CALIBRATION AND SOLUTION METHOD

4.1 MATHEMATICAL MODEL

The mathematical model was chosen carefully in order to cover all significant sources of geometric errors and estimate all significant correction parameters for those errors. (Samtaney, 1999) explored this model in detail. It was derived from the fundamental collinearity equations. This model relates two coordinate systems to each other. It maps the coordinates from the object space into the image space (Mikhail, bethel and McGlone, 2001). There are two types of parameters. First, the exterior parameters which include the location and orientation parameters. Lens distortion and focal length are examples of the second type, which are called the interior parameters. The model specifically covers and takes into account the lens distortion through some parameters that model radial, decentering, and affinity distortion.

$$\begin{aligned} x - x_o &= x' - x_o + \Delta x \\ &= -f\,\frac{r_{11}(X - X_c) + r_{12}(Y - Y_c) + r_{13}(Z - Z_c)}{r_{31}(X - X_c) + r_{32}(Y - Y_c) + r_{33}(Z - Z_c)} \end{aligned} \tag{1a}$$

$$\begin{aligned} y - y_o &= y' - y_o + \Delta y \\ &= -f\,\frac{r_{21}(X - X_c) + r_{22}(Y - Y_c) + r_{23}(Z - Z_c)}{r_{31}(X - X_c) + r_{32}(Y - Y_c) + r_{33}(Z - Z_c)} \end{aligned} \tag{1b}$$

Where (x, y) and (x', y') are the ideal and measured target coordinates in image space. x_o, y_o are the principal point coordinates in image space. $\Delta x, \Delta y$ are distortion corrections in x, y directions in image space, see equation (2). f is the camera focal length and $r_{i,j}$ is the ith row and jth column element of the orientation matrix R , see equation (3). (X, Y, Z) are the target coordinates in object space and (X_c, Y_c, Z_c) are exposure station coordinates in object space.

The distortion effects including radial, lens decentering, and affinity were computed through the equations below.

$$\Delta x = \bar{x}(k_1 r^2 + k_2 r^4 + k_3 r^6) + p_1(r^2 + 2\bar{x}^2) + 2p_2\bar{x}\ \bar{y} \tag{2a}$$

$$\Delta y = \bar{y}(k_1 r^2 + k_2 r^4 + k_3 r^6) + 2p_1\bar{x}\ \bar{y} + p_2(r^2 + 2\bar{y}^2) + a_1\bar{x} + a_2\bar{y} \tag{2b}$$

In which $\bar{x} = x' - x_o$, $\bar{y} = y' - y_o$ and $r^2 = \bar{x}^2 - \bar{y}^2$. k_i are the radial distortion coefficients, p_i are the decentering distortion coefficients and a_i are the affinity distortion coefficients. The rotation matrix R expresses the orientation of the image coordinate system with respect to the object coordinate system. It is used in the model to relate the target coordinates in both systems. Rotations around the three principle axes x, y, and z by the three angles ω, ϕ, and k generate the matrix R as seen in equation (3).

$$R = R_z(k)R_y(\phi)R_x(\omega) \tag{3}$$

The two condition equations for each target will be:

$$\begin{aligned} F_x = {} & \bar{x} + \bar{x}(k_1 r^2 + k_2 r^4 + k_3 r^6) + p_1(r^2 + 2\bar{x}^2) + 2p_2\overline{xy} \\ & + f\,\frac{r_{11}(X - X_c) + r_{12}(Y - Y_c) + r_{13}(Z - Z_c)}{r_{31}(X - X_c) + r_{32}(Y - Y_c) + r_{33}(Z - Z_c)} = 0 \end{aligned} \tag{4a}$$

$$\begin{aligned} F_y = {} & \bar{y} + \bar{y}(k_1 r^2 + k_2 r^4 + k_3 r^6) + 2p_1\overline{xy} + p_2(r^2 + 2\bar{y}^2) + a_1\bar{x} + a_2\bar{y} \\ & + f\,\frac{r_{21}(X - X_c) + r_{22}(Y - Y_c) + r_{23}(Z - Z_c)}{r_{31}(X - X_c) + r_{32}(Y - Y_c) + r_{33}(Z - Z_c)} = 0 \end{aligned} \tag{4b}$$

From the equations above, each target observation will generate two equations. Consequently, the number of equations will be twice the number of targets in the image for each camera.

4.2 SOLUTION METHOD

The unified least squares approach was used to solve this system since some *a priori* knowledge is available for a number of parameters (Mikhail and Ackerman, 1976). Using the *a priori* knowledge of the parameters is the distinction between ordinary least squares and unified least squares. This *a priori* knowledge is utilized to give those parameters initial values and weights. In this sense, some of the parameters were treated as observations with low precision by assigning large variances to them. Since the system is non-linear, the parameter values will be updated iteratively by adding the correction to them.

The system will converge when the correction vector values are negligible. Then the final correction will be added to the parameters to get the final estimated values. In our case here, the system converges with few iterations since the precision of the observations was very high.

5. DISTORTION ANALYSIS

After determining the camera parameters including distortion parameters, distortion curves were drawn for visual and computational analysis. Radial and decentering (tangential) distortions are discussed in this section.

5.1 RADIAL DISTORTION

The technical term for the displacement of an imaged object radially either towards or away from the principle point is radial distortion (Atkinson, 1996). The magnitude of this displacement (radial distortion) is usually determined to micrometer precision and it varies with the lens focusing. Radial Distortion is included in the math model and its magnitude can be calculated as follows:

$$\Delta r = k_1 r^3 + k_2 r^5 + k_3 r^7 \tag{5}$$

$$\delta_x = \Delta r * \bar{x} / r \qquad \delta_y = \Delta r * \bar{y} / r$$

The radial distortion curve was constructed based on the equation above as shown in figure 6. The resulting curves were obtained for all four cameras and the maximum radial distortion was around 30 micrometers.

The following step was done to level or balance the curve based on equalizing the maximum and the minimum distortion values. This procedure is done only to balance the positive and negative excursions of the distortion function about zero. This step has no effect on the final results of the corrected coordinates; it is just cosmetic but accepted professional practice. Mathematically, balancing the curve leads to a change in the radial distortion parameters and consequently the focal length and other related camera parameters. The aim of this balancing procedure is to make $|d_{\max}| = |d_{\min}|$ as shown in figure 6 and the condition equation will be:

$$r_{\max} - CFL \times \tan(\alpha_{\max}) + r_{\min} - CFL \times \tan(\alpha_{\min}) = 0 \tag{6}$$

So the new focal length is

$$CFL = \frac{r_{\max} + r_{\min}}{\tan(\alpha_{\max}) + \tan(\alpha_{\min})} \tag{7}$$

After getting the revised focal length, the calibration adjustment program is run again but with a fixed focal length (CFL). Also, the orientation angles were fixed during this adjustment. This will require adjusting other parameters also to produce the balanced curve in addition to radial distortion parameters k1, k2 and k3. The other parameters are principal point shift, decentering and affine distortion parameters. Since these parameters are not independent of the radial distortion parameters, the equalization procedure will be repeated until we get the balanced curve. If all parameters other than the radial distortion parameters are fixed, then the balanced curve will be obtained from one iteration. All of that processing was handled automatically except for the red camera, that curve was balanced manually.

The distortion curves for each iteration of the green band camera are shown in figure 6. Also the radial distortion magnitudes and their orientations throughout the image plane are shown along with the principal point, PPS, and the fiducial center, FC, in figure 7.

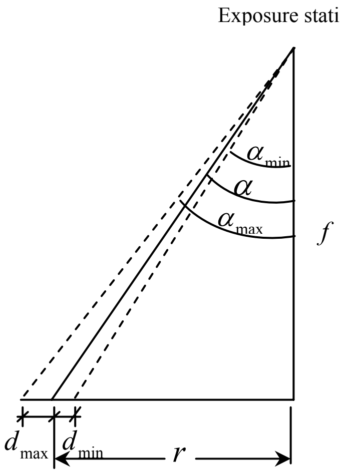

Figure 5: image plane cross section.

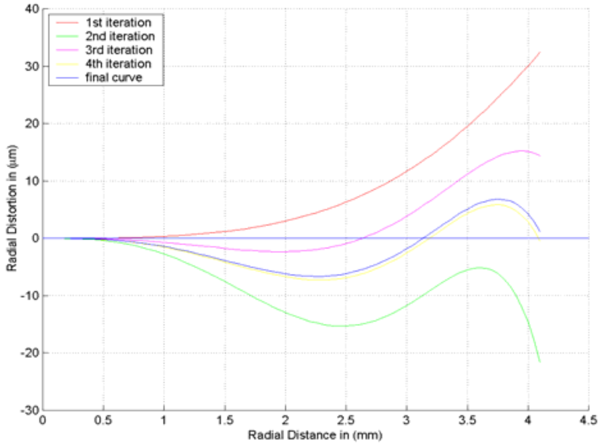

Figure 6: radial distortion for the green camera in CAMIS sensor

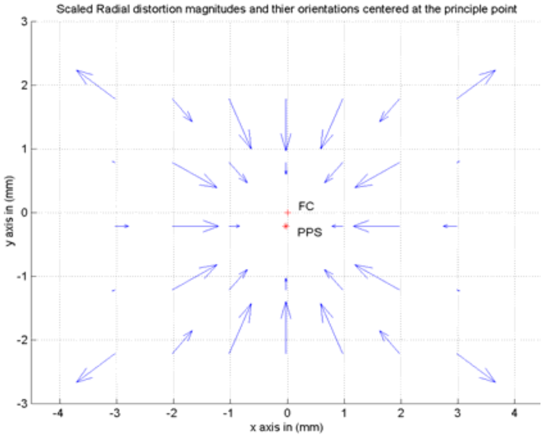

Figure 7a: Scaled radial distortion on image plane centered at PPS for the green camera

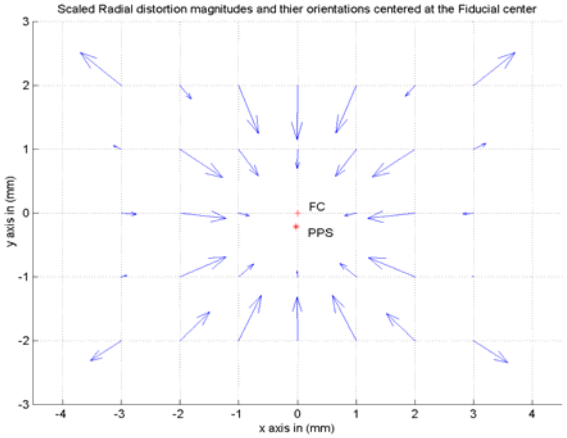

Figure 7b: Scaled radial distortion on image plane centered at FC for the green camera

5.2 DECENTERING DISTORTION

When a lens is manufactured, all its components should be aligned perfectly. But such perfection is not possible. The misalignment will lead to systematic image displacement errors. This undesired geometric displacement in the image is called decentering distortion. In this calibration procedure the following mathematical model is used (Samtaney, 1999; Atkinson, 1996),

$$\begin{aligned}\delta_x &= p_1[r^2 + 2(x - x_o)^2] + 2p_2(x - x_o)(y - y_o)\\ \delta_y &= p_2[r^2 + 2(y - y_o)^2] + 2p_1(x - x_o)(y - y_o)\end{aligned} \tag{8}$$

As mentioned earlier, the equalization procedure for the radial distortion has an affect on the other parameters. So, in each equalization iteration, the decentering parameters will have new values since their behavior will be adjusted according to the modification of the focal length. Nevertheless, the equalization technique does not change the final corrected coordinate values and the main purpose for it is to make the distortion correction balanced in magnitude. Figure 8 shows the scaled magnitudes of the decentering distortions and their orientations throughout the image plane with respect to the principal point (PPS) and the fiducial center (FC) of the image.

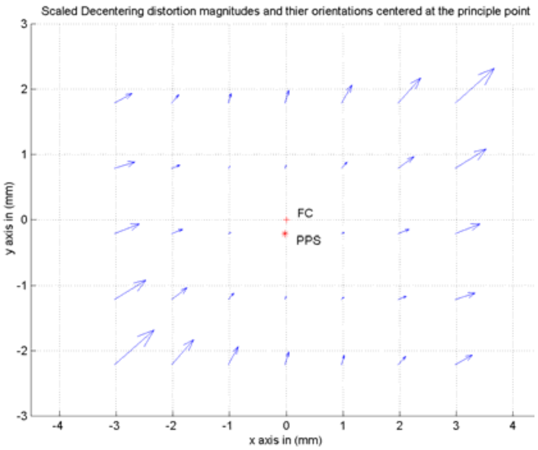

Figure 8a: Scaled Decentering Distortion on image plane centered at PPS for the Green camera

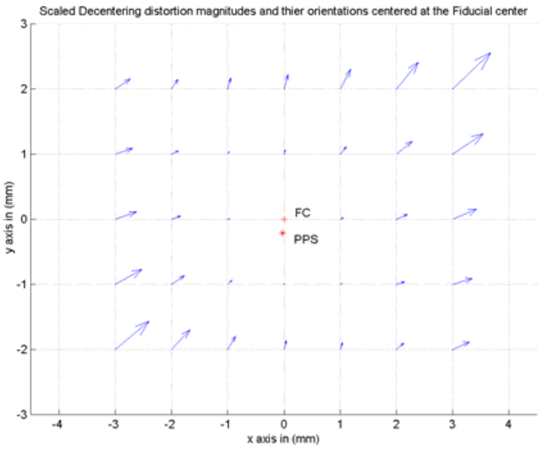

Figure 8b: Scaled Decentering Distortion on image plane centered at FC for the Green camera

6. Results and Discussion

The resulting calibration parameters for the four cameras are summarized in the table below. Those parameters can be used to refine the coordinate observations in image space for each camera, respectively. We tried during this work to automate the calibration process as much as possible. We anticipate that this careful calibration will improve the results from bundle block adjustment using the CAMIS sensor. Verification of this will have to await more testing. The interesting contributions of this research have been, the setup and measurements of the targets and the cameras, the automation of the target locations in the images, and their subsequent refinement, and the automatic process for balancing the radial lens distortion in the presence of other correlated parameters.

Parameter	Blue Camera Working band 450nm	Green Camera Working band 550nm	Red Camera Working band 650nm	Alpha Camera Working band 800nm
f	16.168 mm	16.154 mm	16.177 mm	16.174 mm
x_o	0.084357 mm	-0.024693 mm	-0.253464 mm	-0.014537 mm
y_o	-0.239466 mm	- 0.213401 mm	- 0.109878 mm	-0.158923 mm
k_1	$-1.696019*10^{-3}$	$-1.709735*10^{-3}$	$-2.011666*10^{-3}$	$-1.712994*10^{-3}$
k_2	$0.257710*10^{-3}$	$0.274246*10^{-3}$	$0.337008*10^{-3}$	$0.260639*10^{-3}$
k_3	$-0.009089*10^{-3}$	$-0.010202*10^{-3}$	$-0.013096*10^{-3}$	$-0.009190*10^{-3}$
p_1	$0.053187*10^{-3}$	$0.036416*10^{-3}$	$-0.134155*10^{-3}$	$-0.009700*10^{-3}$
p_2	$0.113262*10^{-3}$	$0.036419*10^{-3}$	$0.066029*10^{-3}$	$0.014206*10^{-3}$
a_1	$1.162203*10^{-3}$	$0.279185*10^{-3}$	$-0.059959*10^{-3}$	$0.130802*10^{-3}$
a_2	$0.059299*10^{-3}$	$-0.663338*10^{-3}$	$-0.637141*10^{-3}$	$0.278204*10^{-3}$

Table 1: Estimated parameters of the four sensors.

ACKMOWLEDGEMENT

The authors would like to acknowledge the support of the Army Research Office and the Topographic Engineering Center.

REFERENCES

Atkinson, K. B., (1996). *Close Range Photogrammetry and Machine Vision*.

Batista, Jorge., Araujo, Helder., Almeida, A. T,. (1998). Iterative Multi-Step Explicit Camera Calibration, 1998 *IEEE* Int. Conf. on Computer Vision (ICCV98), Bombay, India, January 4-7.

Bethel, James S., Mikhail, Edward M., (2001). *Introduction to Modern Photogrammetry*.

Mikhail, Edward M., Ackermann, F., (1976). *Observation and Least Square*.

Moffit, Francis H., Mikhail, Edward M., (1980). *Photogrammetry*, third edition.

Pollefeys, Mark., Koch, Reinhard., Gool, Lue Van. (1999). Self-Calibration and Metric Reconstruction in spite of Varying and Unknown Internal Camera Parameters, *International Journal of Computer Vision*, 32(1), 7-25.

Ravi Samtaney. (1999). A Method to Solve Interior and Exterior Camera Calibration Parameters for Image Resection, *NAS*-99-03.

Geometric Calibration Report of CAMIS Sensor

For

Topographic Engineering Center

By

A. Alharthy & J. Bethel

School of Civil Engineering

Purdue University

25 MAY, 2001

Table of Content

1. Abstract:

The CAMIS sensor consists of four co-baresighted area-CCD cameras with filters to scan. The scan radiance in the blue, green, red, and near infrared spectral bands. In this report, we summarize the work that has been done during the geometric calibration of the CAMIS sensor. The procedure required many preliminary steps such as preparing the calibration site which involved target layout, setting up the coordinate system and locating objects to that system. Theodolites and a steel tape were used to measure the angles and distances in the network of calibration targets. In order to adjust those measurements and to get the target coordinates in the reference coordinate system, we developed network bundle adjustment program. Images of the target field were then taken by each of the four cameras of the CAMIS sensor. The coordinates of the targets in both the object and the image system were used as observations for estimating the sensor parameters. Two matching techniques were used to determine and refine the target locations in the image space. We modified the matching algorithm to overcome certain radiometric effects and thereby found the location of the target centers in image space.

After planning the data flow, the images were taken and the calibration procedure was started. To cover the most significant parameters, a full math model was used. A description of this model and its use are attached to this report. The Unified least square approach was used iteratively to solve this nonlinear over determined system since we have some prior knowledge about a number of the sensor parameters. Finally, in order to see the distortion behavior, the radial and decentering distortions were calculated along the radial distance and plotted separately. Then the radial distortion curve was equalized and the corresponding changes to the sensor parameters were recorded. We repeated the procedure for each camera individually and consequently our results, which are presented in this report, have four sets of adjusted parameters, one per camera. In the appendices, the report also outlines the basic steps and algorithms that were used during the calibration process.

2. Calibration:

The aim of this work was to make a laboratory calibration for the geometric parameters of the CAMIS sensor. CAMIS stands for Computerized Airborne Multicamera Imaging System. It is very advanced system and is designed to utilize modern solid-state imaging and data acquisition technology. It is composed of four CCD cameras with band pass optical filters to obtain four band images. The center wavelength of those bands is as follows: 450, 550, 650 and 800 nm. However, each sensor has its own optics and obtains its own image based on its working band independently from the others at the same time. Those four images can be integrated into a composite image or viewed individually. The CAMIS sensor has been used in multispectral imaging and mapping purposes by mounting it on an airplane with GPS and INS systems. Moreover, the PC that is used with this sensor is capable of recording and managing simultaneous image capture.

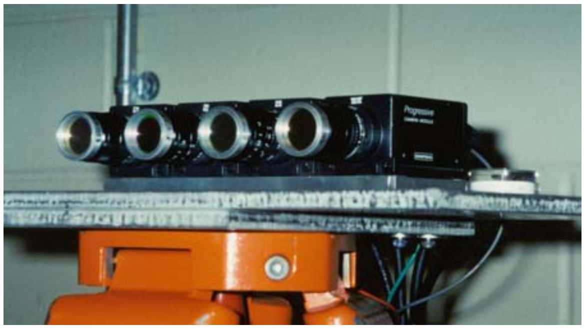

Figure 1a: the four cameras

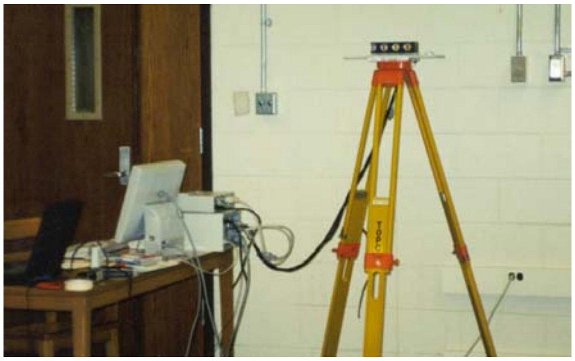

Figure 1b: CAMIS sensor

The procedure required a number of steps and they are summarized below:

2.1 Site preparation:

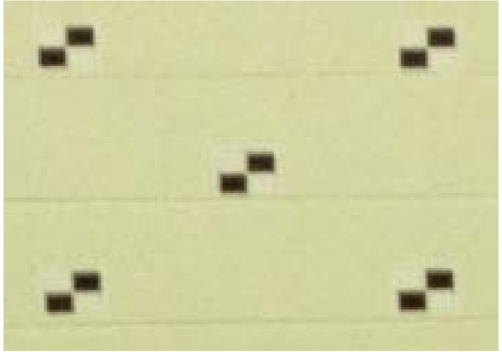

Figure 2: targets shape

The idea of the calibration was to layout some targets in the object space, locate them accurately, and acquire an image of those targets by the sensor. Then, we relate the coordinates of the targets in both systems, image and object space, in order to obtain the camera parameters. So, the procedure starts by setting up the calibration site. First, we designed the targets to be in cross shapes so their center positions will be read very easily. Then they have been laid out to be distributed in the image scene in a specific way that enables us to cover most geometric and systematic errors as shown in figure 3. Those targets were placed on an almost flat service wall and the sensor position was located around 8 meters away from that wall.

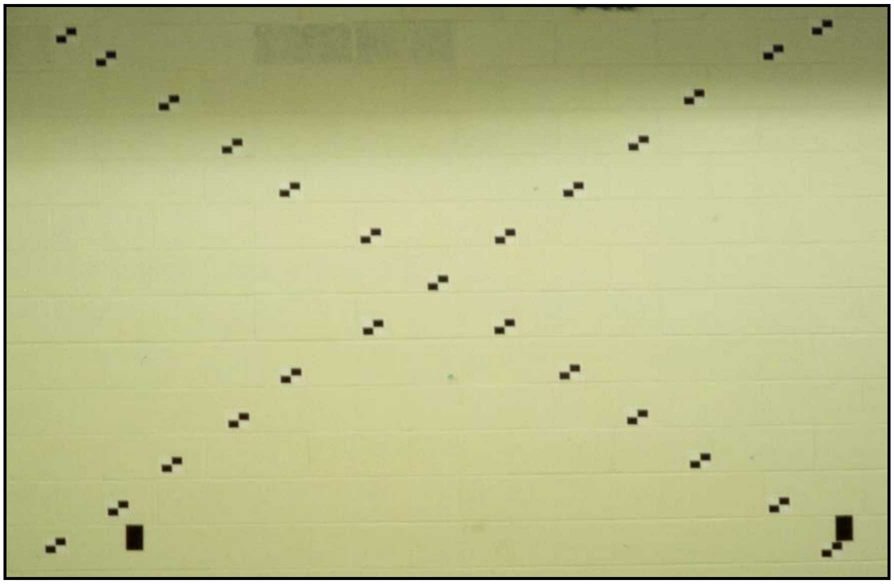

Figure 3: targets layout

In order to register the objects in the scene, an object space coordinate system was established at the site and two other instrument stations were marked to use in the measurements.

2.2 Measurements and adjustment in object space:

Figure 4: measuring angles

Two 3 arc-seconds accuracy theodolites were mounted at these two stations and were used to measure the angles between the targets themselves on one hand and between the targets and the four exposure stations of the CAMIS cameras on the other hand. The origin of the object space was chosen to be theodolite 1 at station one in the right of the sensor position. Many manual measurements were made of the camera physical layout, using machinist calipers. The lenses were also placed on an optical bench for determine the locations of the nodal points. A cross section of one camera is shown in figure 6. This was needed to locate the camera front nodal point with respect to the camera body which would be located in the network by theodolite observations. The spacings between the targets were measured with a steel tape. Having all these observations, we end up with an over determined system of equations. So, we developed a bundle adjustment program to adjust those coordinates of the targets and the instrument stations. As a result of that, we determined precisely all our targets and stations in the object space and the next step was capturing images by the sensor.

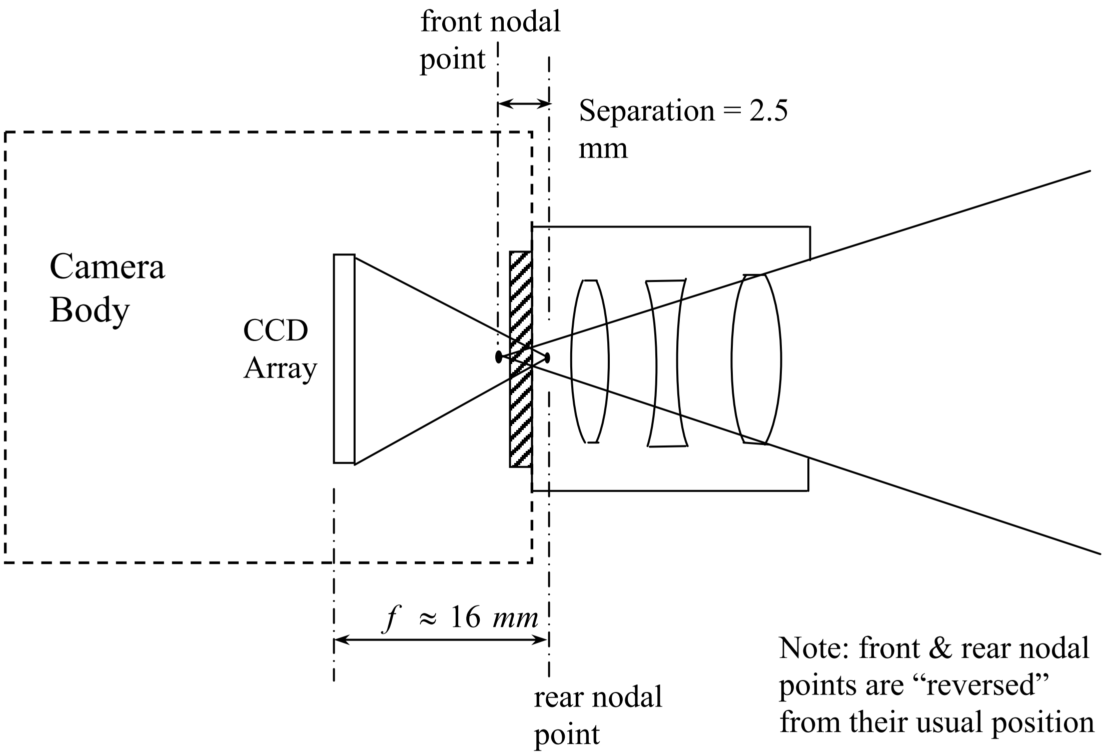

Figure 6: cross section of one camera showing the lenses, rear and front nodal points.

2.3 Capturing Images and obtaining image space coordinates:

Before the measurements, the sensor was mounted on leveled plate over a tripod. In this sense, the exposure stations were fixed and accurately determined. The image-capturing step was operated by a team from TEC and observed by the Purdue team. In this step we tried to simulate the real working conditions by setting the lenses to the infinity focus position. Images were viewed at the site to make sure that as many as possible of the targets were exposed. After this step, the site work ended and the processing procedure started.

2.4 Image space calculations:

Once the images were captured, we ran a cross correlation matching code to get rough approximation of target positions in the image space to within a few pixels. The cross correlation matching function works by computing the similarity between two same sized widows. One window patch contains the ideal target shape and the other contains a window from the image. In general, a matching problem is a key algorithm for other applications and image analysis. This function is explored more in appendix A2. Despite the fact that, the cross correlation matching results showed that we are only away from the exact position by a pixel or less, we needed more accurate and precise methods to define the exact location with a hundredth of a pixel or so. This step is very essential for the coming refinement step. This level of accuracy is mandatory for a camera calibration problem. Least Square matching is very adequate technique for this purpose and very powerful. LSQ matching utilizes the first derivative (gradient) of the intensity in both directions x,y to obtain the best match and the exact matching can be reached by moving one window towards the other one. Some obstacles were faced and solved by modifying the algorithm, see

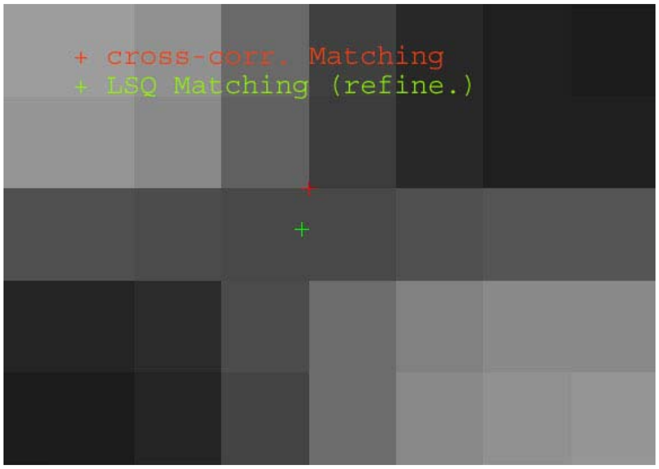

Figure 5: Target's center using positioning using two matching algorithms.

appendix A3 for more details. As a result of this step, the image space coordinates for the targets have been obtained with a fine accuracy. Results using both techniques are shown in figure 5.

2.5 Camera parameters estimation:

First, a full math model was chosen to perform the geometric calibration and estimate the sensor parameters. In this math model, Ravi Samtaney(1999) tried to cover most factors that might occur in geometric calibration. This model is explored in more details in appendix B. The model relates the target coordinates in object space and image space through the camera parameters. This overdetermined and non-linear system needs an optimization criterion to be solved. Since we have some initial values for a number of the camera parameters and their ranges, we decided to use the Unified Least Square algorithm iteratively to solve the system. Using the resulting distortion parameters, plots were drawn to describe the radial and decentering distortion behavior. Finally, the radial distortion curve was equalized by small changes in corresponding parameters.

The results of the process are tabulated for each sensor individually. Also, a numerical example is illustrated in appendix C to demonstrate the use of those parameters.

3 Results:

3.1 Blue Camera:

- Sensor type: working band (450 nm) 'Blue band'.

Camera Model:	CAMIS Model 4768P
Sensor type:	Sony XC-8500 CE ½" CCD Progressive Scan Camera.
Lens type:	TV Lens made by Cosmicar Pentax, Japan.
Shutter speed:	1/50 up to 1/10,000 sec.
Spec. CCD array size:	782 x 582 pixel.
Actual CCD array size:	768 x 576 pixel.
Nominal Focal Length:	16.000 mm.

- Estimated Parameters for the sensor:

Parameter symbol	Calibrated value	Short Description
f	16.168 mm	Calibrated Focal Length "EFL"
x_o	0.084357 mm	Principal Point x coordinate
y_o	- 0.239466 mm	Principal Point y coordinate
k_1	-1.696019 $*10^{-3}$	Radial Distortion parameters
k_2	0.257710 $*10^{-3}$	
k_3	-0.009090 $*10^{-3}$	
p_1	0.053188 $*10^{-3}$	Lens decentering parameters
p_2	0.113262 $*10^{-3}$	
a_1	1.162204 $*10^{-3}$	Affinity Distortion parameters
a_2	0.059300 $*10^{-3}$	

- See math model for more details.
- Conversion factor: 1 pixel = 0.0083 mm.

3.2 Green Camera:

- Sensor type: working band (550 nm) ‘Green band’.

Camera Model:	CAMIS Model 4768P
Sensor type:	Sony XC-8500 CE ½” CCD Progressive Scan Camera.
Lens type:	TV Lens made by Cosmicar Pentax, Japan.
Shutter speed:	1/50 up to 1/10,000 sec.
Spec. CCD array size:	782 x 582 pixel.
Actual CCD array size:	768 x 576 pixel.
Nominal Focal Length:	16.000 mm.

- Estimated Parameters for the sensor:

Parameter symbol	Calibrated value	Short Description
f	16.154 mm	Calibrated Focal Length “EFL”
x_o	-0.024693 mm	Principal Point x coordinate
y_o	- 0.213401 mm	Principal Point y coordinate
k_1	$-1.709735 * 10^{-3}$	Radial Distortion parameters
k_2	$0.274246 * 10^{-3}$	
k_3	$-0.010202 * 10^{-3}$	
p_1	$0.036417 * 10^{-3}$	Lens decentering parameters
p_2	$0.036419 * 10^{-3}$	
a_1	$0.279185 * 10^{-3}$	Affinity Distortion parameters
a_2	$-0.663339 * 10^{-3}$	

- See math model for more details.
- Conversion factor: 1 pixel = 0.0083 mm.

3.3 Red Camera:

- Sensor type: working band (650 nm) ‘Red band’.

Camera Model:	CAMIS Model 4768P
Sensor type:	Sony XC-8500 CE ½” CCD Progressive Scan Camera.
Lens type:	TV Lens made by Cosmicar Pentax, Japan.
Shutter speed:	1/50 up to 1/10,000 sec.
Spec. CCD array size:	782 x 582 pixel.
Actual CCD array size:	768 x 576 pixel.
Nominal Focal Length:	16.000 mm.

- Estimated Parameters for the sensor:

Parameter symbol	Calibrated value	Short Description
f	16.195 mm	Calibrated Focal Length “EFL”
x_o	-0.252689 mm	Principal Point x coordinate
y_o	- 0.108910 mm	Principal Point y coordinate
k_1	$-1.490695 * 10^{-3}$	Radial Distortion parameters
k_2	$0.267886 * 10^{-3}$	
k_3	$-0.010391 * 10^{-3}$	
p_1	$-0.140914 * 10^{-3}$	Lens decentering parameters
p_2	$0.057370 * 10^{-3}$	
a_1	$-0.062786 * 10^{-3}$	Affinity Distortion parameters
a_2	$-0.608008 * 10^{-3}$	

- See math model for more details.
- Conversion factor: 1 pixel = 0.0083 mm.

3.4 Near Infra Red:

- Sensor type: working band (800 nm) ‘Near Infra Red band’.

Camera Model:	CAMIS Model 4768P
Sensor type:	Sony XC-8500 CE ½” CCD Progressive Scan Camera.
Lens type:	TV Lens made by Cosmicar Pentax, Japan.
Shutter speed:	1/50 up to 1/10,000 sec.
Spec. CCD array size:	782 x 582 pixel.
Actual CCD array size:	768 x 576 pixel.
Nominal Focal Length:	16.000 mm.

- Estimated Parameters for the sensor:

Parameter symbol	Calibrated value	Short Description
f	16.173 mm	Calibrated Focal Length “CFL”
x_o	-0.014533 mm	Principal Point x coordinate
y_o	-0.158918 mm	Principal Point y coordinate
k_1	$-1.739689 * 10^{-3}$	Radial Distortion parameters
k_2	$0.263932 * 10^{-3}$	
k_3	$-0.009311 * 10^{-3}$	
p_1	$-0.009317 * 10^{-3}$	Lens decentering parameters
p_2	$0.014705 * 10^{-3}$	
a_1	$0.131437 * 10^{-3}$	Affinity Distortion parameters
a_2	$0.276288 * 10^{-3}$	

- See math model for more details.
- Conversion factor: 1 pixel = 0.0083 mm.

Appendix A: Target Locations in image space (Matching)

A.1 Introduction

In order to find the exact target locations in the image, two matching approaches were used. First, the approximate locations are obtained using the cross correlation matching. Second, we refine the results of the first algorithm using least squares matching.

A.2 Cross-correlation matching

Cross-correlation determines the similarity between two corresponding patches. The cross-correlation approach cannot give the precise location of an object due to many factors. Differences in attitude, distortion, and signal noise are some examples that affect the correspondence in geometry and radiometry. However, this algorithm usually gives an approximate location of the correspondence within a few pixels.

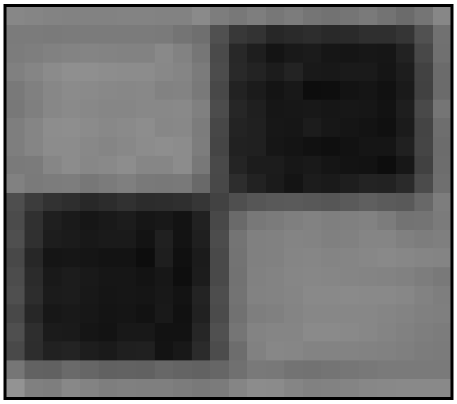

Figure A1: image patch (v)

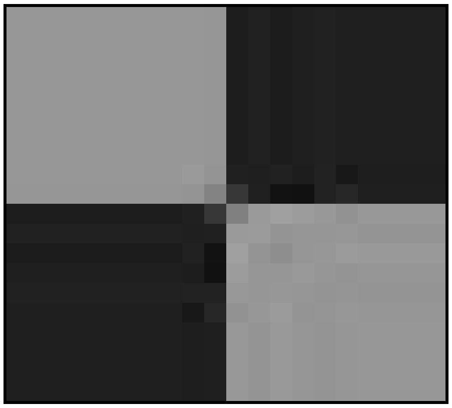

Figure A2: ideal template (u)

The cross-correlation matching function over two windows of N pixels each can be written as:

$$C_{uv} = \frac{\sum_{i=1}^{N} (u_i - \bar{u})\ (v_i - \bar{v})}{\left[\sum_{i=1}^{N} (u_i - \bar{u})\ \sum_{i=1}^{N} (v_i - \bar{v}) \right]^{1/2}} \qquad \text{eq(A1).}$$

Where: C_{uv} : match function between the template window (u) and image window (v).

u_i, v_i: intensity value at position i.

$\bar{u}, \bar{v}$: mean intensity value of the window $\frac{\sum_{i=1}^{N} u_i}{N}$, $\frac{\sum_{i=1}^{N} v_i}{N}$ respectively.

The ideal template will be passed through the image and the matching function will be computed and recorded at the center pixel of the patch. The match function ranges between +1 and -1. The max value equals +1 which means there is a full match between the two windows or, in other words, they are identical. Usually a threshold will be used to distinguish between matches and non-matches. Then the pixels with a cross correlation above the threshold will be considered candidates for the match. A copy of the developed program for this procedure is in the accompanying CD and some patches of the results are shown below. Our results, as shown in figure A3, are off from the center of the target only by a pixel or less. These results enable us to use the least squares matching/refining technique directly.

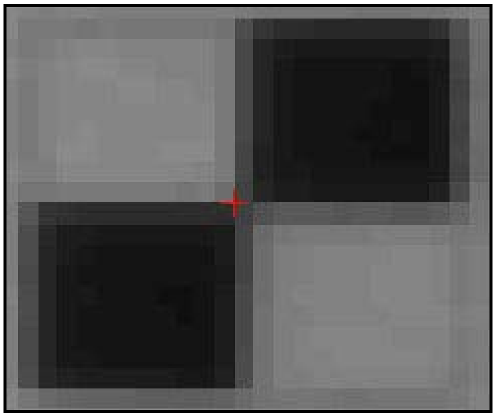

Figure A3a: a cross_corr. Match

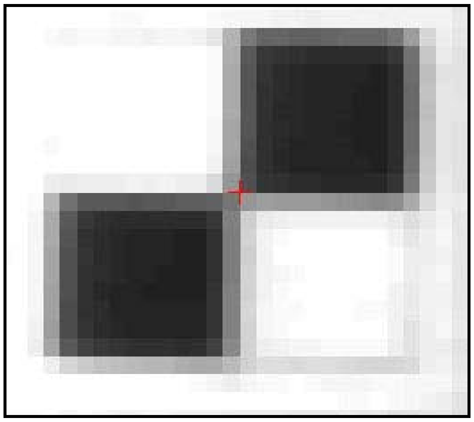

Figure A3b: another cross_corr. match

A.3 Least squares matching (LSQM):

Least squares matching works as a powerful and an accurate technique to refine an object's coordinates in the image space based on the correspondence between two relatively small windows of two images. This technique uses the gradient in the x,y directions in order to move the two patches towards each others to get the perfect match. The match precision that we are looking for with this technique is with in a hundredth of a pixel or so. The similarity between the two spots was only geometrically modeled for this specific problem since the radiometric effect was eliminated through some preprocessing steps, as we will see below. The problem is to match an ideal shape of the target with a small window from the image containing the imaged target. The following steps describe the procedure for setting up the two windows for matching:

i) Get the approximate location of the imaged target using the first matching approach (cross correlation) as described above in appendix A2. Those locations should be within a few pixels of the exact location in order to make the geometric model in LSQM converge and to produce accurate results.

ii) Having the rough estimated location, a window around that location from the image with adequate size will be extracted for matching purposes. This is all done systematically inside the code.

iii) Then, the pixel gray level values in this window will be used to assemble the ideal target for matching as shown in figure A4. In the extracted patch, the center of the target can be seen very clearly while in the image patch it not clear. Moreover, the similarity in the intensity is preserved between the two windows. Also, we tried to preserve the gradient by gradually distributing the change in the intensity between the black and gray regions. In this sense the radiometric effect on the correspondence will be diminished.

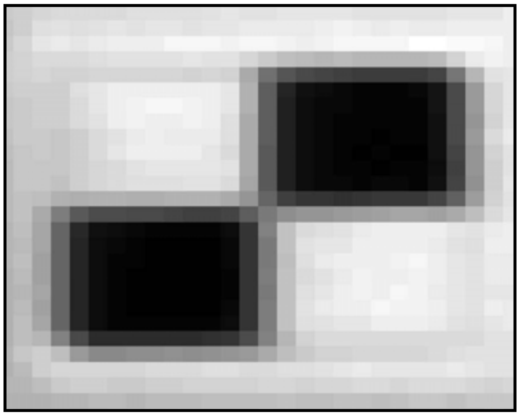

Figure A4a: the target in Image patch

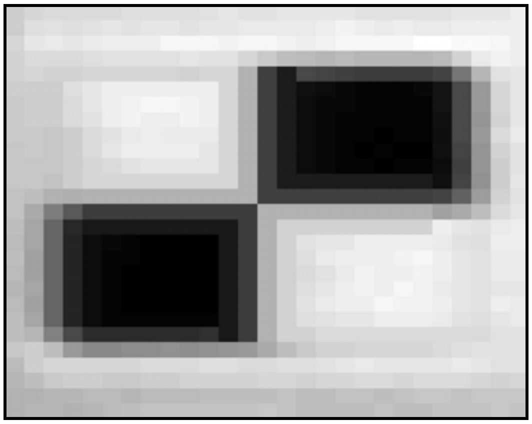

Figure A4b: the extracted target from Image Patch to use it as the ideal target in matching

After specifying the two windows with the same size for matching the LSQM procedure will take a place. Requiring equality in intensity between each of the two corresponding pixels from the two windows is the basic condition for this procedure as shown below.

$$F = img\ (i, j) - temp\ (i, j) = 0 \qquad \text{eq(A2).}$$

Where 'img' represent the patch that was taken from image in order to match it with 'temp', which represents the ideal template.

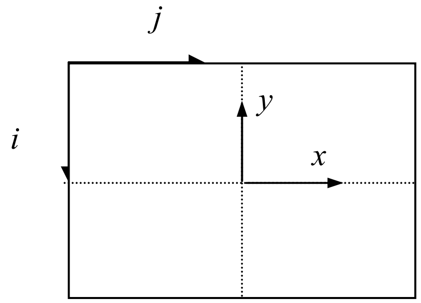

Figure A5a: Image patch

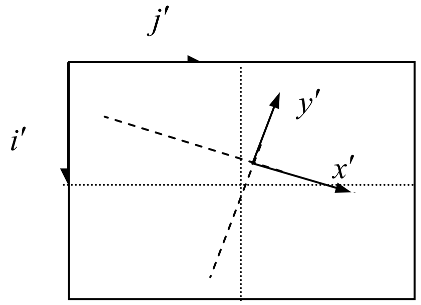

Figure A5a: ideal template

x, y and x', y' are not in the same coordinate system. A transformation, which consists of 6-parameters, is used to link those two systems.

$$\begin{bmatrix} x' \\ y' \end{bmatrix} = \begin{bmatrix} a_1 & a_2 \\ b_1 & b_2 \end{bmatrix} \begin{bmatrix} x \\ y \end{bmatrix} + \begin{bmatrix} a_o \\ b_o \end{bmatrix}$$

in which a_1, a_2, b_1, b_2 are the elements of the transformation matrix R and a_o, b_o are the elemenst of the shift vector t. Then the linearized form of the least square is used to estimate those parameters.

$$v + B\Delta = f \qquad \text{eq(A3),}$$

Where v is a vector of the residuals to the parameters and B is a matrix consists of the partial derivatives of the condition equation with respect to the parameters as shown below. Δ is the correction vector to those parameters and $f = -F$.

$$B = [\ \frac{\partial F}{\partial a_1} \quad \frac{\partial F}{\partial a_2} \quad \frac{\partial F}{\partial a_o} \quad \frac{\partial F}{\partial b_1} \quad \frac{\partial F}{\partial b_2} \quad \frac{\partial F}{\partial b_o}\ ]$$

taking the derivatives via the chain rule, the above expression will be:

$$\frac{\partial F}{\partial a_1} = -\frac{\partial\, temp}{\partial a_1} = -\frac{\partial\, temp}{\partial x'}\frac{\partial x'}{\partial a_1}$$

in which $\frac{\partial temp}{\partial x'} = g_x$ and $\frac{\partial x'}{\partial a_1} = x$

The first part of the each partial derivative in B (gx and gy) was estimated by the gradients in the x and y directions respectively as follows:

$$g_y = -\frac{temp(i+1, j) - temp(i-1, j)}{2}, \qquad g_x = \frac{temp(i, j+1) - temp(i, j-1)}{2}$$

Consequently the matrix B will be:

$$B_{(k,6)} = [\ -g_x x \quad -g_x y \quad -g_x \quad -g_y x \quad -g_y y \quad -g_y\ ]$$

From the above drawing in figure 5,

$$x = j - (size_{patch}/2)\ ; \qquad y = -(i - (size_{patch}/2))$$

and $$f_{(k,1)} = -(img(i,j) - temp(i,j)),$$

B and f will be calculated for each pixel and its corresponding pixel in the other patch. The two patches that we should work with should be the same size (m,n). So, $k = m * n$. Using all pixels (k), the least squares technique will estimate the 6-parameters for the first iteration, assuming unit weights,

$$\Delta = inv(B' * B)(B' * f)$$

This correction vector will be added to the 6-parameter initial values. Those corrected parameters will be used to calculate the new coordinates x', y' in order to use them in resampling the grid for the template window. We used bilinear interpolation to estimate the intensity values during this resampling procedure.

The whole procedure will be repeated as needed but using the new template window with the new intensity values every time and the parameters will be accumulatively updated. The match will be achieved when the system converges and those 6-parameters do not change any further. The system might diverge if there is no similarity between the two patches or the approximate location of the match far off from the real one by more than several pixels. For more details, see the matlab LSQM matching program that is in the accompanying CD.

For the purpose of comparison, the match from cross-correlation and LSQM are viewed in figure A6. We can see clearly how the match moved towards the right center of the targets using LSQM.

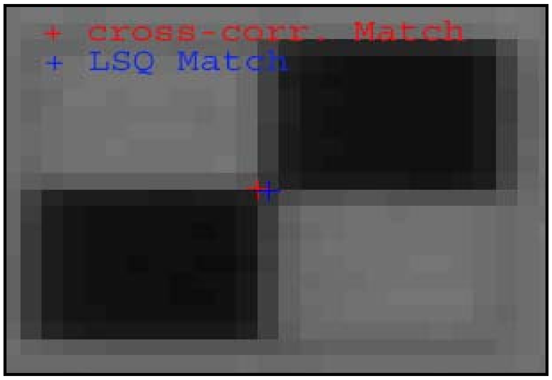

Figure A6: matching results using cross-Correlation and LSQ matching techniques.

Appendix B: Math Model

B.1 Math model

The math model was chosen carefully in order to cover all possible sources of geometric errors and estimate all significant correction parameters for those errors as in eq B1. Samtaney (1999) explored this model in detail. It was derived from the fundamental collinearity equations. This model relates two coordinate systems to each other. It maps the coordinates from the object space into the image space and vice versa taking in account that it is unique only in one direction. There are two types of parameters. First, the *extrinsic* parameters which include the location and orientation parameters. Lens distortion and focal length are examples of the second type, which are called the *intrinsic* parameters. The model specifically covers and takes into account the lens distortion influence through some factors such as radial, decentering, and affinity distortion see eq B2.

$$x - x_o = x' - x_o + \Delta x$$

$$= -f \frac{r_{11}(X - X_c) + r_{12}(Y - Y_c) + r_{13}(Z - Z_c)}{r_{31}(X - X_c) + r_{32}(Y - Y_c) + r_{33}(Z - Z_c)} \qquad \text{eq B1a}$$

$$y - y_o = y' - y_o + \Delta y$$

$$= -f \frac{r_{21}(X - X_c) + r_{22}(Y - Y_c) + r_{23}(Z - Z_c)}{r_{31}(X - X_c) + r_{32}(Y - Y_c) + r_{33}(Z - Z_c)} \qquad \text{eq B1b}$$

(x, y) ; (x', y') : ideal and measured targets projected coordinates in image space.

x_o, y_o : principal point coordinates in image space.

$\Delta x, \Delta y$: distortion correction in x, y directions in image space, see eq B2.

f : camera focal length.

$r_{i,j}$: the ith row and jth column element of the orientation matrix R , see eq B3.

(X,Y,Z): target coordinates in object space.

(X_c,Y_c,Z_c): exposure station coordinates in object space.

The distortion effects including radial, lens decentering, and affinity were computed through the equations below.

$$\Delta x = \bar{x}(k_1 r^2 + k_2 r^4 + k_3 r^6) + p_1(r^2 + 2\bar{x}^2) + 2p_2\bar{x}\ \bar{y}$$

$$\Delta y = \bar{y}(k_1 r^2 + k_2 r^4 + k_3 r^6) + 2p_1\bar{x}\ \bar{y} + p_2(r^2 + 2\bar{y}^2) + a_1\bar{x} + a_2\bar{y} \qquad \text{eq B2}$$

in which: $\bar{x} = x' - x_o$, $\bar{y} = y' - y_o$, $r^2 = \bar{x}^2 - \bar{y}^2$.

k_i : radial distortion coefficients.

p_i : decentering distortion coefficients.

a_i : affinity distortion coefficients.

The rotation matrix R expresses the orientation of the image coordinate system with respect to the object coordinate system. It is used in the model to relate the target coordinates in both systems. Rotations around the three principle axes x, y, and z by the three angles ω, ϕ, and k generate the matrix R as seen in eq B3.

$$R = R_z(k)\,R_y(\phi)\,R_x(\omega) \qquad \text{eq B3}$$

and those rotations are given by:

$$R_x(\omega) = \begin{bmatrix} 1 & 0 & 0 \\ 0 & \cos\omega & \sin\omega \\ 0 & -\sin\omega & \cos\omega \end{bmatrix} , \ R_y(\phi) = \begin{bmatrix} \cos\phi & 0 & -\sin\phi \\ 0 & 1 & 0 \\ \sin\phi & 0 & \cos\phi \end{bmatrix} , \ R_z(k) = \begin{bmatrix} \cos k & \sin k & 0 \\ -\sin k & \cos k & 0 \\ 0 & 0 & 1 \end{bmatrix}$$

The two condition equations for each target will be:

$$\begin{aligned} Fx = {} & \bar{x} + \bar{x}(k_1 r^2 + k_2 r^4 + k_3 r^6) + p_1(r^2 + 2\bar{x}^2) + 2p_2\overline{xy} \\ & + f\,\frac{r_{11}(X - X_c) + r_{12}(Y - Y_c) + r_{13}(Z - Z_c)}{r_{31}(X - X_c) + r_{32}(Y - Y_c) + r_{33}(Z - Z_c)} = 0 \end{aligned} \qquad \text{eq B4a}$$

$$\begin{aligned} Fy = {} & \bar{y} + \bar{y}(k_1 r^2 + k_2 r^4 + k_3 r^6) + 2p_1\overline{xy} + p_2(r^2 + 2\bar{y}^2) + a_1\bar{x} + a_2\bar{y} \\ & + f\,\frac{r_{21}(X - X_c) + r_{22}(Y - Y_c) + r_{23}(Z - Z_c)}{r_{31}(X - X_c) + r_{32}(Y - Y_c) + r_{33}(Z - Z_c)} = 0 \end{aligned} \qquad \text{eq B4b}$$

From the equations above, each target will form two equations. Consequently, the number of equations will be twice the number of targets in the image. So, we can conclude that the number of calibration targets in each image should be at least half of the number of camera parameters that we want to estimate in order to solve this system. However, in a calibration process like this we want the number of equations to exceed the minimum requirement in order to have an *overdetermined* system. Such a system enhances the reliability of the result. In this problem, 13 parameters were estimated and the number of targets that were used was 20 and 21 in some cases. So, the redundancy we had during the procedure was 27.

B.2 Solution method

The Unified least squares approach was used to solve this system since some *a priori* knowledge is available for a number of parameters. Using the a priori knowledge of the parameters is the distinction between the ordinary least squares and the unified least squares. This a priori knowledge is utilized to give those parameters initial values and weights. In this sense, some of the parameters were treated as observations with low precision by assigned large variances to them. Since the system is non-linear, the parameter values will be updated iteratively by adding the correction vector , Δ, to them.

$$\Delta = (N + W_{xx})^{-1} * (t - W_{xx} f_x) \qquad \text{eq B5}$$

in which,

$$\begin{aligned} N &= B' * (A * Q * A')^{-1} * B \\ t &= B' * (A * Q * A')^{-1} * f_o \\ f_o &= -(F + A * (L - L_o)) \end{aligned} \qquad \text{eq B6}$$

Geometric Calibration of the CAMIS Sensor

Abdullatif Alharthy & James Bethel

Geomatics Area, School of Civil Engineering

Purdue University

May 6, 2002

Presentation Outline

- 1) Introduction:
  - Research Objectives
  - Sensor Description
- 2) Laboratory work:
  - Site preparation
  - Measurements and adjustment in object space
  - Capturing Images
- 3) Target Locations in image space (Matching):
  - Cross-correlation matching (CCM)
  - Least squares matching (LSQM)

- 4) Mathematical Model:
  - Mathematical model
  - Solution method
- 5) Distortion Analysis:
  - Radial Distortion
  - Decentering Distortion
- 6) Results and Discussion

1.1 Research Objectives

- CAMIS sensor has been used in multispectral imaging and mapping purposes by mounting it in an airplane with GPS and INS systems.
- These auxiliary sensors provide very good position and attitude data for stabilizing the subsequent bundle block adjustment.
- The aim of this work was to make a laboratory calibration for the geometric parameters of the CAMIS sensor.

1.2 Sensor Description

- CAMIS stands for Computerized Airborne Multicamera Imaging System.
- CAMIS is a system for airborne remote sensing and is designed to utilize modern solid-state imaging and data acquisition technology.
- It consists of four co-boresighted area-CCD cameras with band pass filters: blue, green, red, and near infrared.
- Each sensor has its own optics and obtains its own image independently from the others at the same time.
- The sensor is operated by Topographic Engineering Center and we have worked with Mr. Mitch Pierson to obtain the required data.

CAMIS, the four cameras

CAMIS in Aircraft with Image Display

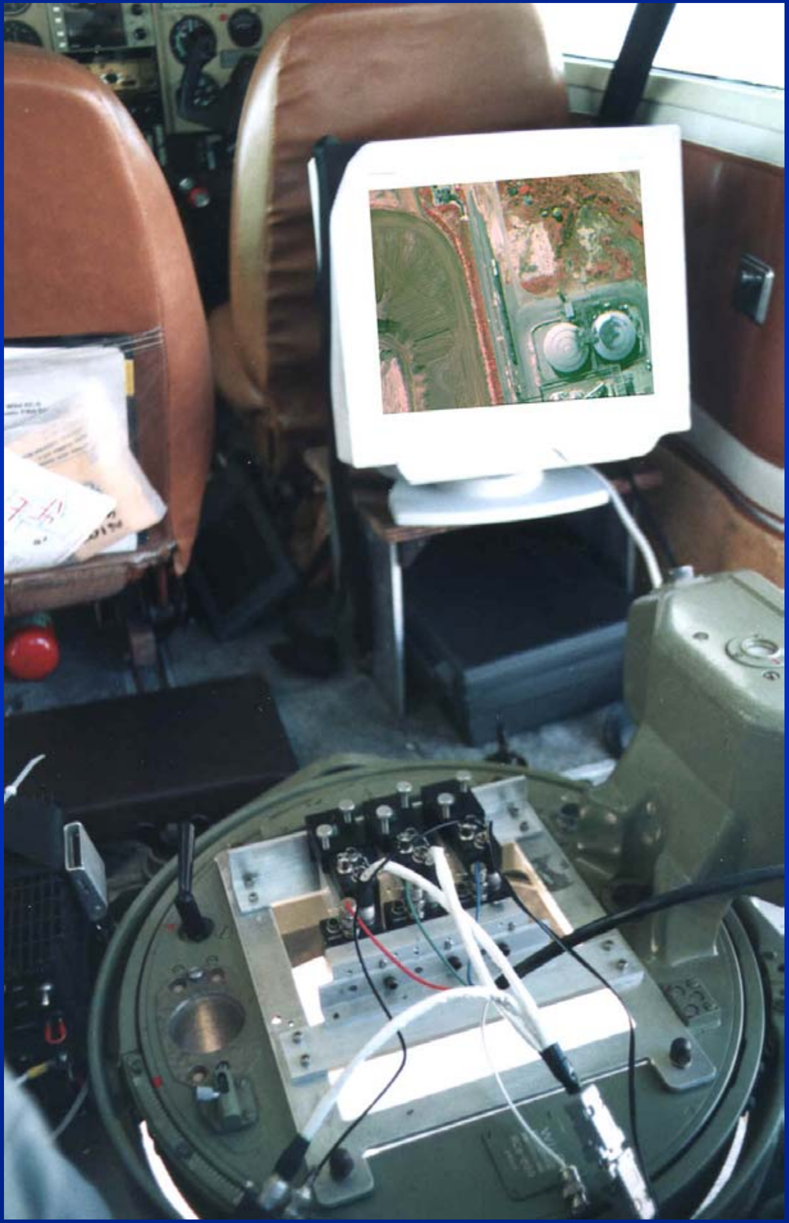

CAMIS 3 Bands and Color Composite

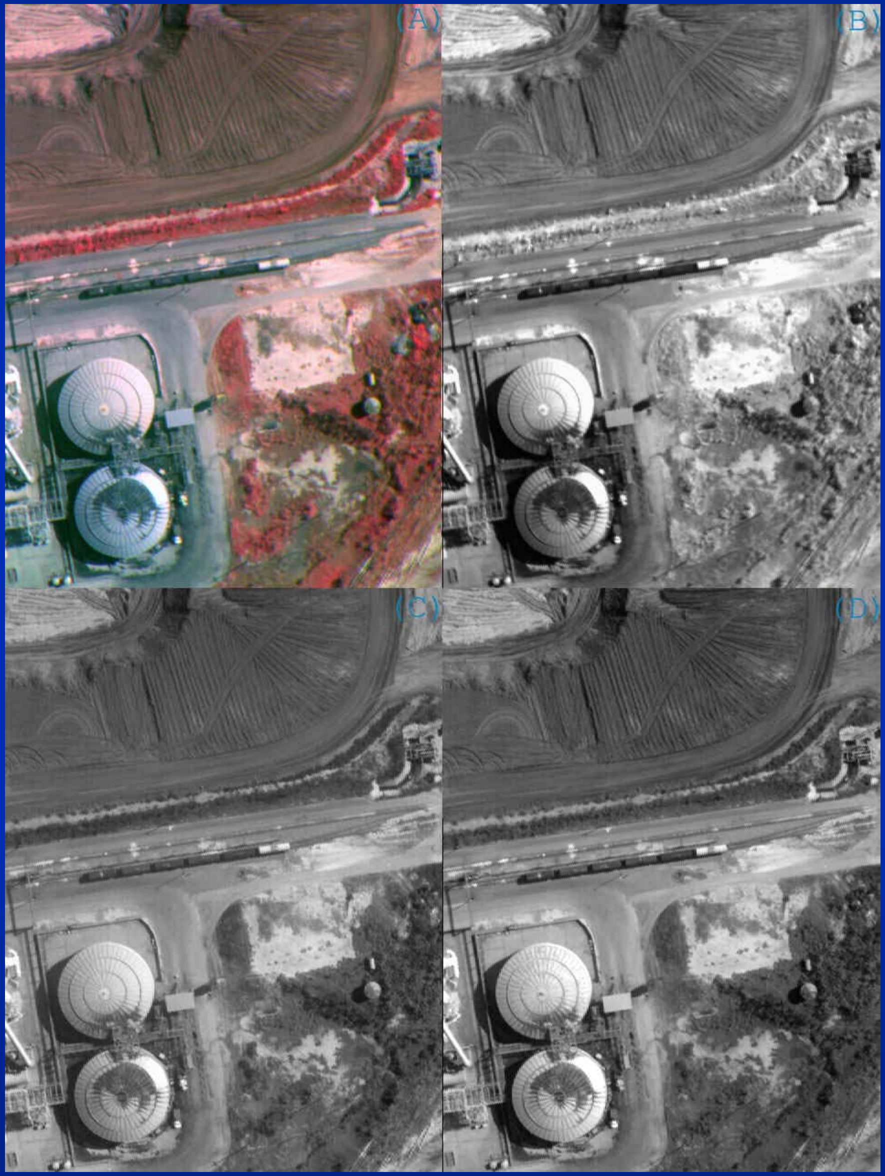

Mosaic from CAMIS Strips

Ft. A.P. Hill Mosaic

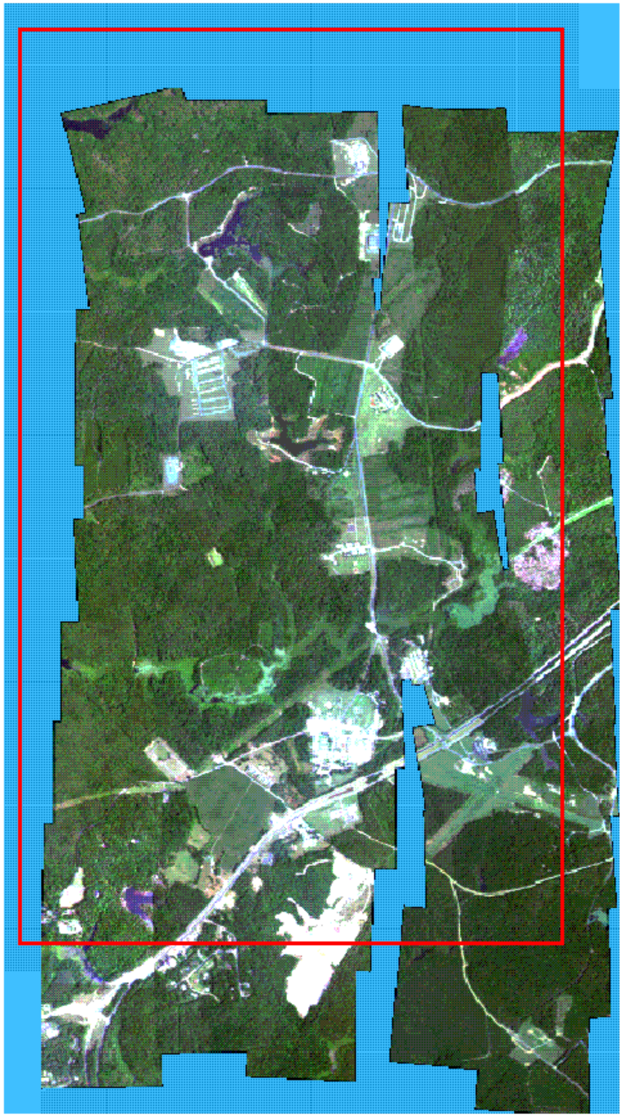

2) Site work

2.1) Calibration site preparation:

- Targets layout
  - Target design
    - cross shape
      - » So their centers positions will be read easily.
  - Targets layout
    - “X” pattern
      - » This layout allows us to recover the needed geometric parameters and systematic errors
  - Exposure stations
    - The sensor was mounted on a leveled plate fixed on a survey tripod which is about 8m from targets (far enough to use infinity focus position)

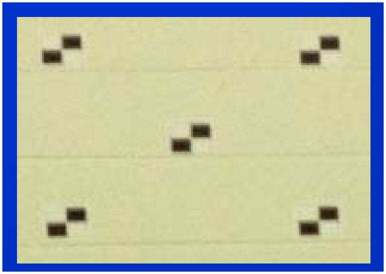

Enlargement showing 5 targets

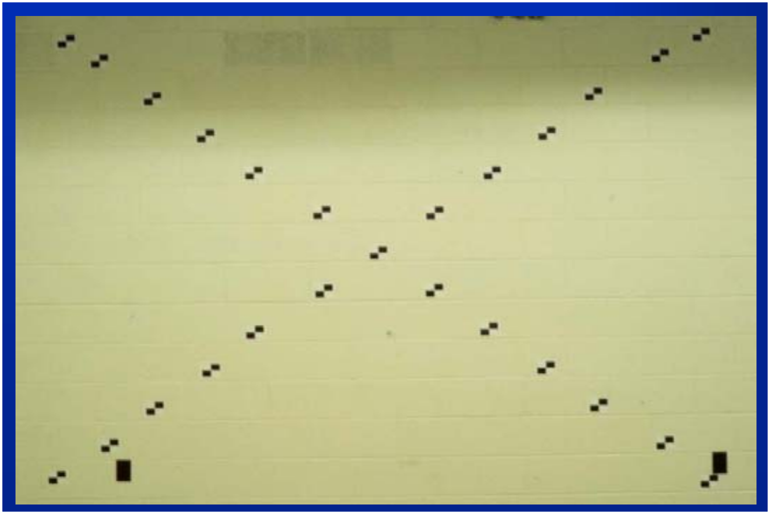

Targets layout

2) Site work steps cont’d

2.2) Measurements and adjustment in object space:

- Laboratory measurements
  - Two 3 arc-second accuracy theodolites were stationed and referenced to measure directions.
    - target centers
    - theodolite locations
    - camera case monuments
  - Steel tape and machinist calipers to measure distances
  - Optical bench to determine the locations of the nodal points

Measurements in the calibration site

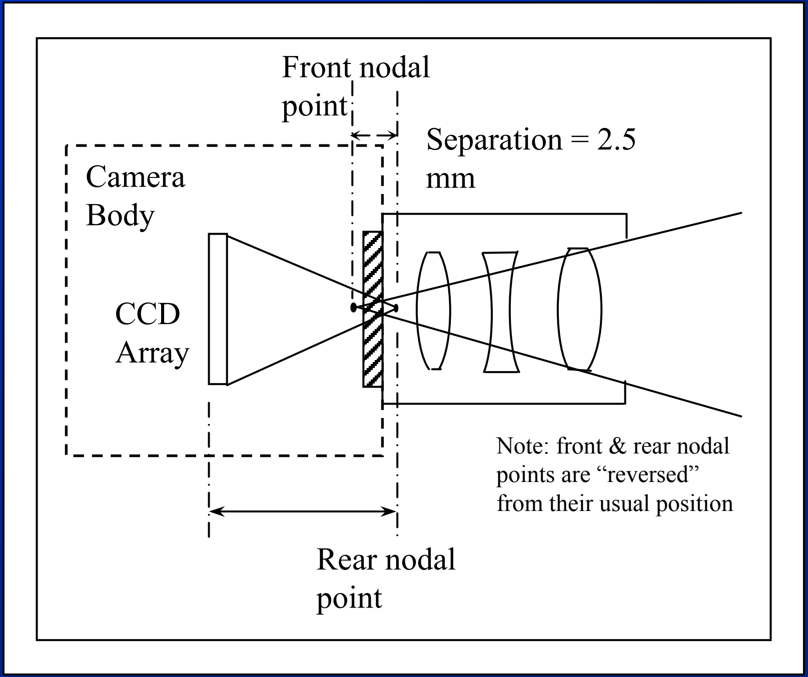
Front nodal point
Separation = 2.5 mm
Camera Body
CCD Array
Note: front & rear nodal points are “reversed” from their usual position
Rear nodal point

cross section of one camera showing the lenses, rear and front nodal points

2) Site work steps cont’d

2.2) Measurements and adjustment in object space cont’d

– Network adjustment

- Having all these observations, we end up with an over determined system of equations.
- A bundle adjustment program was developed to adjust those coordinates of the targets and the instrument stations.
- As a result of that, we determined precisely all our targets and stations in the object space which is a necessity for the calibration purpose.

2.3) Capturing Images

- This step was operated by a team from TEC and observed by the Purdue team
- We tried to simulate the real working conditions by setting the lenses to the “working” infinity focus position
- Images were viewed at the site to make sure that as many as possible of the targets were exposed.

3) Target Locations in Image Space

3.1) Cross Correlation Matching (CCM)

- A cross correlation matching program was used to get rough approximation of target positions in the image space to within a pixel.

- This was done by computing the similarity between a window patch containing the ideal target and the another window from the captured image.

- Despite the fact that, the CCM results showed that we are only away from the exact position by a pixel or less, we needed more accurate and precise methods to define the exact location within a hundredth of a pixel or so.

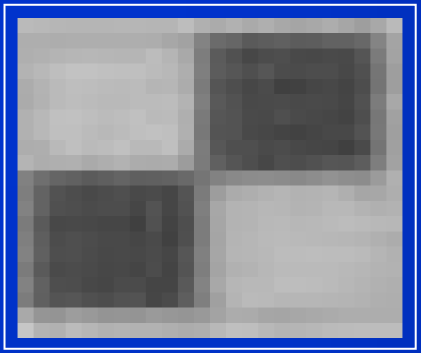

image patch (v)

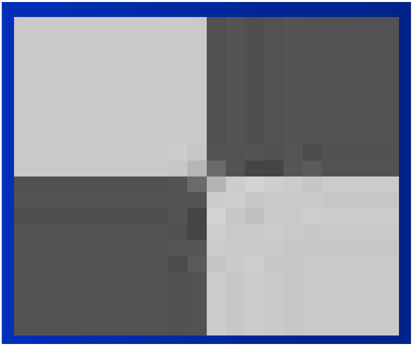

ideal template (u)

$$C_{uv} = \frac{\sum_{i=1}^{N} (u_i - \overline{u})\,(v_i - \overline{v})}{\left[\sum_{i=1}^{N} (u_i - \overline{u}) \; \sum_{i=1}^{N} (v_i - \overline{v}) \right]^{1/2}}$$

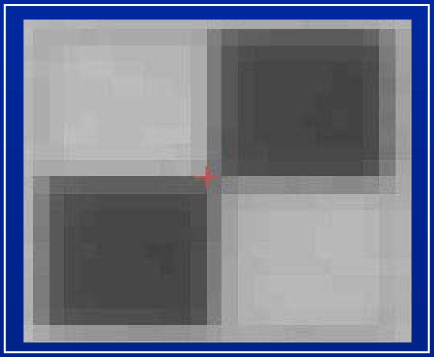

CCM Match

Response to Coarse Alignment via Template Matching

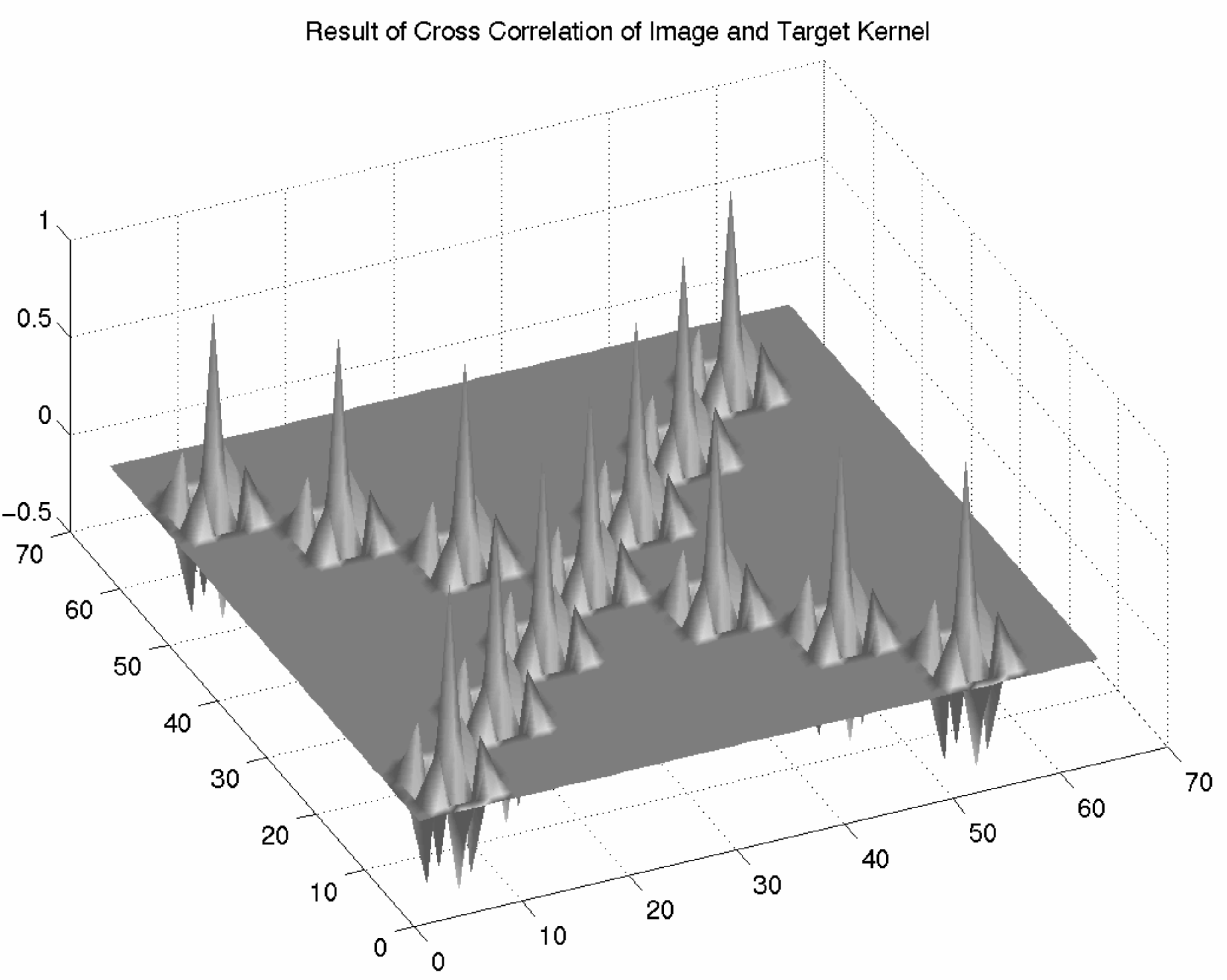

3) Target Locations in Image Space cont’d

3.2) Least squares matching (LSQM)

- LSQM utilizes the first derivative of the intensity in both x and y directions to refine the best correspondence and the exact matching can be reached by moving one window with respect to the other one while minimizing some of squares of differences of intensity values.
- The similarity between the two spots was only geometrically modeled since the radiometric effect was eliminated.
  - Get the approximate location of the imaged target using the first matching approach. Those locations should be within a few pixels of the exact location.
  - A window around that location from the image with adequate size will be extracted.
  - The ideal or template target is retrieved at this point. Similarity in the intensity is enforced between the two windows.

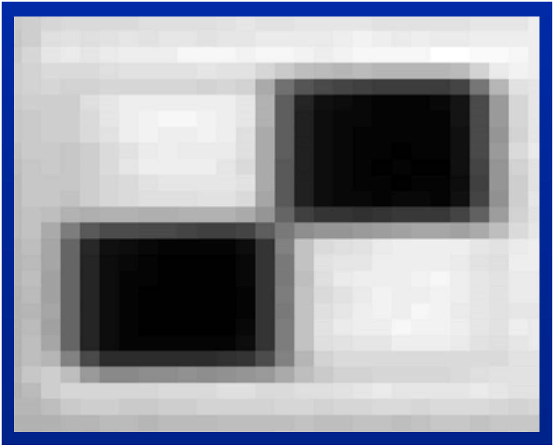

the target in Image patch

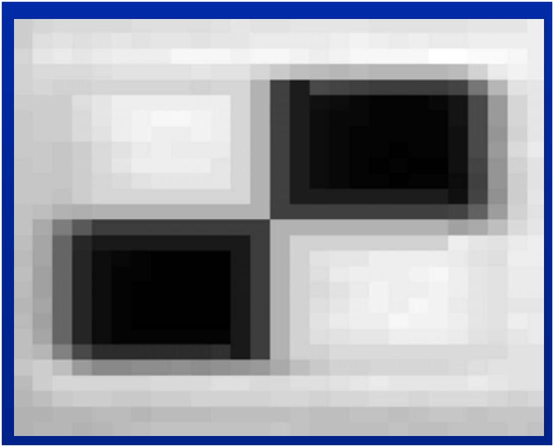

the extracted target

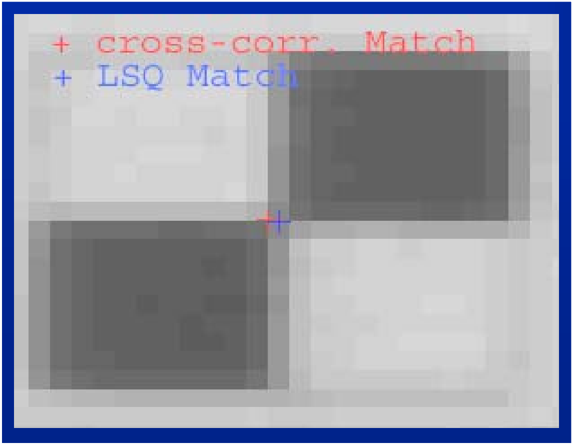

matching results using two methods in succession

4) Math Model and Solution Method

4.1) Math Model

- The mathematical model was chosen carefully in order to recover all significant sources of geometric errors and estimate all significant correction parameters for those errors.

$$x - x_o = x' - x_o + \Delta x \qquad = -f\,\frac{r_{11}(X - X_c) + r_{12}(Y - Y_c) + r_{13}(Z - Z_c)}{r_{31}(X - X_c) + r_{32}(Y - Y_c) + r_{33}(Z - Z_c)}$$

$$y - y_o = y' - y_o + \Delta y \qquad = -f\,\frac{r_{21}(X - X_c) + r_{22}(Y - Y_c) + r_{23}(Z - Z_c)}{r_{31}(X - X_c) + r_{32}(Y - Y_c) + r_{33}(Z - Z_c)}$$

- Samtaney (1999) explored this model in detail.
  - It was derived from the fundamental collinearity equations. It maps the coordinates from the object space into the image space through some parameters.
    - Exterior parameters which include the location and orientation parameters
    - Interior parameters, lens distortion and focal length are examples of the second type.

4) Math Model cont’d

– The model specifically covers and takes into account the lens distortion through some parameters that model radial, decentering, and affinity distortion.

$$\Delta x = \bar{x}(k_1 r^2 + k_2 r^4 + k_3 r^6) + p_1(r^2 + 2\bar{x}^2) + 2 p_2 \bar{x}\ \bar{y}$$

$$\Delta y = \bar{y}(k_1 r^2 + k_2 r^4 + k_3 r^6) + 2 p_1 \bar{x}\ \bar{y} + p_2(r^2 + 2\bar{y}^2) + a_1 \bar{x} + a_2 \bar{y}$$

where: $r^2 = \bar{x}^2 - \bar{y}^2, \quad \bar{x} = x' - x_o, \quad \bar{y} = y' - y_o$

$k_i, \ p_i, \ a_i$: radial , decentering, affinity distortion coefficients

4) Math Model cont'd

$$F_x = \bar{x} + \bar{x}(k_1 r^2 + k_2 r^4 + k_3 r^6) + p_1(r^2 + 2\bar{x}^2) + 2p_2\overline{xy}$$
$$+ f\,\frac{r_{11}(X - X_c) + r_{12}(Y - Y_c) + r_{13}(Z - Z_c)}{r_{31}(X - X_c) + r_{32}(Y - Y_c) + r_{33}(Z - Z_c)} = 0$$

$$F_y = \bar{y} + \bar{y}(k_1 r^2 + k_2 r^4 + k_3 r^6) + 2p_1\overline{xy} + p_2(r^2 + 2\bar{y}^2) +$$
$$a_1\bar{x} + a_2\bar{y} + f\,\frac{r_{21}(X - X_c) + r_{22}(Y - Y_c) + r_{23}(Z - Z_c)}{r_{31}(X - X_c) + r_{32}(Y - Y_c) + r_{33}(Z - Z_c)} = 0$$

- Each target observation will generate two equations. Consequently, the number of equations will be twice the number of targets in the image for each camera.

4) Math Model cont’d

4.2) Solution Method

- In a calibration process like this we want the number of equations to exceed the minimum requirement in order to have an *overdetermined* system. Such a system enhances the reliability and precision of the result. In this problem, 13 parameters were estimated and the number of targets that were used was 20 and 21 in some cases. So, the redundancy we had during the procedure was 27.

- The Unified least squares approach was used to solve this system since some *a priori* knowledge is available for a number of parameters. This a priori knowledge is utilized to give those parameters initial values and weights.

- In this sense, some of the parameters were treated as observations with low precision by assigned large variances to them. Since the system is non-linear, the parameter values will be updated iteratively until convergence by adding the correction vector

5) Distortion Analysis

- After determining the camera parameters including distortion parameters, distortion curves were drawn for visual and computational analysis.

5.1) Radial Distortion

It is the displacement of an imaged object radially either towards or away from the principle point

$$\Delta r = k_1 r^3 + k_2 r^5 + k_3 r^7$$

$$\delta_x = \Delta r * \overline{x} / r \qquad \delta_y = \Delta r * \overline{y} / r$$

The resulting curves were obtained for all four cameras and the maximum radial distortion was less than 40 micrometers.

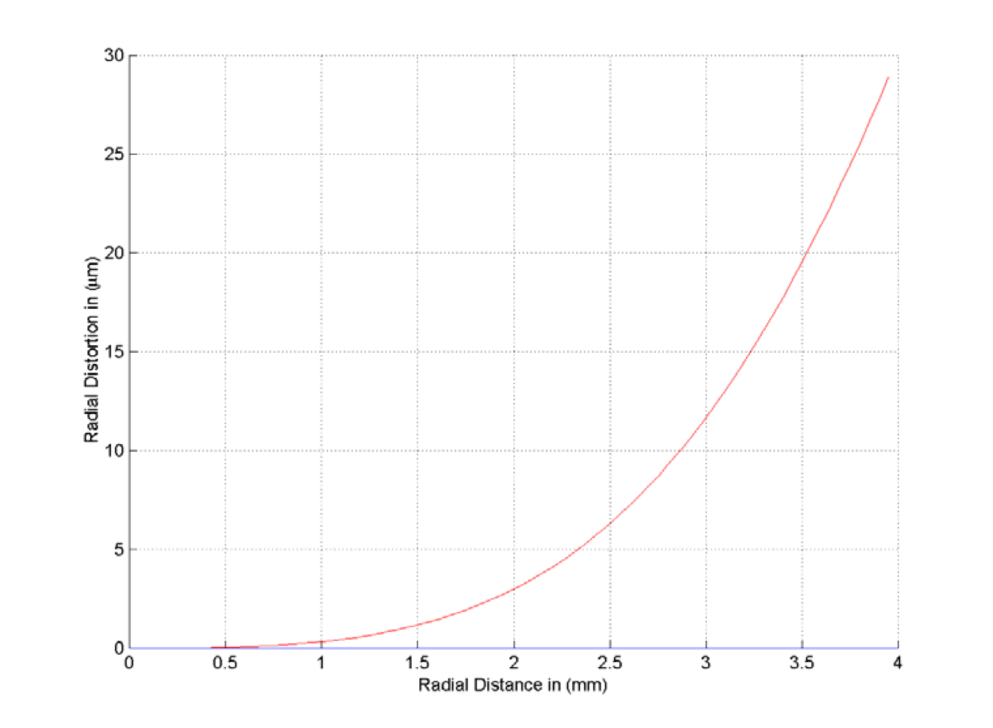

Radial distortion curve of the blue camera

5) Distortion Analysis cont'd

- Radial distortion curve equalization

- The following step was done to level or balance the curve based on equalizing the maximum and the minimum distortion values. This step has no effect on the final results of the corrected coordinates; it is just cosmetic but accepted professional practice.

- Mathematically, balancing the curve leads to a change in the radial distortion parameters and consequently the focal length and other related camera parameters. So this procedure was done iteratively and the parameters were updated.

- CFL: Calibrated focal length.

$$r_{\max} - CFL \times \tan(\alpha_{\max}) + r_{\min} - CFL \times \tan(\alpha_{\min}) = 0$$

$$CFL = \frac{r_{\max} + r_{\min}}{\tan(\alpha_{\max}) + \tan(\alpha_{\min})}$$

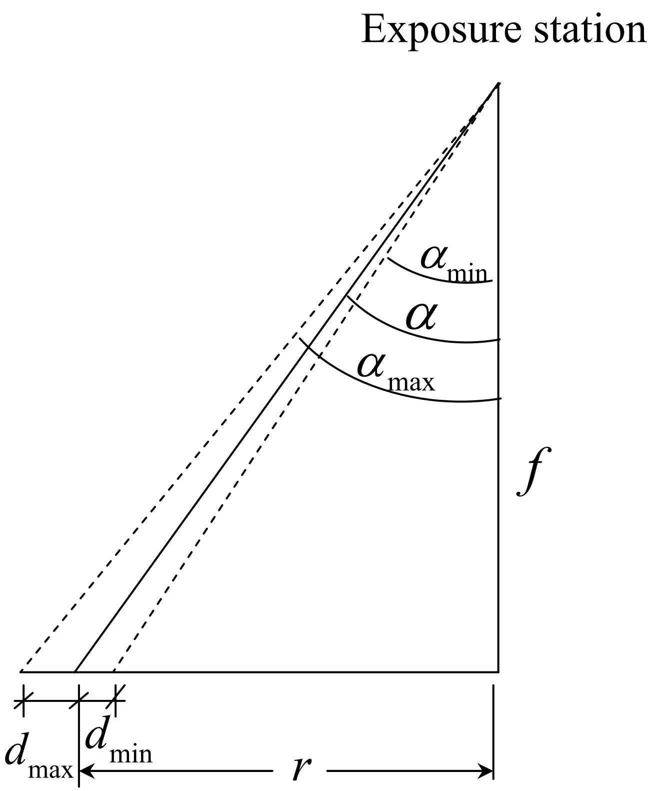

image plane cross section

We want dmax and dmin to have approximately the same magnitude.

5) Distortion Analysis cont'd

Radial distortion (RD) resulting curves

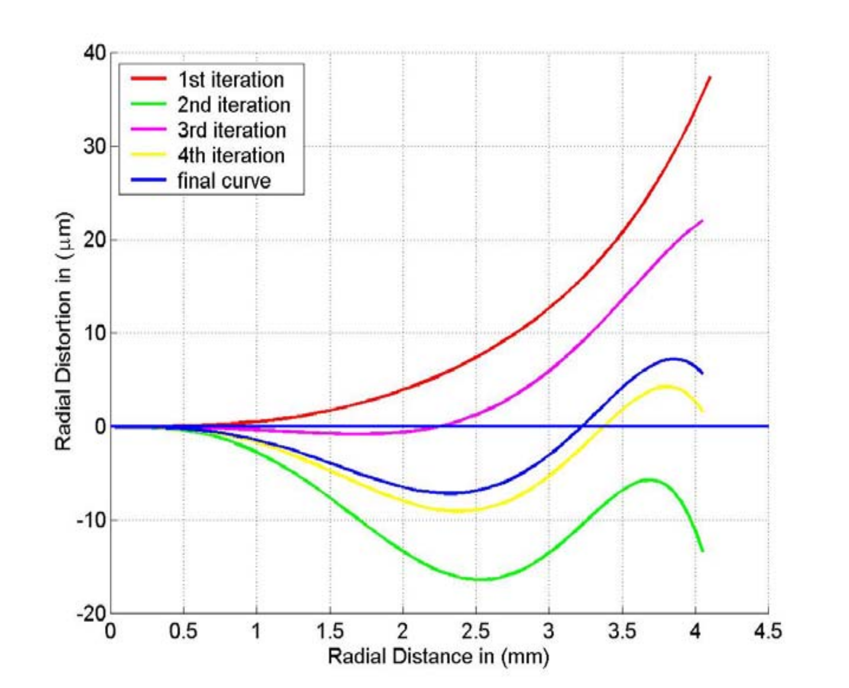

Radial distortion (Equalization iteration for the Blue camera)

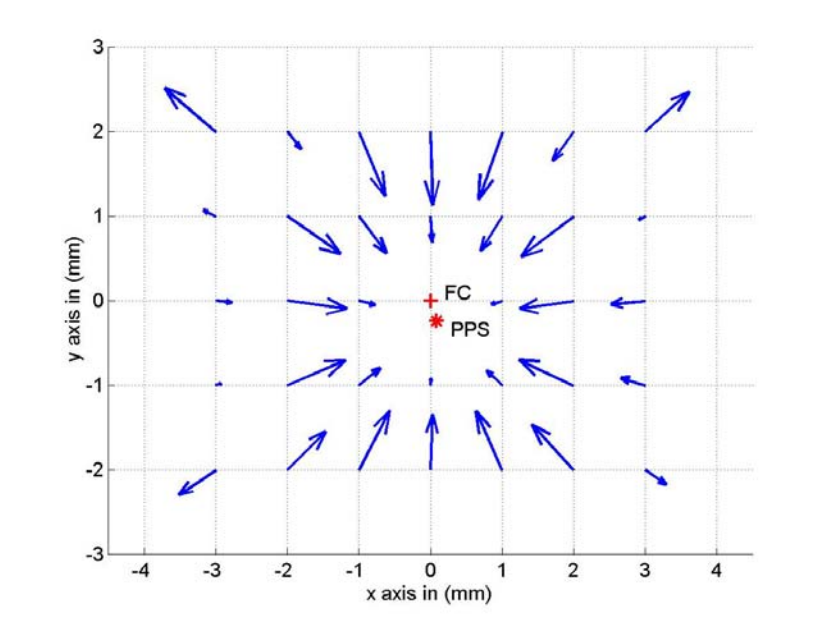

. Scaled RD centered at FC for the Blue camera

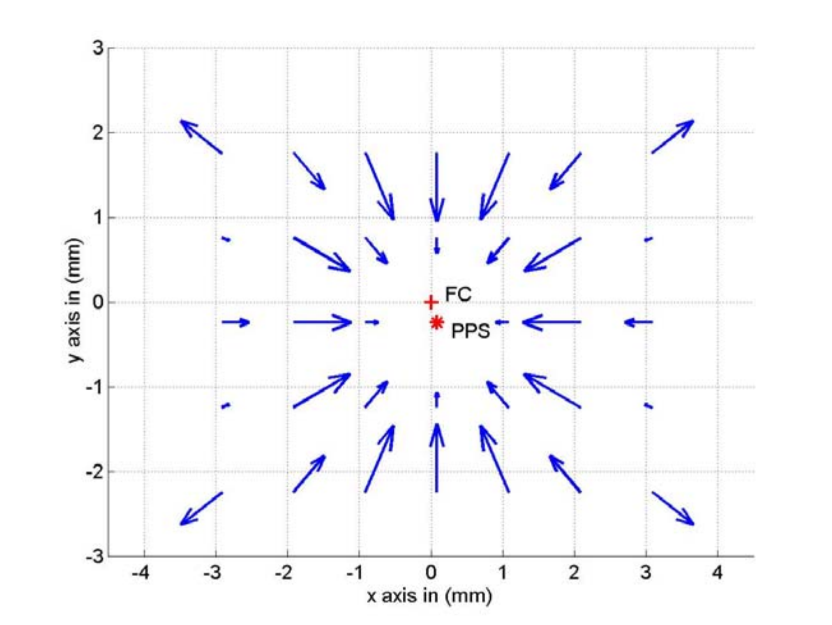

. Scaled RD centered at PPS for the Blue camera

FC: fiducial center.

PPS: principal point of best symmetry.

5) Distortion Analysis cont’d

5.2) Decentering Distortion (DD)

- The misalignment between lens components will lead to systematic image displacement errors which is called Decentering Distortion.

$$\delta_x = p_1[r^2 + 2(x - x_o)^2] + 2p_2(x - x_o)(y - y_o)$$

$$\delta_y = p_2[r^2 + 2(y - y_o)^2] + 2p_1(x - x_o)(y - y_o)$$

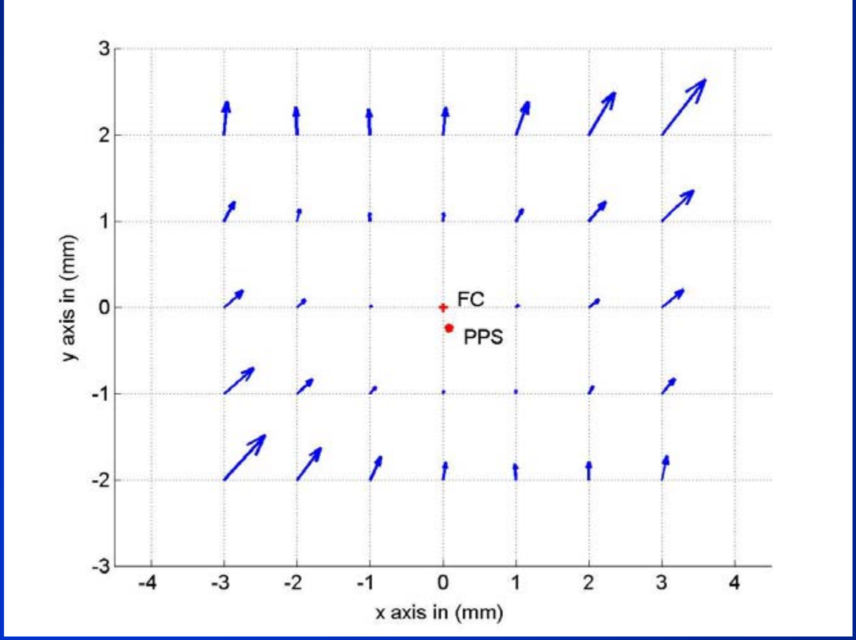

. Scaled DD centered at PPS for the Blue camera

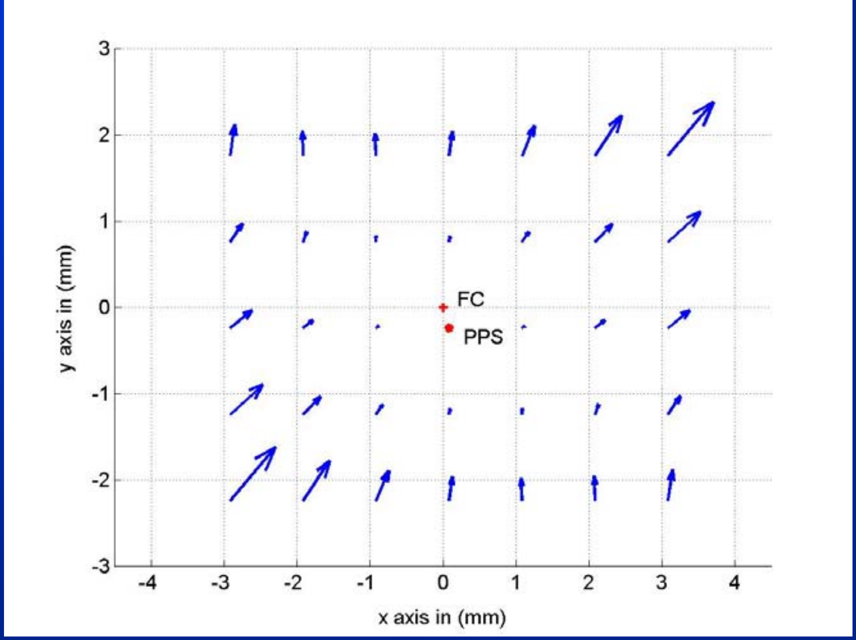

. Scaled DD centered at FC for the Blue camera

6) Results and Discussion

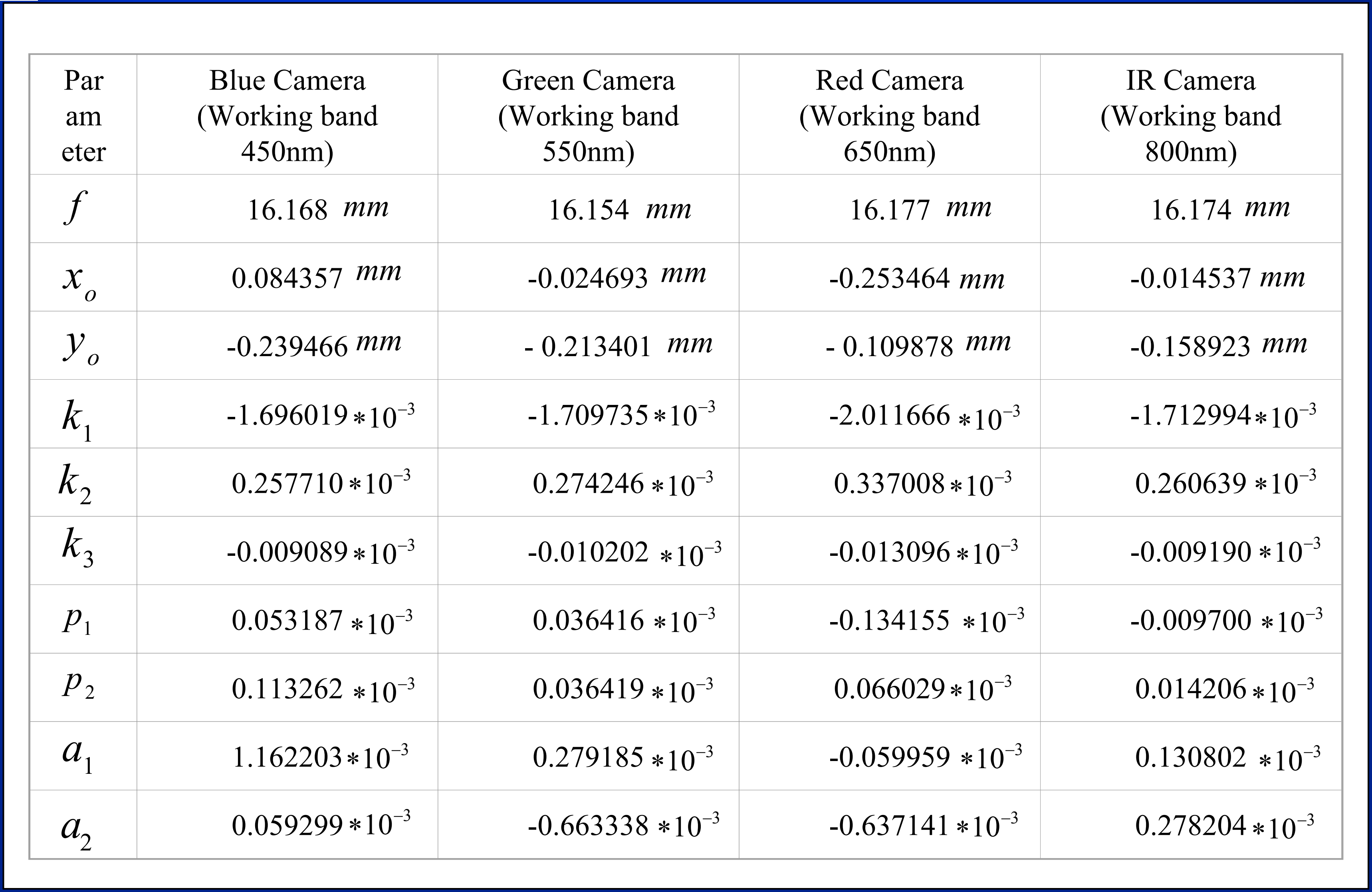

Par am eter	Blue Camera (Working band 450nm)	Green Camera (Working band 550nm)	Red Camera (Working band 650nm)	IR Camera (Working band 800nm)
f	16.168 mm	16.154 mm	16.177 mm	16.174 mm
x_o	0.084357 mm	-0.024693 mm	-0.253464 mm	-0.014537 mm
y_o	-0.239466 mm	- 0.213401 mm	- 0.109878 mm	-0.158923 mm
k_1	-1.696019 $*10^{-3}$	-1.709735 $*10^{-3}$	-2.011666 $*10^{-3}$	-1.712994 $*10^{-3}$
k_2	0.257710 $*10^{-3}$	0.274246 $*10^{-3}$	0.337008 $*10^{-3}$	0.260639 $*10^{-3}$
k_3	-0.009089 $*10^{-3}$	-0.010202 $*10^{-3}$	-0.013096 $*10^{-3}$	-0.009190 $*10^{-3}$
p_1	0.053187 $*10^{-3}$	0.036416 $*10^{-3}$	-0.134155 $*10^{-3}$	-0.009700 $*10^{-3}$
p_2	0.113262 $*10^{-3}$	0.036419 $*10^{-3}$	0.066029 $*10^{-3}$	0.014206 $*10^{-3}$
a_1	1.162203 $*10^{-3}$	0.279185 $*10^{-3}$	-0.059959 $*10^{-3}$	0.130802 $*10^{-3}$
a_2	0.059299 $*10^{-3}$	-0.663338 $*10^{-3}$	-0.637141 $*10^{-3}$	0.278204 $*10^{-3}$

Estimated parameters of the four sensors.

6) Results and discussion cont’d

- For simplicity, the graphical user interface feature in MATLAB was used to create a small user-friendly program to show the results and compute refined image coordinates on a single point basis.

- The parameters of each camera were stored in the file and by inserting the value of the measured line and sample and specifying the corresponding camera, the corrected line and sample will be calculated and printed in the window for the user.

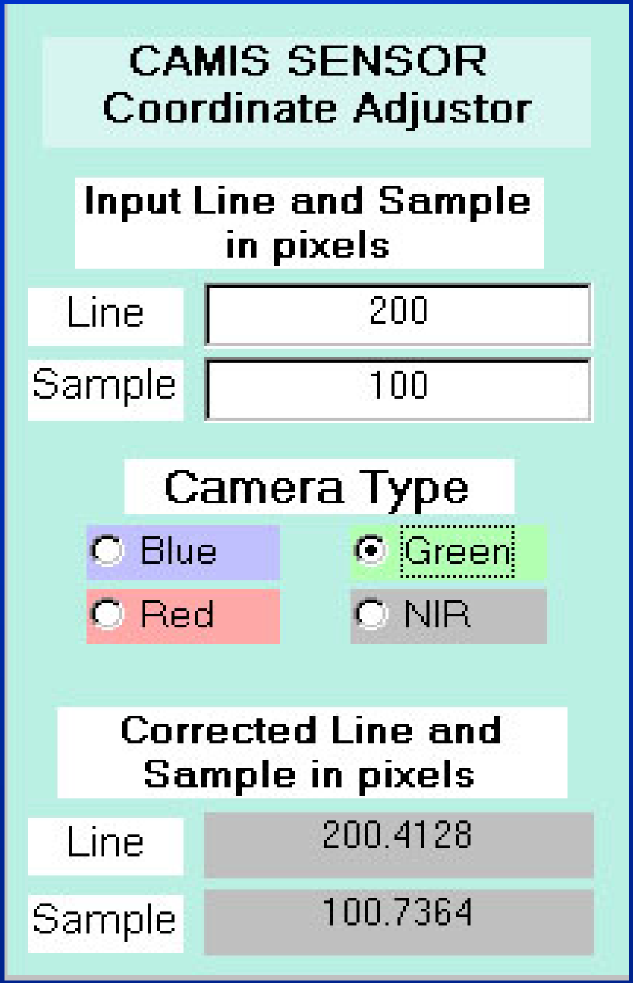

CAMIS SENSOR
Coordinate Adjustor

Input Line and Sample in pixels

Line	200
Sample	100

Camera Type

○ Blue ● Green
○ Red ○ NIR

Corrected Line and Sample in pixels

Line	200.4128
Sample	100.7364

Large Blocks May Require Robust Estimation

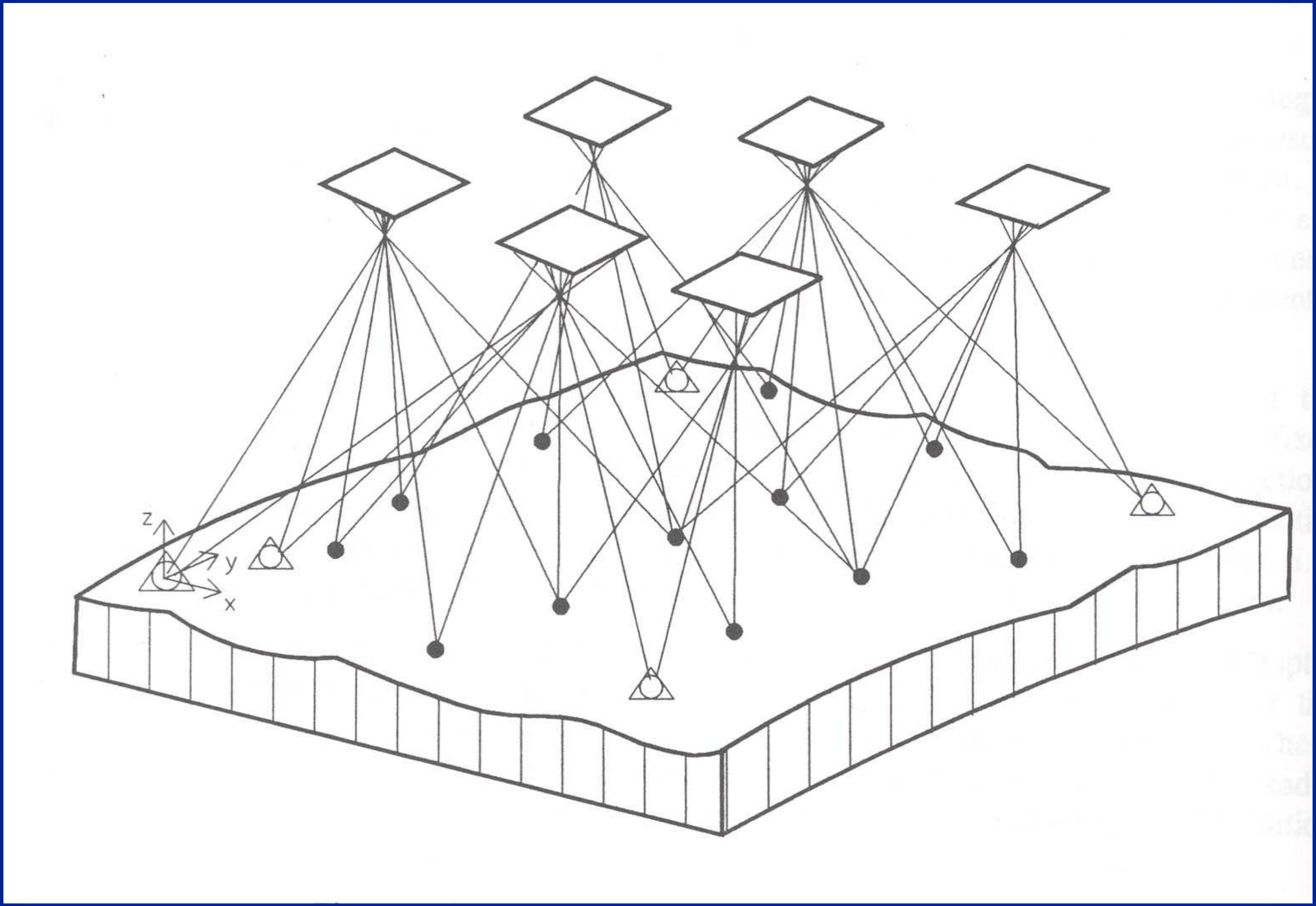

Possible Techniques: Data Snooping, IRLS,L1,LMS,L-M

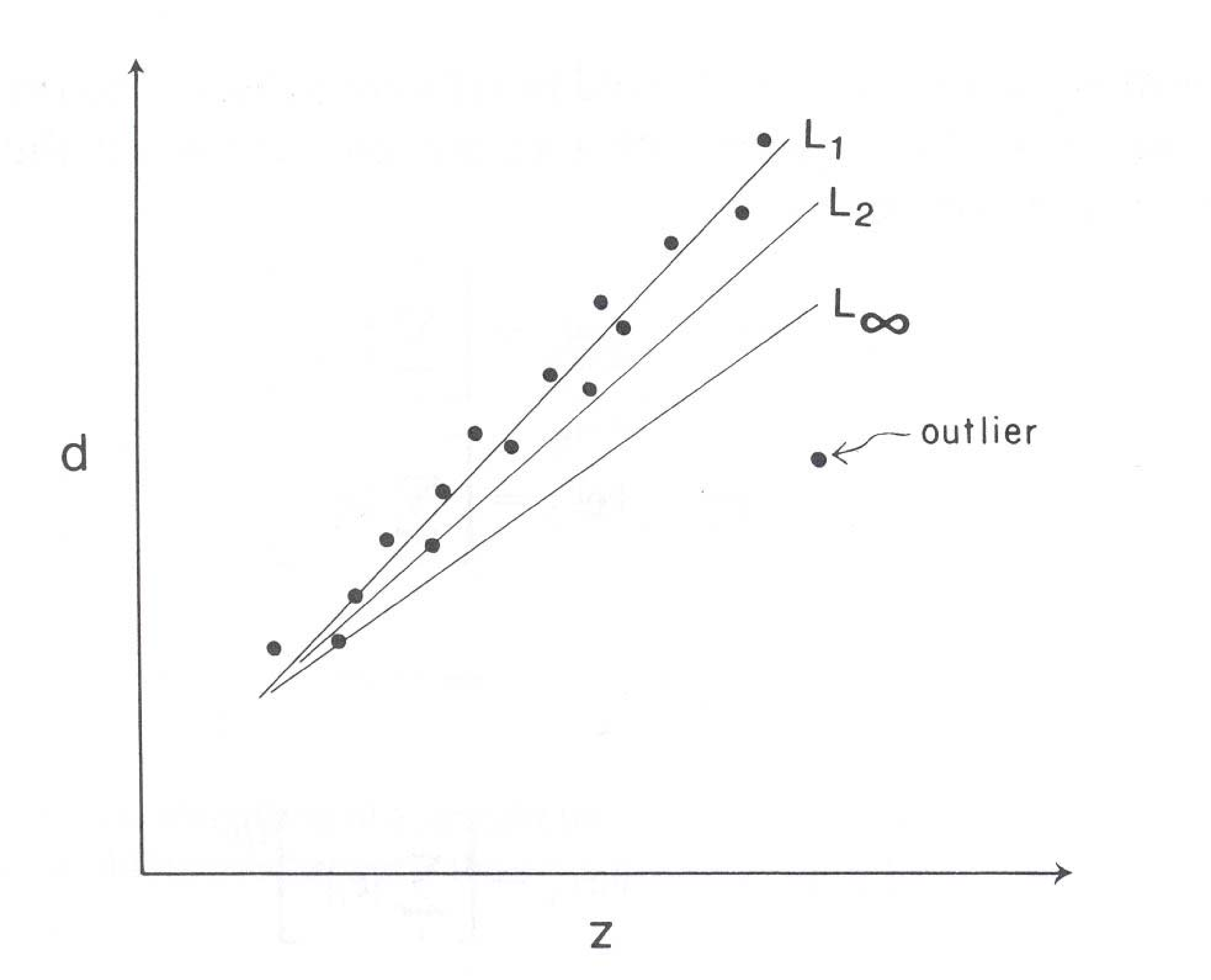

Blocks Often Have Regular Structure of Normal Equations

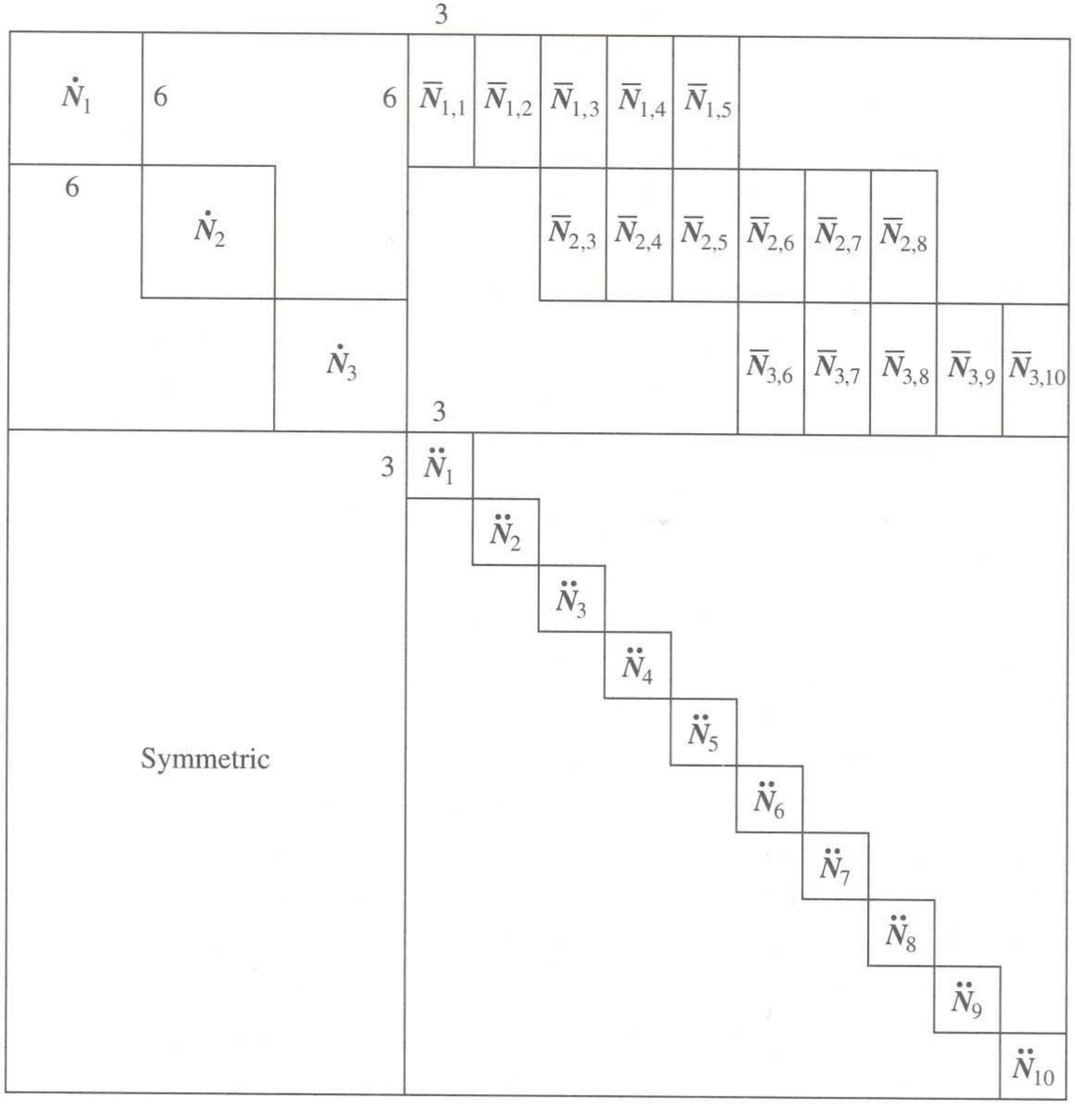

Figure 5-14 Unreduced normal equation structure.

Parameter Ordering with Regular Blocks Creates Sparse Matrix

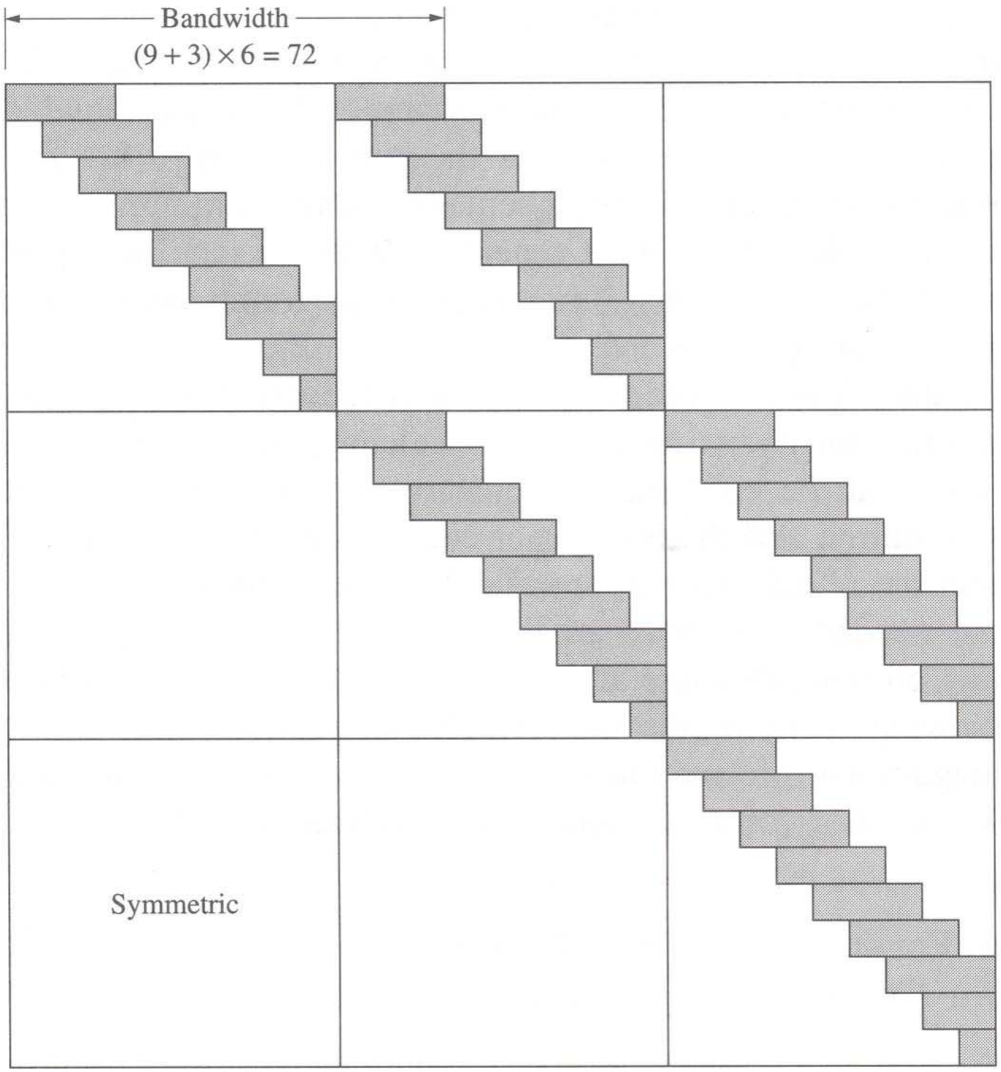

Figure 5-16 Reduced normal equations using down-strip numbering, with three flightlines and nine photos/strip.

The interesting contributions of this research

- We tried during this work to automate the calibration process as much as possible.
- The setup and measurements of the targets and the cameras.
- The automation of the target locations in the images, and their subsequent refinement.
- The automatic process for balancing the radial lens distortion in the presence of other correlated parameters.

- ## ACKNOWLEDGEMENT
- We would like to acknowledge the support of the Army Research Office and the Topographic Engineering Center.

Blunder Detection in Aerial Triangulation

Three algorithms were tested for the purpose of detecting and locating blunders in the triangulation of conventional, frame aerial photographs. It is believed that results from this limited testing will actually apply to a much wider selection of camera and sensor models. A MATLAB coding of the collinearity based bundle block algorithm was produced with a graphical user interface (GUI) for ease of running and evaluating. The data selected for the testing was a block of two images from a larger clock of about 30 images taken over the Purdue University campus. The scale is nominally 1:4000, the two photos selected 1-7 and 1-9 were a 60% overlap pair. The block actually contained 80% forward overlap imagery but the intervening image(1-8) was omitted to reflect the more common collection geometry.

The photos are shown below.

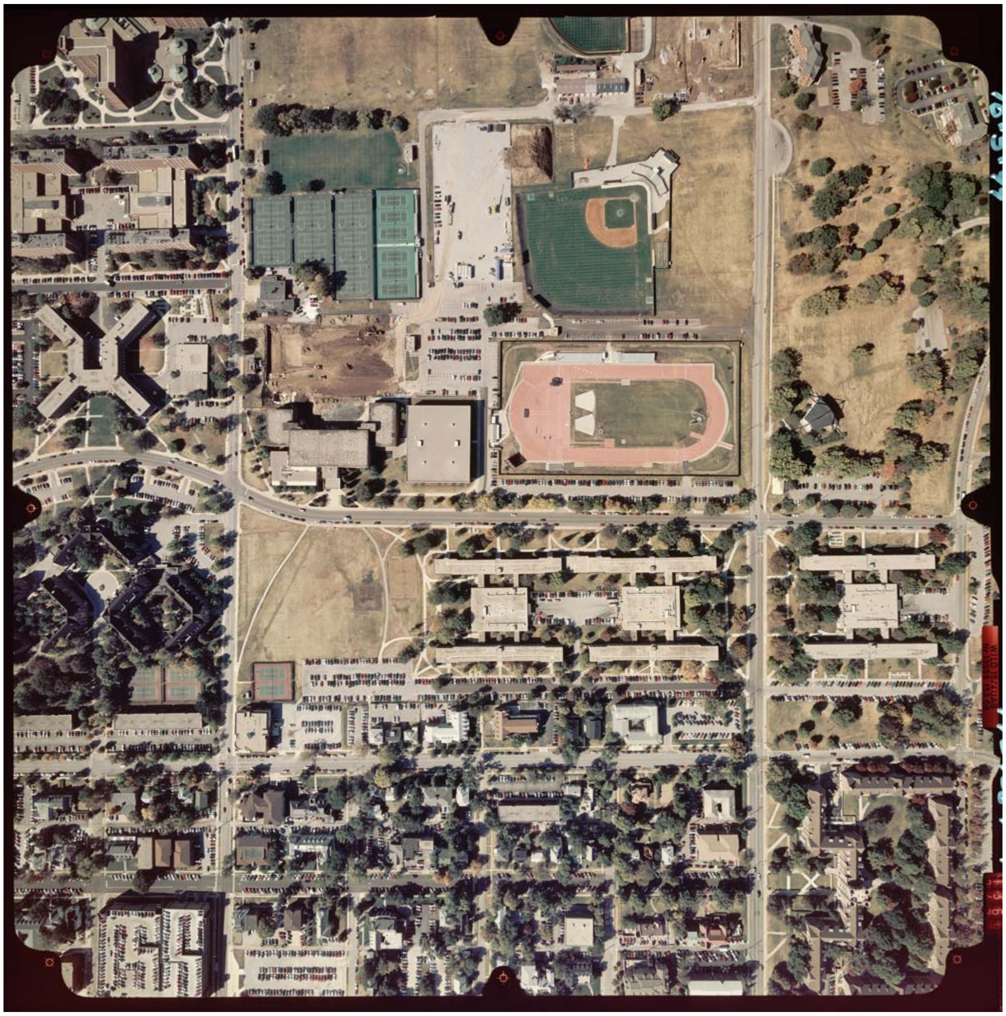

Figure 1 Left Photo 1-7

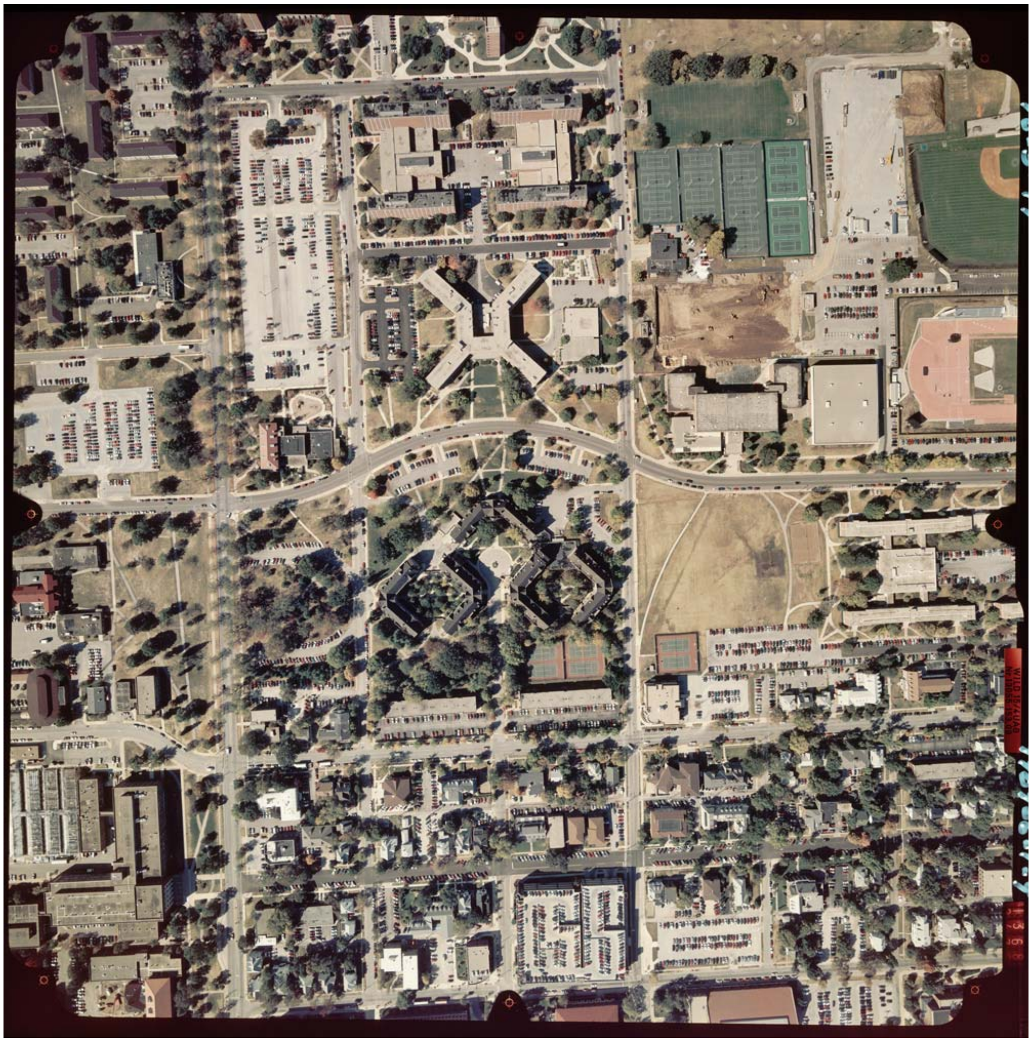

Figure 2. Right Photo 1-9

50 points have been read, distributed over the stereo model, including 3 ground control points. Errors have been artificially inserted into 3 of the observations to evaluate the three different adjustment algorithms. (1) L2 norm minimization (least squares) converges and it is clear that errors are present, but it is difficult to locate them because the effects are spread around neighboring points. (2) likewise IRLS (iteratively reweighted least squares) works well, but the weight function for adjusting the weights at each iteration seems disturbingly dependent on the particular application. (3) L1 norm minimization appears to work the best. As one can see from the numerical results and the graphical depiction of the residual vectors, all of the error is correctly placed into the 3 observations where it originally occurred. They were all y-errors since, in a 2 model block, x-errors are not detectable.

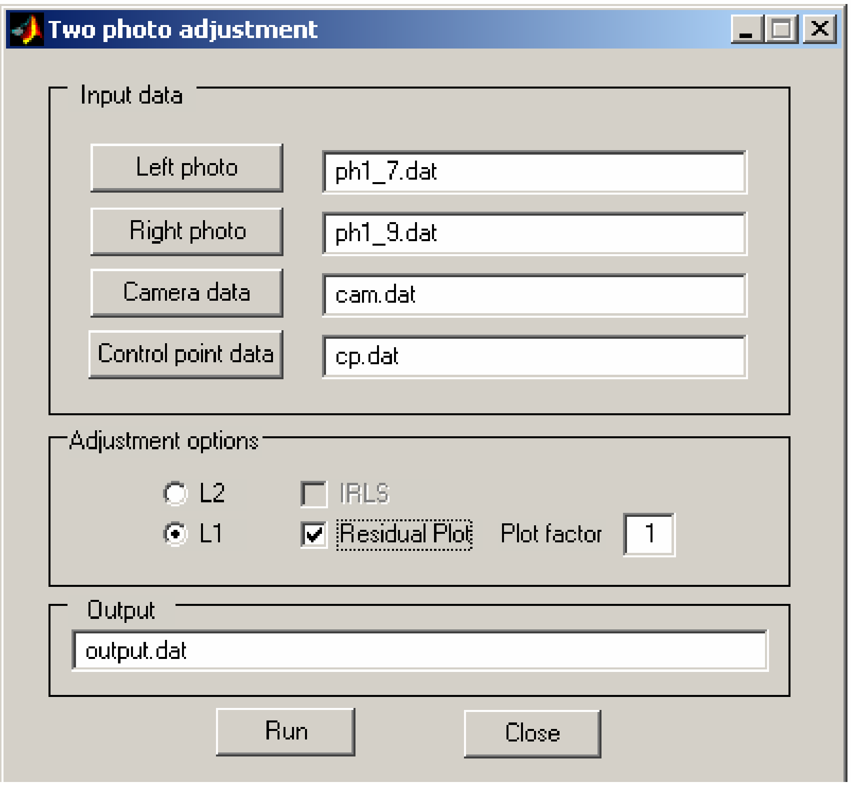

Input data

Left photo: ph1_7.dat

Right photo: ph1_9.dat

Camera data: cam.dat

Control point data: cp.dat

Adjustment options

○ L2 □ IRLS

● L1 ☑ Residual Plot Plot factor 1

Output

output.dat

Figure 3. GUI Program with selections for L1

The output listing showing the 5 iterations and the final residuals follows.

```
Number of control points: 3
Number of total parameters: 162
Number of adjusted parameters:155
Number of equations: 200
Number of fixed parameters: 7
Redundancy: 45

begin iterations

***************************************************
iter =
     1
Optimization terminated successfully.
parameter corrections
pc =
   -0.0085   -0.0024   -0.0009   -3.9883    5.0264   -1.3021
    0.0374   -0.0366   -0.0509   -2.7118    4.8994    1.6004
dspv =
    1.0000    0.0000    0.4914    0.0000   -0.0000
    2.0000    0.0000    0.7580    0.0000   -0.0000
    3.0000    0.0000    0.1657    0.0000   -0.0000
  101.0000    0.0000   30.6690    0.0000   -0.0000
  102.0000    0.0000   -0.0072    0.0000   -0.0000
  103.0000    0.0000    0.0122    0.0000   -0.0000
  104.0000    0.0000   -0.0000    0.0000   -0.0000
  105.0000    0.0000   30.1345    0.0000   -0.0000
  106.0000    0.0000   -0.0464    0.0000   -0.0000
  107.0000    0.0000   -0.0245    0.0000   -0.0000
  108.0000    0.0000   -0.0099    0.0000   -0.0000
  109.0000    0.0000    0.0380    0.0000   -0.0000
  110.0000    0.0000   -0.0376    0.0000   -0.0000
  111.0000    0.0000    0.0000    0.0000   -0.0000
  112.0000    0.0000    0.0256    0.0000   -0.0000
  113.0000    0.0000    0.0363    0.0000   -0.0000
  114.0000    0.0000   -0.0148    0.0000   -0.0000
  115.0000    0.0000   -0.0454    0.0000   -0.0000
  116.0000    0.0000   -0.0300    0.0000   -0.0000
  117.0000    0.0000   -0.0241    0.0000   -0.0000
  118.0000    0.0000    0.0552    0.0000   -0.0000
  119.0000    0.0000    0.0053    0.0000   -0.0000
  120.0000    0.0000   -0.0586    0.0000   -0.0000
  121.0000    0.0000   -0.0311   -0.0000   -0.0000
  122.0000    0.0000    0.0187   -0.0000   -0.0000
  123.0000    0.0000   -0.0146    0.0000   -0.0000
  124.0000    0.0000   -0.0268   -0.0000   -0.0000
  125.0000    0.0000   28.9544    0.0000   -0.0000
  201.0000    0.0000   -0.0153    0.0000   -0.0000
  202.0000    0.0000    0.0288    0.0000   -0.0000
  203.0000    0.0000    0.0107    0.0000   -0.0000
  204.0000    0.0000   -0.0205    0.0000   -0.0000
  205.0000    0.0000    0.0065    0.0000   -0.0000
  206.0000    0.0000   -0.0317    0.0000   -0.0000
  207.0000    0.0000    0.0256    0.0000   -0.0000
  208.0000    0.0000    0.0000   -0.0000   -0.0000
  209.0000    0.0000    0.0047   -0.0000   -0.0000
  210.0000    0.0000   -0.0016    0.0000   -0.0000
  211.0000    0.0000    0.0137    0.0000   -0.0000
  212.0000    0.0000   -0.0000    0.0000   -0.0000
  213.0000    0.0000   -0.0623    0.0000   -0.0000
  214.0000    0.0000    0.0182    0.0000   -0.0000
  215.0000    0.0000    0.0187   -0.0000   -0.0000
  218.0000    0.0000    0.0087    0.0000   -0.0000
  219.0000    0.0000   -0.0000    0.0000   -0.0000
  220.0000    0.0000   -0.0087    0.0000   -0.0000
  221.0000    0.0000   -0.0416    0.0000   -0.0000
  222.0000    0.0000   -0.0507    0.0000   -0.0000
  223.0000    0.0000   -0.0036    0.0000   -0.0000
  225.0000    0.0000   -0.0388    0.0000   -0.0000

***************************************************
iter =
     2
Optimization terminated successfully.
parameter corrections
pc =
    0.0080    0.0018    0.0010    3.5852   -4.7558    1.3144
    0.0063   -0.0002    0.0022    2.7585   -4.5207   -1.2844
dspv =
    1.0000   -0.0000    0.0000   -0.0000   -0.0000
    2.0000   -0.0000    0.0000   -0.0000   -0.0099
    3.0000   -0.0000   -0.0000    0.0000   -0.0000
  101.0000   -0.0000   29.9364   -0.0000   -0.0000
  102.0000   -0.0000   -0.0185   -0.0000   -0.0000
  103.0000   -0.0000    0.0060   -0.0000   -0.0000
  104.0000   -0.0000    0.0017   -0.0000   -0.0000
  105.0000   -0.0000   29.9776   -0.0000   -0.0000
  106.0000   -0.0000   -0.0451   -0.0000   -0.0000
  107.0000   -0.0000   -0.0061   -0.0000   -0.0000
  108.0000   -0.0000   -0.0086   -0.0000   -0.0000
  109.0000   -0.0000    0.0390   -0.0000   -0.0000
  110.0000   -0.0000    0.0000   -0.0000    0.0138
  111.0000   -0.0000    0.0105   -0.0000   -0.0000
  112.0000   -0.0000    0.0000   -0.0000   -0.0280
  113.0000   -0.0000    0.0000   -0.0000   -0.0362
  114.0000   -0.0000    0.0000   -0.0000    0.0057
  115.0000   -0.0000    0.0000   -0.0000    0.0161
  116.0000   -0.0000   -0.0000   -0.0000    0.0207
  117.0000   -0.0000   -0.0000   -0.0000    0.0262
  118.0000    0.0000    0.0000   -0.0000   -0.0538
  119.0000   -0.0000    0.0000    0.0000   -0.0058
  120.0000   -0.0000    0.0000   -0.0000    0.0359
  121.0000   -0.0000   -0.0000   -0.0000    0.0313
  122.0000   -0.0000    0.0000   -0.0000   -0.0000
  123.0000   -0.0000    0.0000   -0.0000    0.0275
  124.0000   -0.0000    0.0000   -0.0000    0.0109
  125.0000   -0.0000    0.0000   -0.0000  -28.4591
  201.0000   -0.0000   -0.0267   -0.0000   -0.0000
  202.0000   -0.0000    0.0342   -0.0000   -0.0000
  203.0000   -0.0000    0.0041   -0.0000   -0.0000
  204.0000   -0.0000   -0.0091   -0.0000   -0.0000
  205.0000   -0.0000    0.0035   -0.0000   -0.0000
  206.0000   -0.0000   -0.0304   -0.0000   -0.0000
  207.0000    0.0000    0.0358   -0.0000   -0.0000
  208.0000   -0.0000    0.0000   -0.0000   -0.0000
  209.0000   -0.0000   -0.0000   -0.0000    0.0103
  210.0000   -0.0000    0.0000   -0.0000    0.0187
  211.0000   -0.0000    0.0000   -0.0000   -0.0050
  212.0000   -0.0000    0.0000   -0.0000   -0.0055
  213.0000   -0.0000    0.0000   -0.0000    0.0447
  214.0000   -0.0000    0.0000   -0.0000   -0.0179
  215.0000    0.0000    0.0000   -0.0000   -0.0190
  218.0000   -0.0000    0.0000   -0.0000   -0.0000
  219.0000   -0.0000    0.0000   -0.0000   -0.0284
  220.0000   -0.0000   -0.0032   -0.0000   -0.0000
  221.0000   -0.0000   -0.0000   -0.0000    0.0150
  222.0000    0.0000   -0.0561   -0.0000   -0.0000
  223.0000   -0.0000   -0.0032   -0.0000   -0.0000
  225.0000   -0.0000    0.0000   -0.0000    0.0343

***************************************************
iter =
     3
Optimization terminated successfully.
parameter corrections
pc =
   -0.0001   -0.0000   -0.0000   -0.0108    0.0651   -0.0398
    0.0000   -0.0001   -0.0000   -0.0712   -0.0450    0.0085
dspv =
    1.0000    0.0000   -0.0007    0.0000    0.0000
    2.0000   -0.0000    0.0000   -0.0000   -0.0164
    3.0000    0.0000    0.0000    0.0000    0.0000
  101.0000    0.0000   29.9454    0.0000    0.0000
  102.0000    0.0000   -0.0128    0.0000    0.0000
  103.0000    0.0000    0.0113    0.0000    0.0000
  104.0000    0.0000    0.0036    0.0000    0.0000
  105.0000    0.0000   29.9858    0.0000    0.0000
  106.0000    0.0000   -0.0427    0.0000    0.0000
  107.0000    0.0000   -0.0067    0.0000    0.0000
  108.0000    0.0000   -0.0084    0.0000    0.0000
  109.0000    0.0000    0.0400    0.0000    0.0000
  110.0000    0.0000   -0.0000    0.0000    0.0112
  111.0000    0.0000    0.0091    0.0000    0.0000
  112.0000   -0.0000    0.0000   -0.0000   -0.0276
  113.0000   -0.0000    0.0000   -0.0000   -0.0375
  114.0000   -0.0000    0.0000    0.0000    0.0019
  115.0000   -0.0000    0.0000    0.0000    0.0098
  116.0000   -0.0000    0.0000    0.0000    0.0224
  117.0000   -0.0000    0.0000   -0.0000    0.0249
  118.0000   -0.0000    0.0000   -0.0000   -0.0563
  119.0000   -0.0000    0.0000   -0.0000   -0.0101
  120.0000   -0.0000    0.0000   -0.0000    0.0275
  121.0000   -0.0000    0.0000   -0.0000    0.0312
  122.0000   -0.0000    0.0000   -0.0000   -0.0061
  123.0000   -0.0000    0.0000   -0.0000    0.0181
  124.0000   -0.0000    0.0000   -0.0000    0.0000
  125.0000   -0.0000    0.0000    0.0000  -28.6231
  201.0000    0.0000   -0.0199    0.0000    0.0000
  202.0000    0.0000    0.0381    0.0000    0.0000
  203.0000    0.0000    0.0066    0.0000    0.0000
  204.0000    0.0000   -0.0081    0.0000    0.0000
  205.0000    0.0000    0.0040    0.0000    0.0000
  206.0000    0.0000   -0.0319    0.0000    0.0000
  207.0000    0.0000    0.0000   -0.0000   -0.0333
  208.0000   -0.0000    0.0000   -0.0000    0.0000
  209.0000   -0.0000    0.0000   -0.0000    0.0083
  210.0000   -0.0000    0.0000   -0.0000    0.0154
  211.0000   -0.0000    0.0000   -0.0000   -0.0140
  212.0000   -0.0000    0.0000   -0.0000   -0.0204
  213.0000   -0.0000    0.0000   -0.0000    0.0357
  214.0000   -0.0000    0.0000   -0.0000   -0.0189
  215.0000   -0.0000    0.0000   -0.0000   -0.0201
  218.0000    0.0000    0.0000    0.0000    0.0000
  219.0000    0.0000    0.0000    0.0000   -0.0316
  220.0000    0.0000   -0.0017    0.0000    0.0000
  221.0000    0.0000   -0.0000    0.0000    0.0122
  222.0000    0.0000   -0.0515    0.0000    0.0000
  223.0000    0.0000    0.0000    0.0000    0.0000
  225.0000   -0.0000    0.0000   -0.0000    0.0261

***************************************************
iter =
     4
Optimization terminated successfully.
parameter corrections
pc =
  1.0e-004 *

   -0.0004    0.0002   -0.0001    0.2307    0.1752   -0.2362
    0.0001    0.0002    0.0001    0.1171   -0.0445   -0.1519
dspv =
    1.0000    0.0000   -0.0007    0.0000    0.0000
    2.0000   -0.0000   -0.0000    0.0000   -0.0164
    3.0000    0.0000   -0.0000    0.0000   -0.0000
  101.0000    0.0000   29.9454    0.0000   -0.0000
  102.0000    0.0000   -0.0128    0.0000   -0.0000
  103.0000    0.0000    0.0113    0.0000    0.0000
  104.0000    0.0000    0.0036    0.0000    0.0000
  105.0000    0.0000   29.9858    0.0000    0.0000
  106.0000    0.0000   -0.0427    0.0000   -0.0000
  107.0000    0.0000   -0.0067    0.0000   -0.0000
  108.0000    0.0000   -0.0084    0.0000    0.0000
  109.0000    0.0000    0.0400    0.0000   -0.0000
  110.0000    0.0000   -0.0000    0.0000    0.0112
  111.0000   -0.0000    0.0091    0.0000   -0.0000
  112.0000   -0.0000    0.0000    0.0000   -0.0276
  113.0000   -0.0000    0.0000    0.0000   -0.0375
  114.0000   -0.0000   -0.0000    0.0000    0.0019
  115.0000   -0.0000   -0.0000    0.0000    0.0098
  116.0000   -0.0000   -0.0000    0.0000    0.0224
  117.0000   -0.0000   -0.0000    0.0000    0.0249
  118.0000   -0.0000    0.0000    0.0000   -0.0563
  119.0000   -0.0000    0.0000    0.0000   -0.0101
  120.0000   -0.0000   -0.0000    0.0000    0.0275
  121.0000   -0.0000   -0.0000    0.0000    0.0312
  122.0000   -0.0000   -0.0000    0.0000   -0.0061
  123.0000   -0.0000   -0.0000    0.0000    0.0181
  124.0000   -0.0000   -0.0000    0.0000    0.0000

  125.0000   -0.0000   -0.0000    0.0000  -28.6231
  201.0000    0.0000   -0.0199   -0.0000   -0.0000
  202.0000    0.0000    0.0381    0.0000   -0.0000
  203.0000    0.0000    0.0066    0.0000   -0.0000
  204.0000    0.0000   -0.0081    0.0000   -0.0000
  205.0000    0.0000    0.0040    0.0000   -0.0000
  206.0000    0.0000   -0.0319    0.0000   -0.0000
  207.0000   -0.0000    0.0000    0.0000   -0.0333
  208.0000   -0.0000   -0.0000    0.0000   -0.0000
  209.0000   -0.0000   -0.0000    0.0000    0.0082
  210.0000   -0.0000    0.0000    0.0000    0.0154
  211.0000   -0.0000   -0.0000    0.0000   -0.0140
  212.0000   -0.0000   -0.0000    0.0000   -0.0204
  213.0000   -0.0000   -0.0000    0.0000    0.0357
  214.0000   -0.0000   -0.0000    0.0000   -0.0189
  215.0000   -0.0000   -0.0000    0.0000   -0.0201
  218.0000    0.0000   -0.0000    0.0000    0.0000
  219.0000    0.0000   -0.0000    0.0000   -0.0315
  220.0000    0.0000   -0.0017    0.0000    0.0000
  221.0000    0.0000   -0.0000    0.0000    0.0122
  222.0000    0.0000   -0.0515    0.0000    0.0000
  223.0000    0.0000   -0.0000    0.0000    0.0000
  225.0000   -0.0000   -0.0000    0.0000    0.0261
```

```
we have converged

residuals
point-id  vx-l  vy-l  vx-r  vy-r
#    1   0.00000   -0.00070    0.00000    0.00000
#    2  -0.00000   -0.00000    0.00000   -0.01644
#    3   0.00000   -0.00000    0.00000   -0.00000
#  101   0.00000   29.94538    0.00000   -0.00000
#  102   0.00000   -0.01281    0.00000   -0.00000
#  103   0.00000    0.01127    0.00000    0.00000
#  104   0.00000    0.00361    0.00000    0.00000
#  105   0.00000   29.98575    0.00000    0.00000
#  106   0.00000   -0.04273    0.00000   -0.00000
#  107   0.00000   -0.00669    0.00000   -0.00000
#  108   0.00000   -0.00840    0.00000    0.00000
#  109   0.00000    0.04005    0.00000   -0.00000
#  110   0.00000   -0.00000    0.00000    0.01124
#  111  -0.00000    0.00914    0.00000   -0.00000
#  112  -0.00000    0.00000    0.00000   -0.02765
#  113  -0.00000    0.00000    0.00000   -0.03753
#  114  -0.00000   -0.00000    0.00000    0.00189
#  115  -0.00000   -0.00000    0.00000    0.00980
#  116  -0.00000   -0.00000    0.00000    0.02236
#  117  -0.00000   -0.00000    0.00000    0.02493
#  118  -0.00000    0.00000    0.00000   -0.05632
#  119  -0.00000    0.00000    0.00000   -0.01009
#  120  -0.00000   -0.00000    0.00000    0.02751
#  121  -0.00000   -0.00000    0.00000    0.03116
#  122  -0.00000   -0.00000    0.00000   -0.00609
#  123  -0.00000   -0.00000    0.00000    0.01809
#  124  -0.00000   -0.00000    0.00000    0.00000
#  125  -0.00000   -0.00000    0.00000  -28.62311
#  201   0.00000   -0.01987   -0.00000   -0.00000
#  202   0.00000    0.03806    0.00000   -0.00000
#  203   0.00000    0.00661    0.00000   -0.00000
#  204   0.00000   -0.00810    0.00000   -0.00000
#  205   0.00000    0.00398    0.00000   -0.00000
#  206   0.00000   -0.03191    0.00000   -0.00000
#  207  -0.00000    0.00000    0.00000   -0.03331
#  208  -0.00000   -0.00000    0.00000   -0.00000
#  209  -0.00000   -0.00000    0.00000    0.00825
#  210  -0.00000    0.00000    0.00000    0.01540
#  211  -0.00000   -0.00000    0.00000   -0.01396
#  212  -0.00000   -0.00000    0.00000   -0.02035
#  213  -0.00000   -0.00000    0.00000    0.03568
#  214  -0.00000   -0.00000    0.00000   -0.01888
#  215  -0.00000   -0.00000    0.00000   -0.02013
#  218   0.00000   -0.00000    0.00000    0.00000
#  219   0.00000   -0.00000    0.00000   -0.03155
#  220   0.00000   -0.00175    0.00000    0.00000
#  221   0.00000   -0.00000    0.00000    0.01222
#  222   0.00000   -0.05155    0.00000    0.00000
#  223   0.00000   -0.00000    0.00000    0.00000
#  225  -0.00000   -0.00000    0.00000    0.02608
left photo w,p,k  xl,yl,zl

omega_l =
       -0.0299735226753904
phi_l =
        0.0195274155794779
kappa_l =
          1.55932710861381
xl_l =
          913722.159060762
yl_l =
          575234.888671137
zl_l =
          758.679524164434
right photo w,p,k  xl,yl,zl

omega_r =
        0.0143402128413725
phi_r =
       -0.0167326674115072
kappa_r =
          1.51038139606387
xl_r =
          913729.425538108
yl_r =
          574874.372672258
zl_r =
          761.308438653024
object points x,y,z
    1   913565.589   575312.953      188.413
    2   913928.656   575198.483      189.867
    3   913421.163   574863.304      188.864
  101   913449.026   574846.372      188.528
  102   913440.177   574922.010      200.675
  103   913435.540   574965.220      189.324
  104   913518.165   575132.684      188.807
  105   913434.248   575308.938      188.547
  106   913562.052   574847.230      205.327
  107   913697.162   574825.802      191.221
  108   913676.814   574975.794      189.464
  109   913654.151   575150.062      202.171
  110   913613.517   575270.275      189.052
  111   913775.073   574879.419      190.584
  112   913868.727   574941.724      190.123
  113   913868.030   575021.060      190.213
  114   913854.092   575141.748      189.913
  115   913837.288   575260.592      199.936
  116   913942.714   574853.346      189.890
  117   913920.787   574981.803      190.062
  118   913921.631   575034.847      190.198
  119   913941.089   575081.310      189.899
  120   913940.164   575218.731      189.726
  121   914039.235   574865.686      188.286
  122   914108.997   574983.294      188.747
  123   914097.685   575078.001      189.460
  124   914022.784   575203.542      189.358
  125   913919.546   575295.806      195.643
  201   913408.619   574931.351      197.214
  202   913537.804   574813.597      202.504
  203   913537.157   574914.501      202.654
  204   913619.271   574814.277      202.756
  205   913618.728   574915.197      202.532
  206   913728.431   574874.684      208.342
  207   913885.559   574842.455      199.319
  208   914039.119   574865.807      188.294
  209   914049.479   574923.479      202.069
  210   914050.830   574958.793      201.987

  211   914075.889   575091.662      189.508
  212   914113.320   575200.907      189.548
  213   913963.994   575211.224      200.330
  214   913873.859   575002.922      190.056
  215   913847.850   575026.485      190.334
  218   913673.822   575036.970      206.215
  219   913644.580   575282.572      189.009
  220   913624.477   575192.311      201.137
  221   913616.112   575283.177      188.907
  222   913437.545   575004.464      188.946
  223   913433.740   575137.764      188.617
  225   913993.507   575155.644      200.014
```

As can be seen by the last residual listing, the three 30mm errors stand our clearly. These are also shown on the following graphical residual plot.

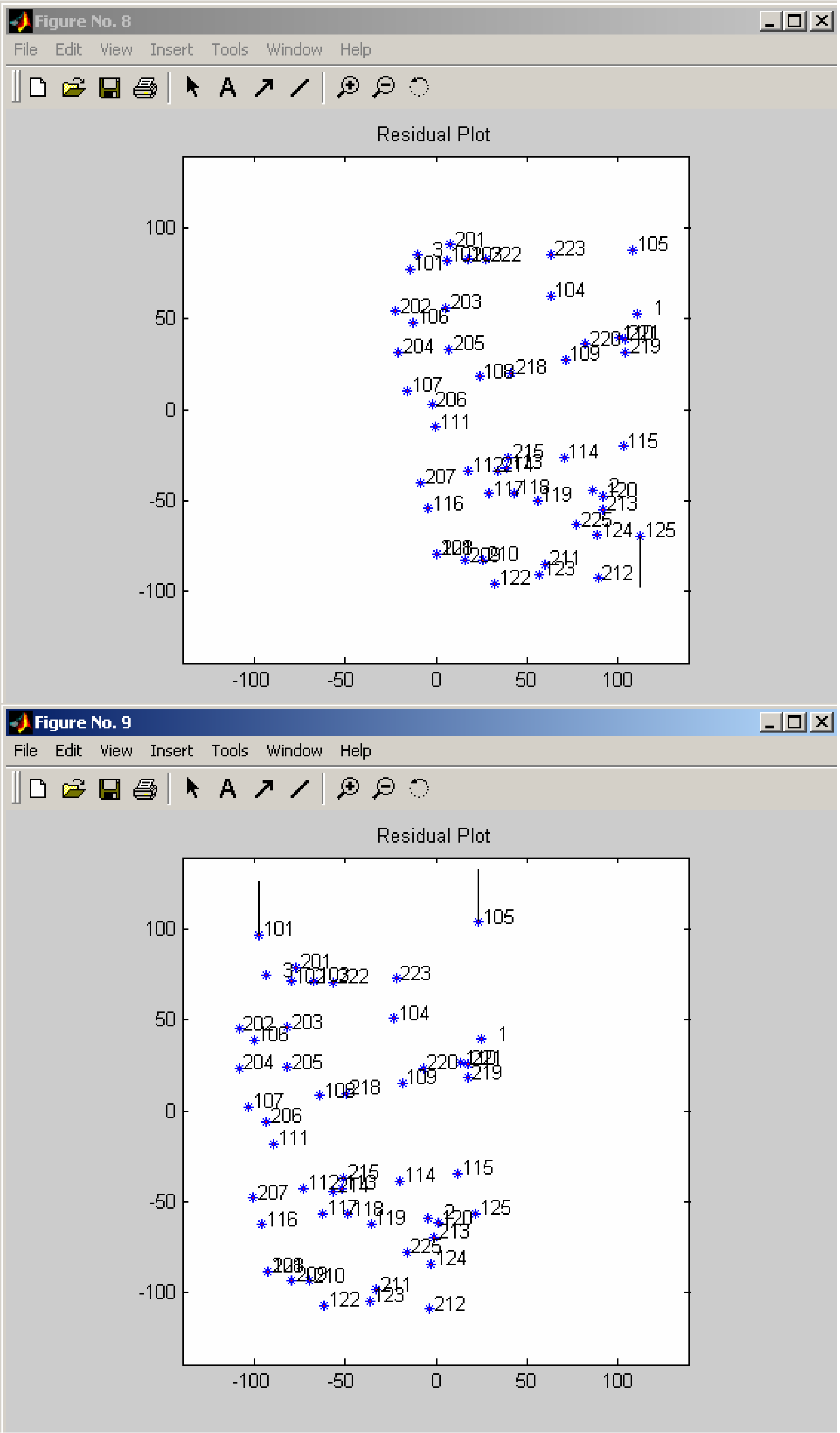

Figure 4. Residual Vectors with 3 Blunders Clearly Evident

Our conclusion from this exercise is that the L1 minimization procedure is a very powerful tool for blunder detection, when there is sufficient redundancy. It is slower than least squares by a factor of 10-20, but when looking for difficult to find blunders, that time can easily be accommodated versus, manual inspection or univariate data snooping.

BAE SYSTEMS

3D Visualization

Joseph Spann
BAE SYSTEMS
(858)592-5853

September 5, 2001

Photogrammetry Using 3-D Graphics and Projective Textures

Joseph R. Spann and Karen S. Kaufman

BAE SYSTEMS Mission Solutions

Oblique photograph of Boulder, Colorado

Aerial photograph of Boulder, Colorado

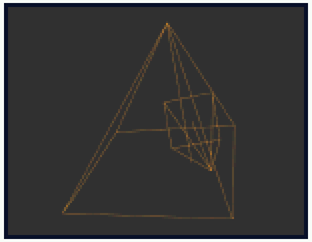

Sensor models

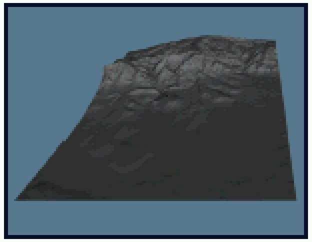

Terrain/feature model of Boulder, Colorado

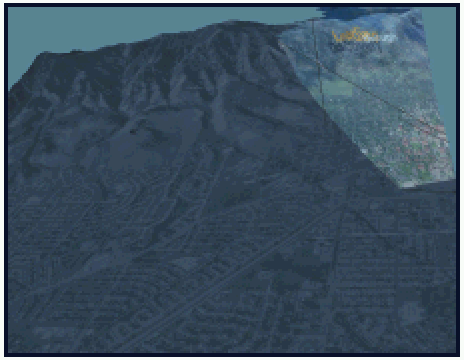

Multiple images simultaneously projected on terrain and features

Sensor projector combines rigorous photogrammetric camera models with 3-D virtual reality

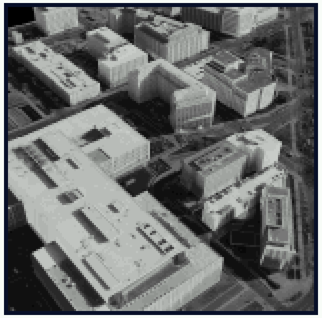

Imagery projected on terrain/feature models, Washington, D.C.

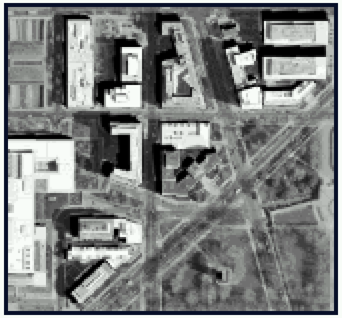

Orthographic view yields true orthographic projection

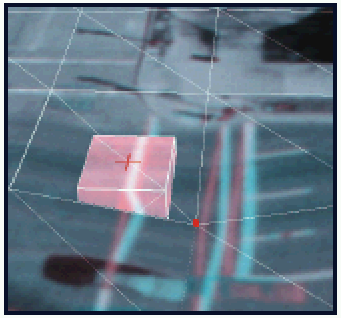

Movable projection surface enables photogrammetric measurements

3D Visualization Background

- VESPER image projection is implemented via a 4 x 4 projection matrix.
- For a frame camera, the projection matrix elements are derived from the frame camera parameters.
- For an orthographic projection, they are readily derived from the orthographic projection parameters.
- Complex sensor models cannot be converted into a single 4 x 4 projection matrix.
- VESPER is being extended to accurately project whole images from sensors other than frame or orthographic.

3D Visualization Objectives

- Expand the concept of sensor projectors to accurately project imagery collected by virtually any type of optical sensor (for instance, pushbroom, whiskbroom, PAN, SPOT, etc). This will increase the breadth of applications for which sensor projectors can be utilized.

- Extend the piecewise frame sensor projector to provide efficient means of storing, moving (internet), and projecting very large quantities of high-resolution imagery from all types of optical sensors.

3D Visualization Approach

- Piecewise frame sensor modeling. Any type of sensor projector will be approximated as a collection of one or more frame sensor projectors.
- Essentially all of the optical sensor types utilized in photogrammetry are represented in the BAE Systems library of sensor models.
- For each sensor type represented, the library has a function that for a given point in the image yields the ray along which light traveled to arrive at that point. This function is known as the imaging locus function.
- Over any sufficiently small section of an optical sensor's image, this function can be approximated as the imaging locus function of a frame sensor with a particular set of parameters.

Approach (continued)

- Develop methods that determine the number of sections into which an image must be divided so that a sufficiently accurate (better than one pixel) frame sensor representation can be determined for each section.
- The simultaneous projection of all the sections of the image, utilizing frame sensor models, will be the equivalent of projecting the entire image using its rigorous sensor model.
- Clipmapping - adapt cliptexture concepts for piecewise frame sensor modeling to run efficiently across computer networks.

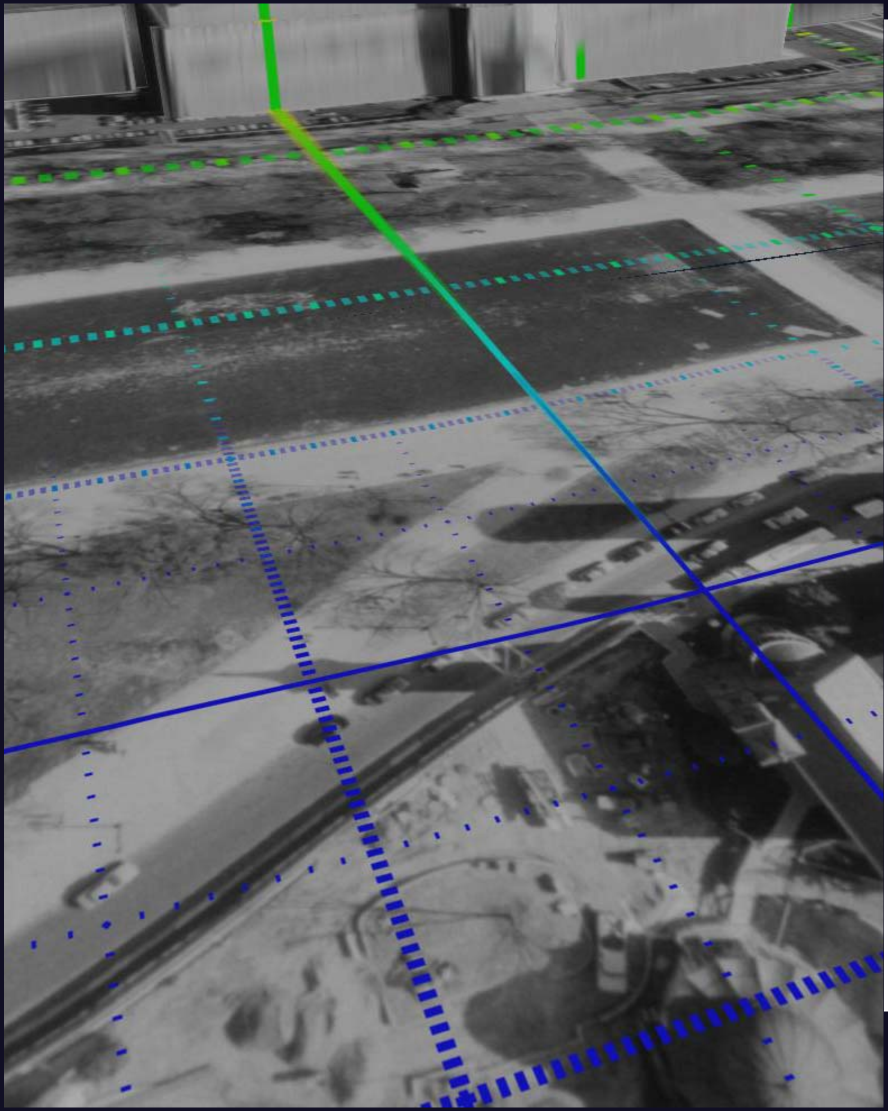

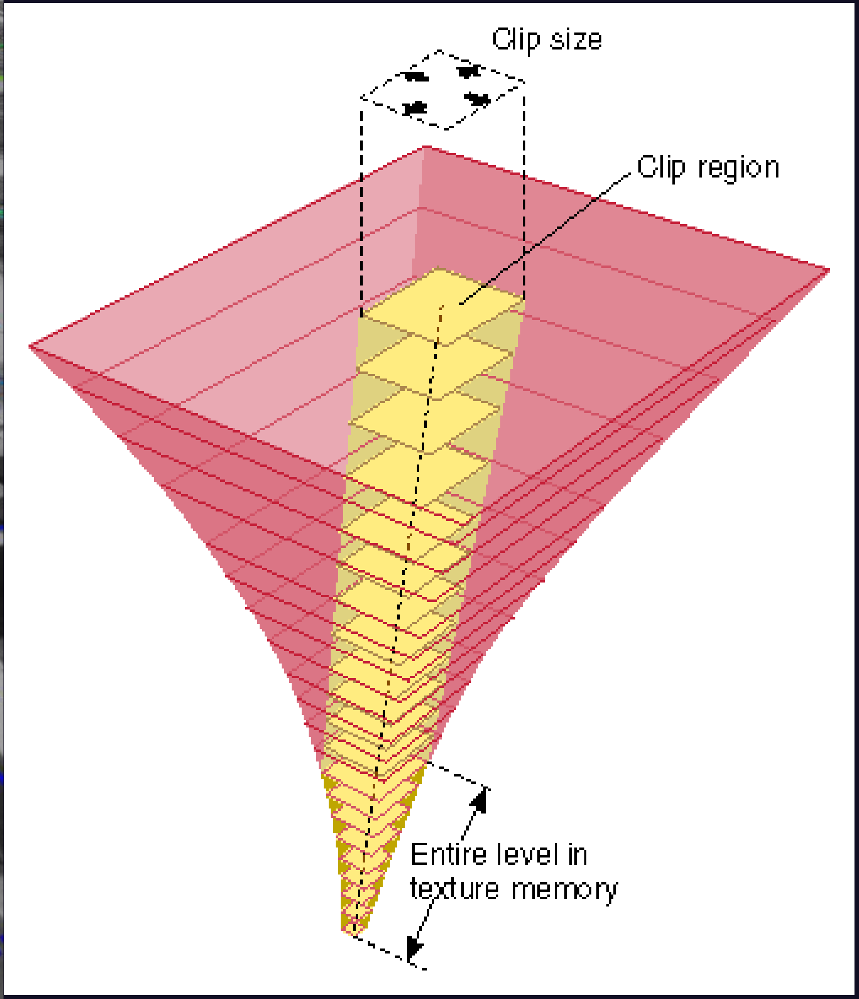
Clip size
Clip region
Entire level in
texture memory

Status

- Autoclip
- ProjectorSensorModelGroup::()
- Divided frame model
- ray() - piecewise frame function
- Classified VESPER lab established

Summary

- Foundation is in place for push to completion
- If IKONOS sensor model becomes available unclassified demonstrations will be possible

VESPER for the Battlespace (VFB)

Rapid and Affordable Sensor-to-Visualization

Joseph R. Spann
BAE SYSTEMS – Mission Solutions
San Diego CA (858) 592-5853
joseph.spann@baesystems.com

Photogrammetry Using 3-D Graphics and Projective Textures

Joseph R. Spann and Karen S. Kaufman

BAE SYSTEMS Mission Solutions

Oblique photograph of Boulder, Colorado

Aerial photograph of Boulder, Colorado

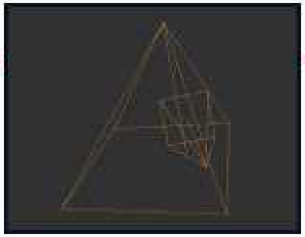

Sensor models

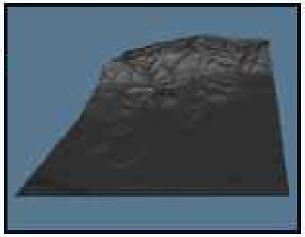

Terrain/feature model of Boulder, Colorado

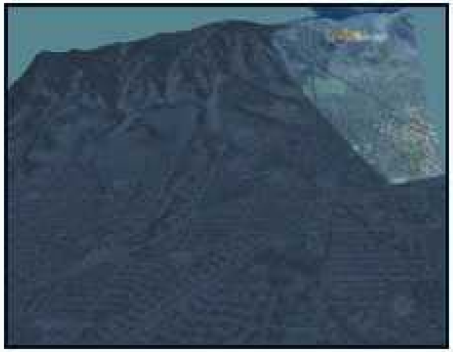

Multiple images simultaneously projected on terrain and features

Sensor projector combines rigorous photogrammetric camera models with 3-D virtual reality

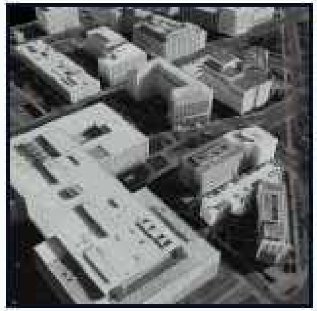

Imagery projected on terrain/feature models, Washington, D.C.

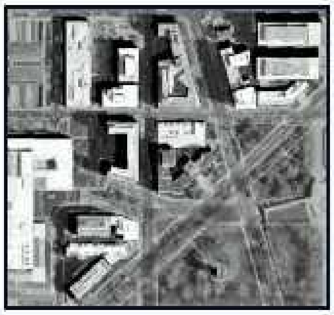

Orthographic view yields true orthographic projection

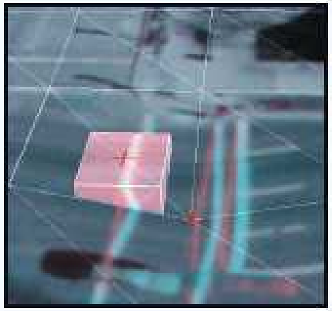

Movable projection surface enables photogrammetric measurements

BAE SYSTEMS

Military Impact

- The VFB will augment the COP to achieve a rapid and affordable "Sensor-to-Visualization" process for time-critical operations such as:
  - intelligence operations
  - mission planning and rehearsal
  - targeting initiatives
  - operational command and control
  - battle damage assessment

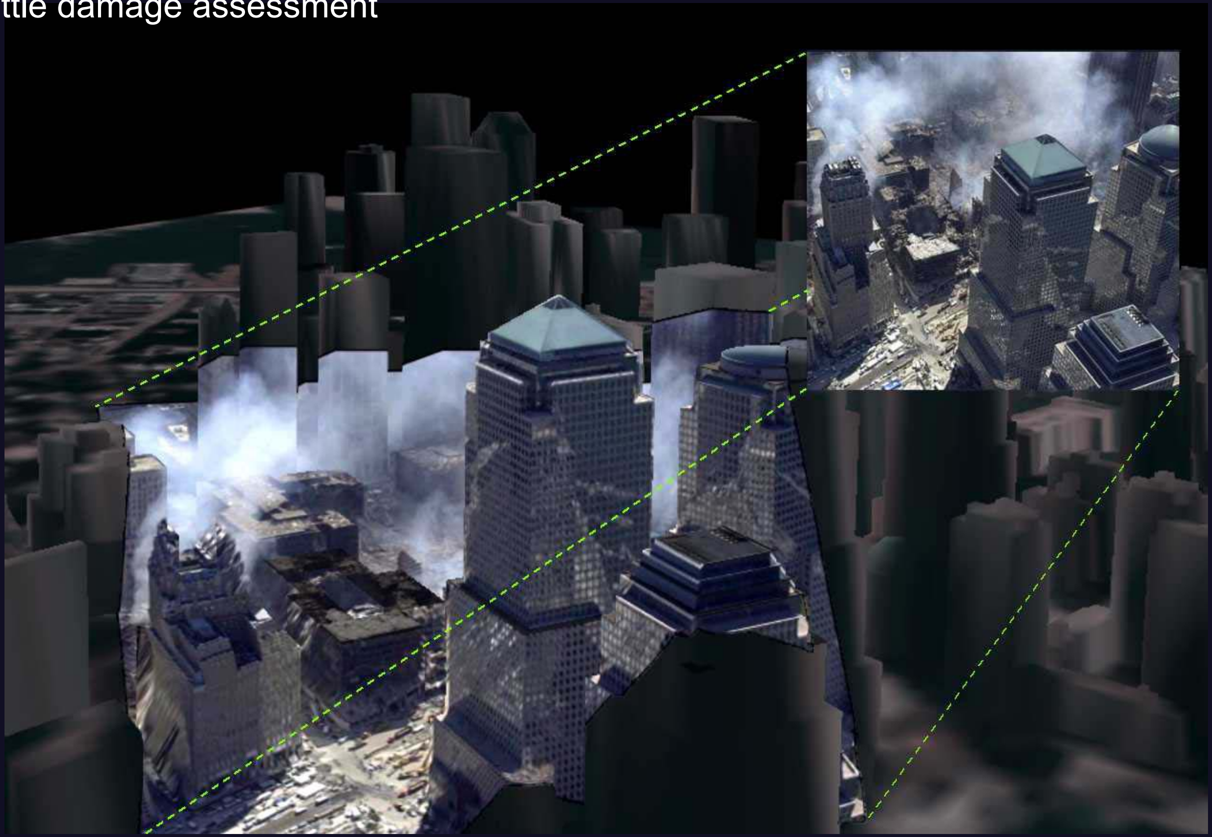

VFB Objectives

- Develop and demonstrate advanced sensor data fusion, 2-D and 3-D visualization capabilities to enhance the Joint Vision 2020 requirement of Dominant Battlespace Awareness.

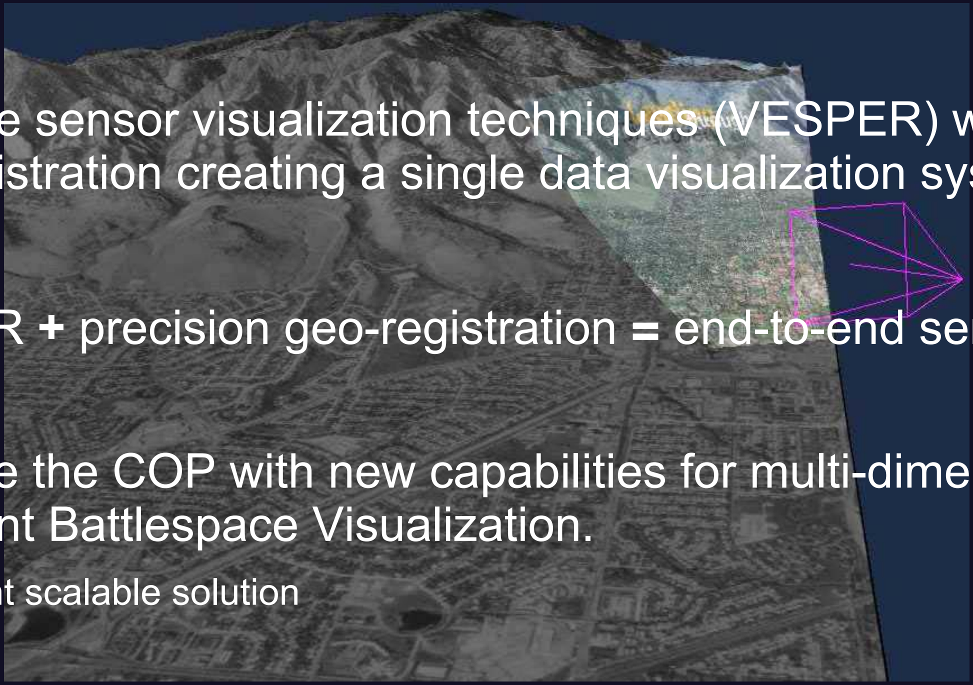

- Combine sensor visualization techniques (VESPER) with precise geo-registration creating a single data visualization system.

- VESPER **+** precision geo-registration **=** end-to-end sensor to visualization

- Enhance the COP with new capabilities for multi-dimensional Dominant Battlespace Visualization.
  - Efficient scalable solution

Provide an integrated "Sensor-to-Visualization" process for time-critical operations such as intelligence operations, mission planning and rehearsal, targeting initiatives, and operational command and control.

VFB Data Flow

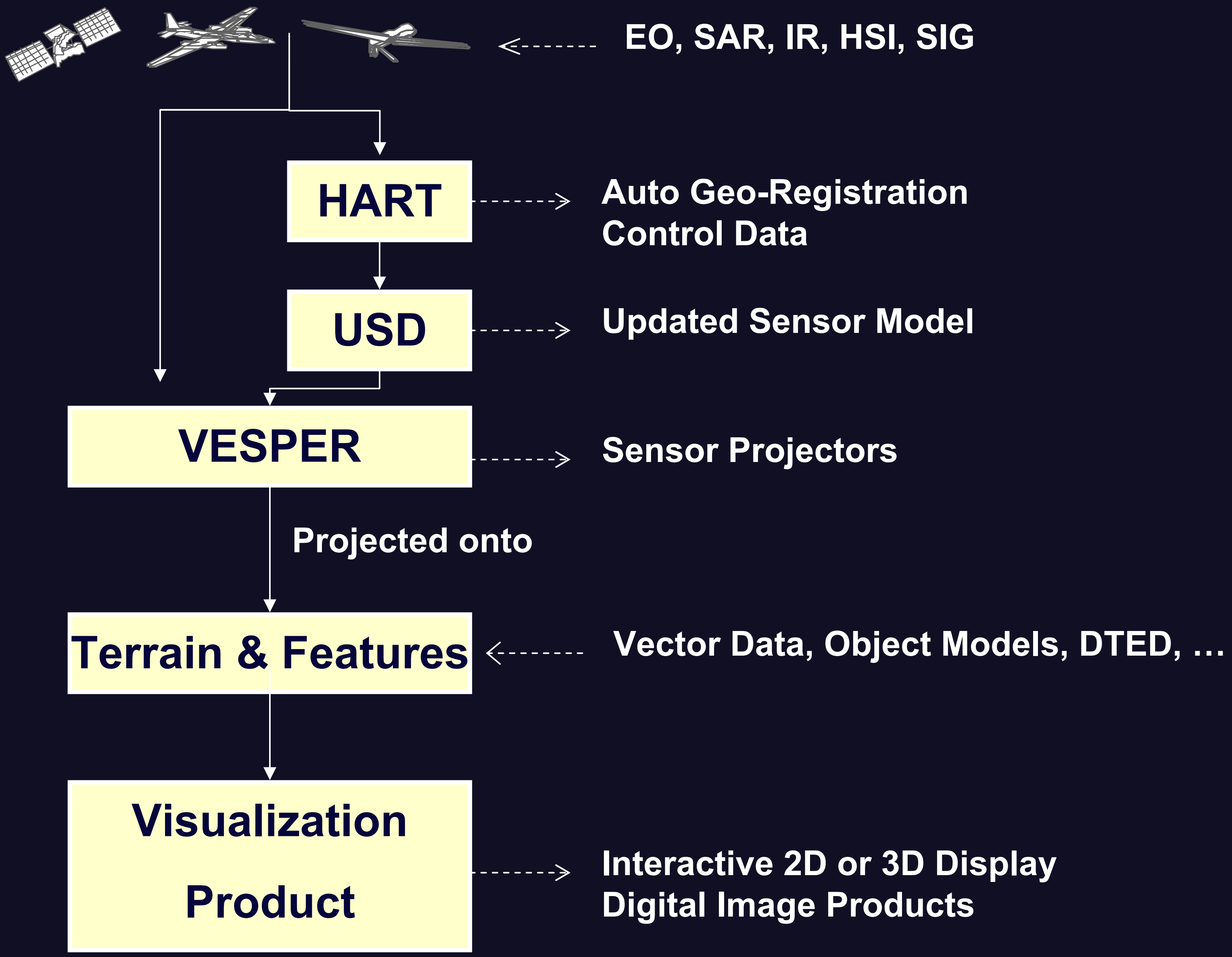

EO, SAR, IR, HSI, SIG

HART

Auto Geo-Registration
Control Data

USD

Updated Sensor Model

VESPER

Sensor Projectors

Projected onto

Terrain & Features

Vector Data, Object Models, DTED, …

Visualization Product

Interactive 2D or 3D Display
Digital Image Products

VFB Improves Current Capability

- VFB eliminates the need for time consuming data preparation
  - Foundation data prep currently takes from days to weeks
  - Current scene visualization can take days to produce and only addresses a specific predefined scenario.
  - VFB automates the process for precise geo-registration and sensor modeling.
- VFB allows the real-time integration of all data sources.
  - Current systems often require image rectification and image to image correlation, resulting in a loss of information and precision.
  - Sensor projectors utilize rigorous sensor models with geo-registration allowing for immediate and precise presentation and fusion of any data source.
- VFB delivers ad-hoc source selection and fusion from any perspective.

VESPER: Reverse the data collection process

Sensor Data

projected onto

Terrain and Feature Data

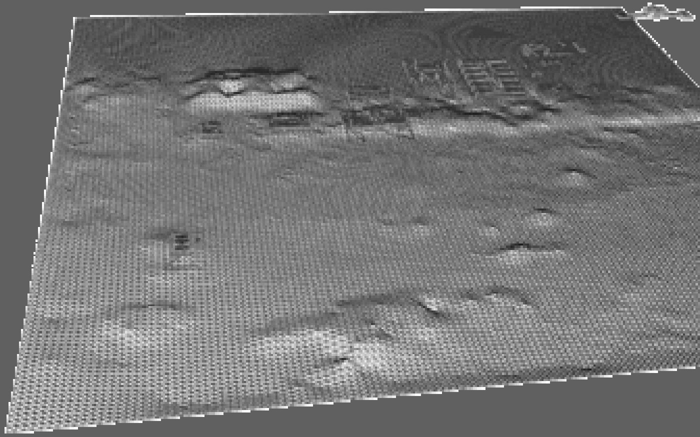

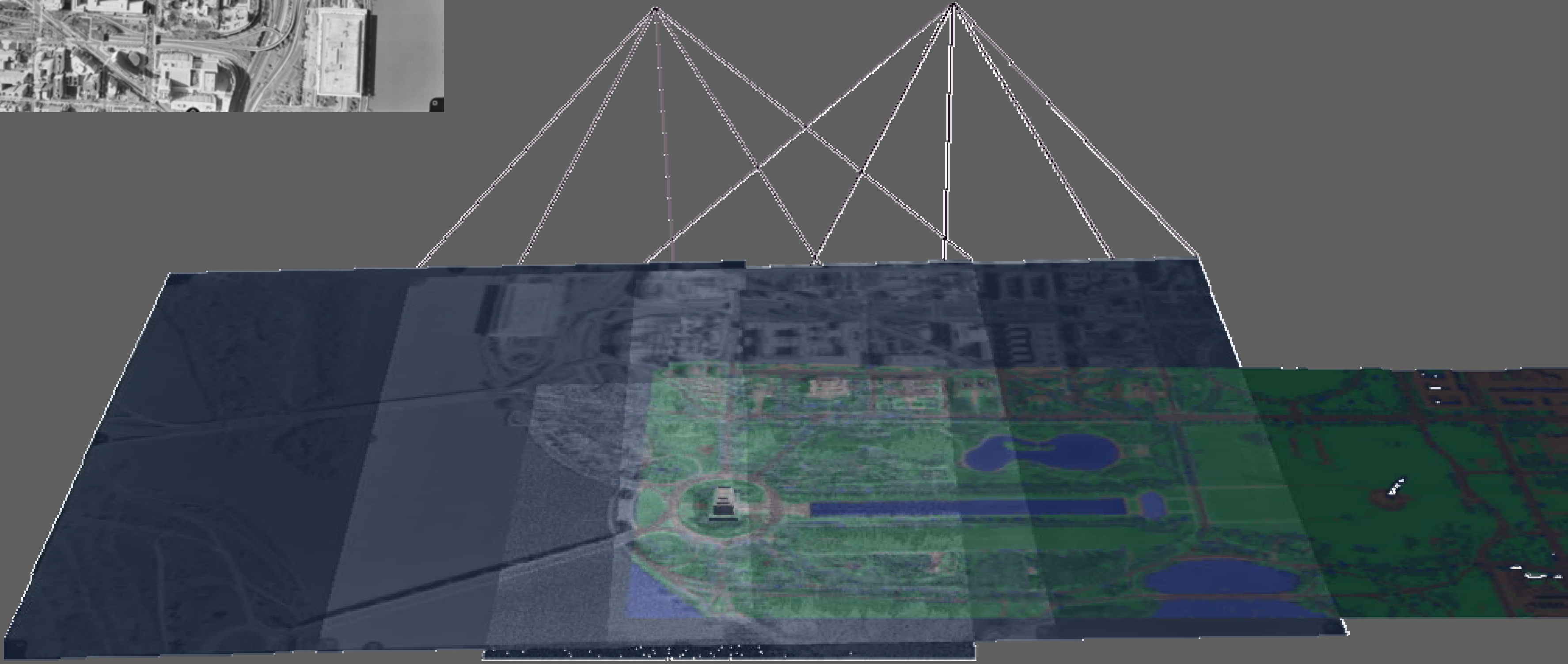

Multi-Image Projection with Color Separation

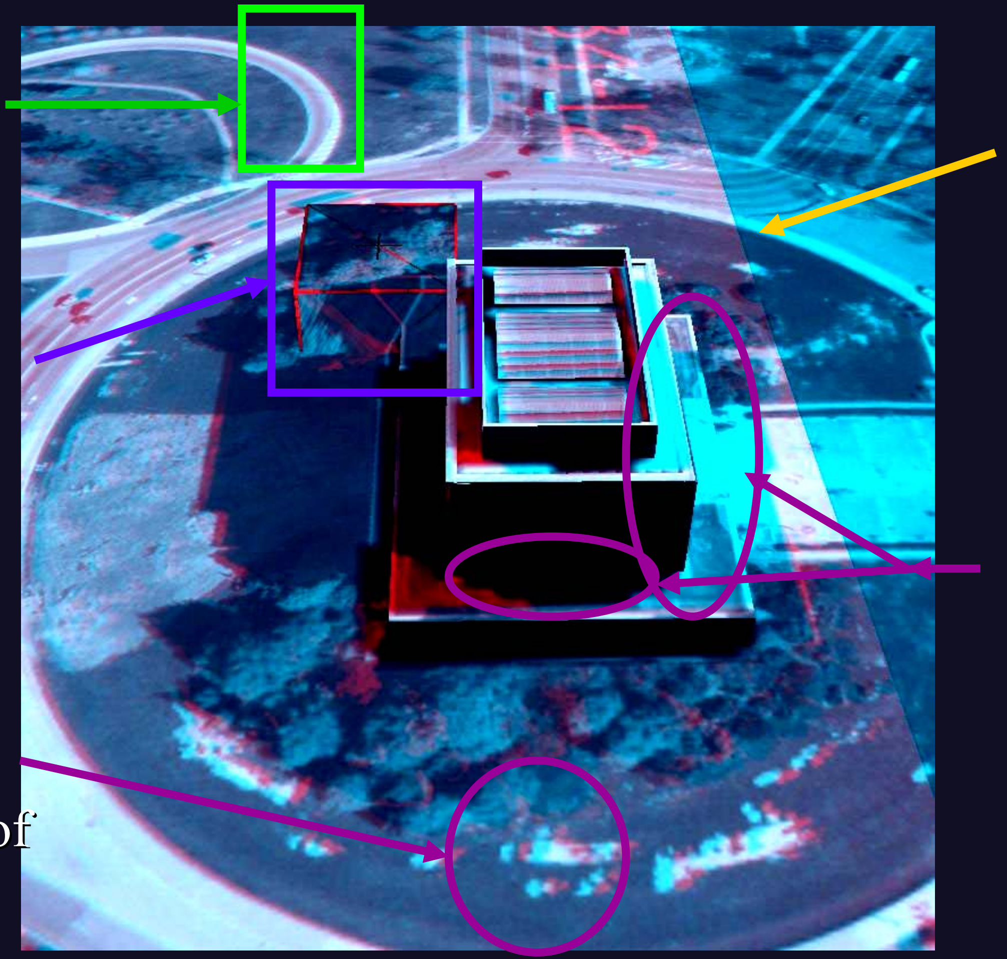

Grayscale confirms accuracy of surface model

Mensuration using cursor cube

Identification of surface model errors

Edge of image overlap

Occluded areas identified

Mensuration and Model Refinement

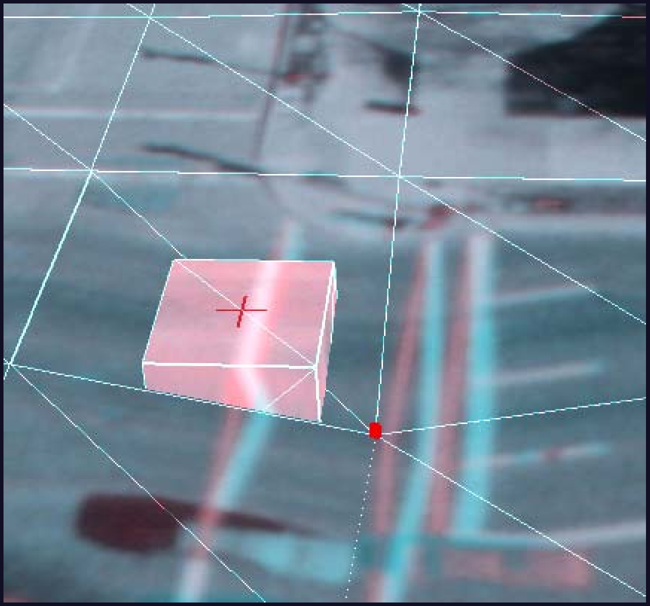

- Refine world model with surface edits until images have a satisfactory alignment

The cursor cube was used to identify a 6.2 foot elevation error in the Digital Terrain Model (DTM).

EXAMPLE 3-D MULTI-IMINT SOURCE FUSION

BAE SYSTEMS

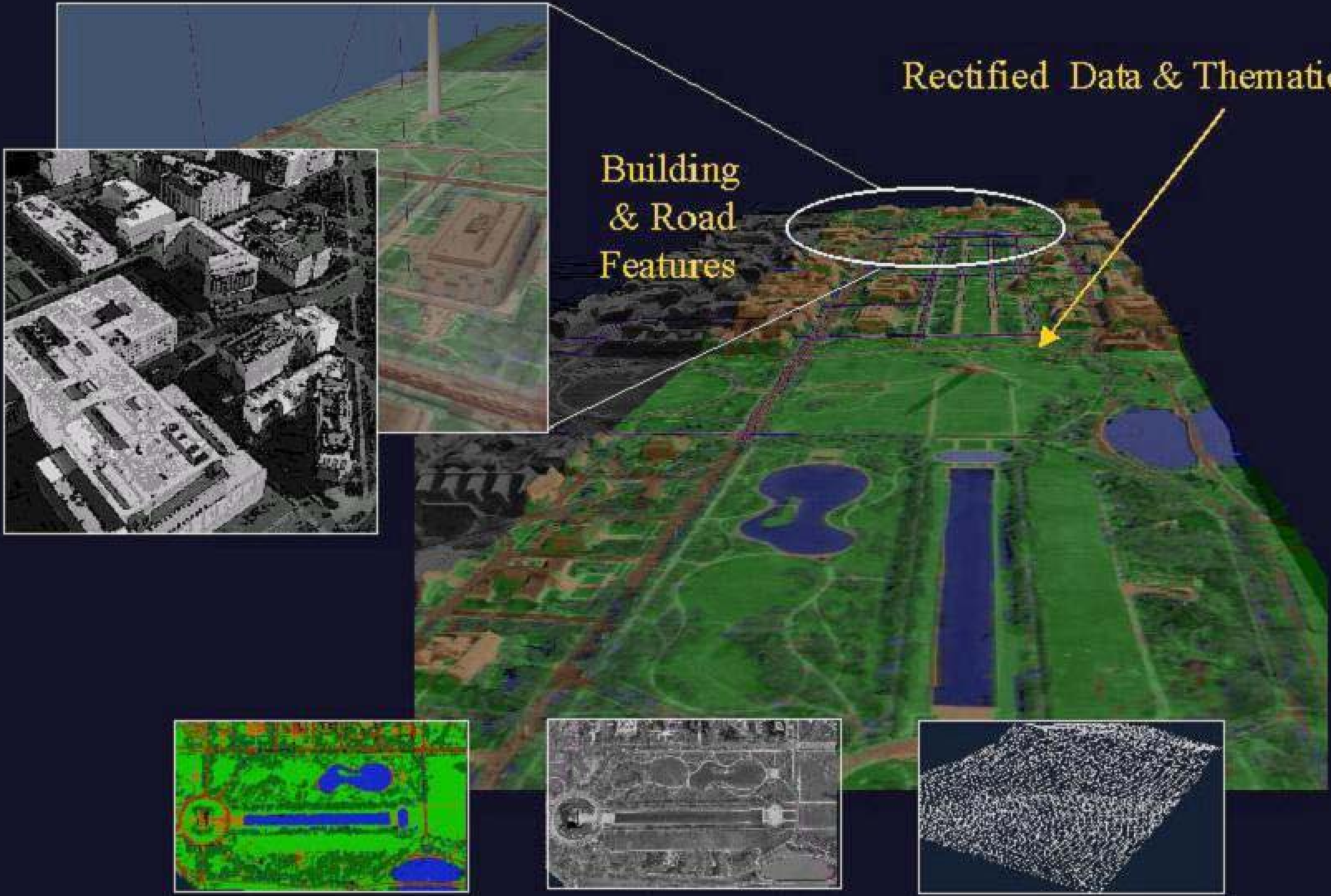

Rectified Data & Thematic Map

Building & Road Features

Multi-Spectral

Optical Image

Elevation Data

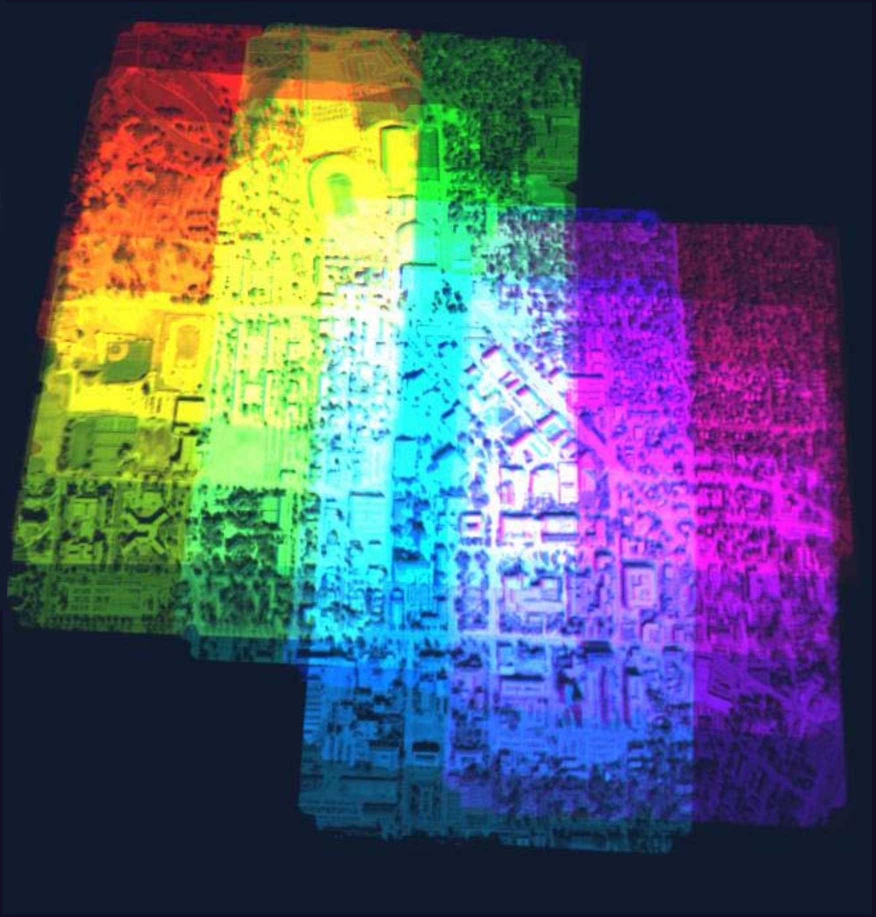

Multi-Image Mensuration via Focus

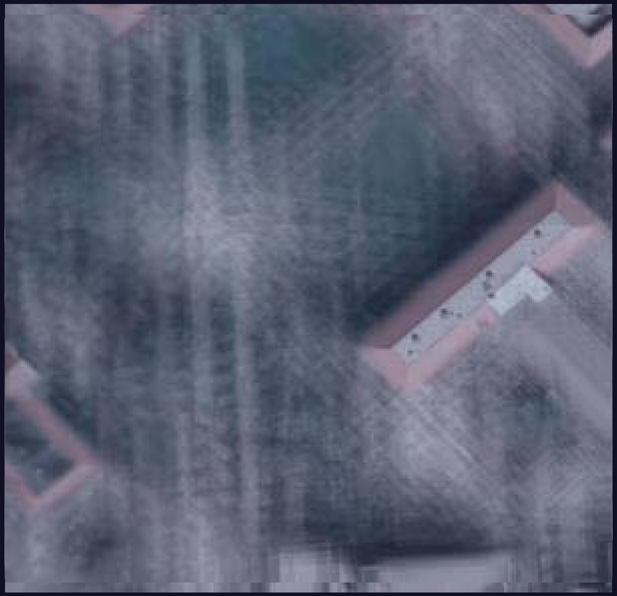

Registered Video Projected to Reference Data

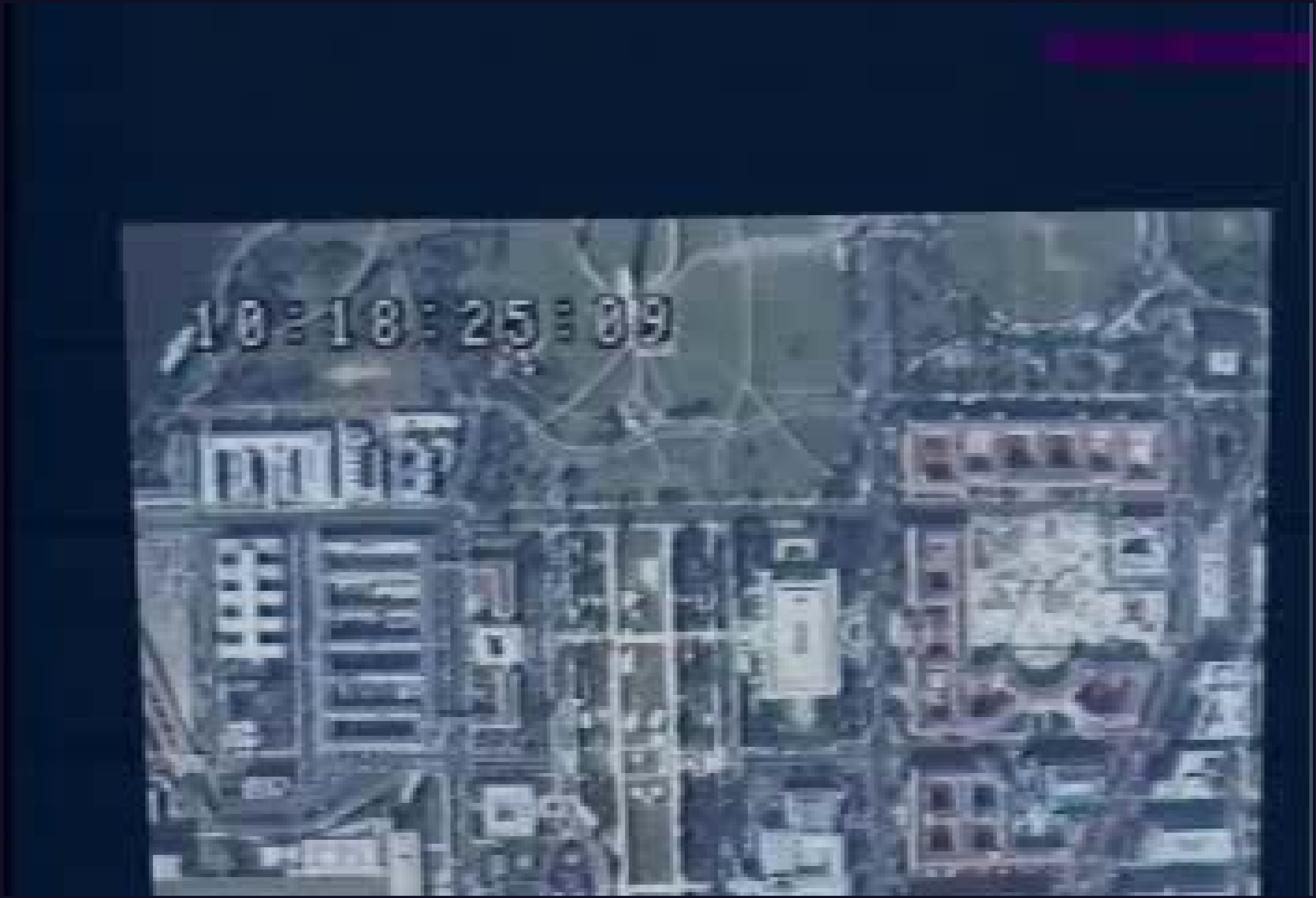

Multi-Int Data Fusion

New Imagery Projected to Reference Data

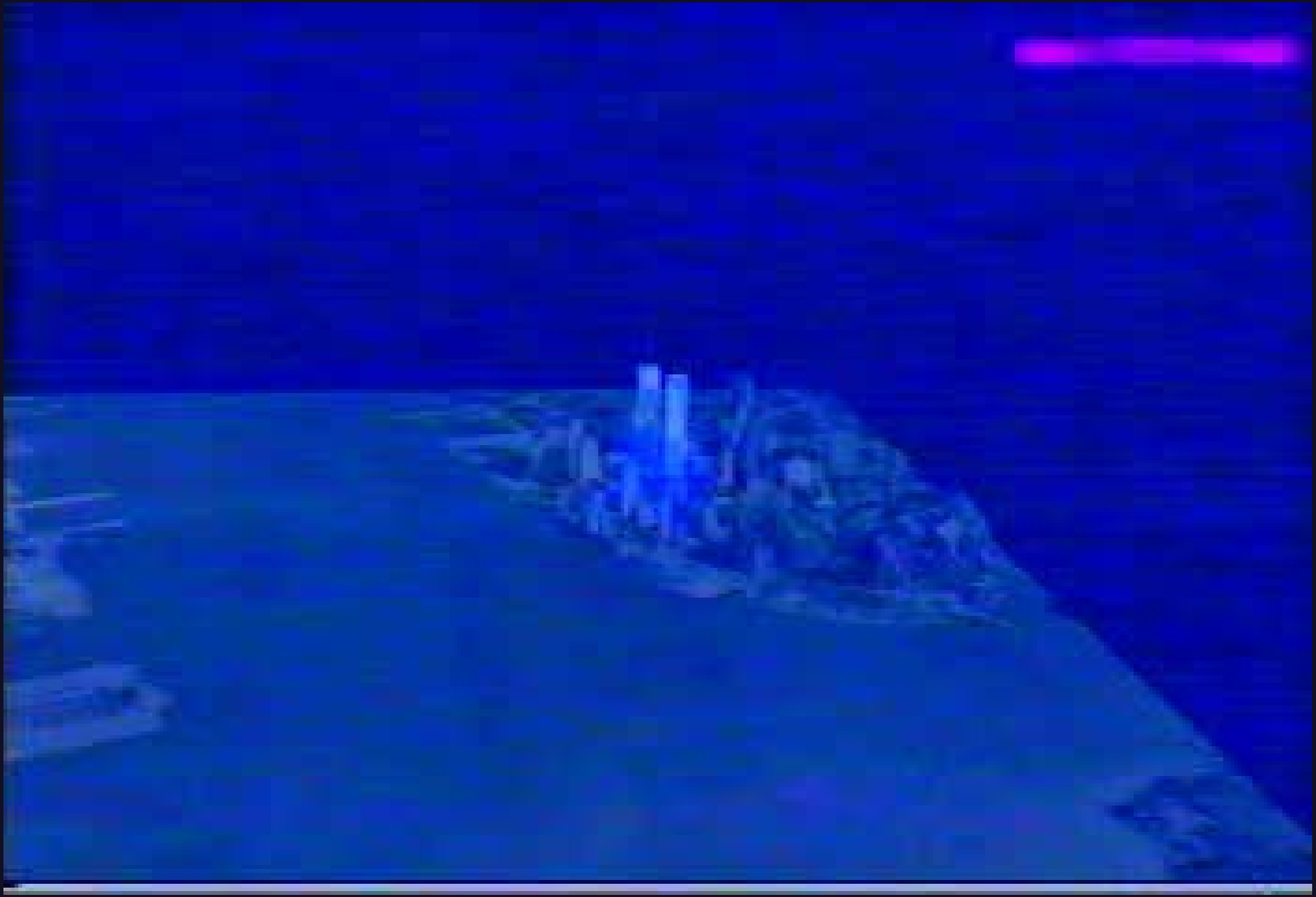

VFB Current Status

- VESPER is the result of 5 years of basic research funded by ARO FY96 - FY01 $1M
  - The Visualization Environment Supporting Photogrammetry and Exploitation Research (VESPER) test bed was used to produce the examples in this presentation.
  - Capable of presenting 30+ sensor types, tactical to NTM, from multiple simultaneous sources (many gigabytes of data) in 2D or 3D displays on the desktop or over networks.
  - This innovation allows many very large images to be viewed in the context of the underlying three-dimensional terrain and features. This enables new visual methods for multi-image photogrammetry, multi source data fusion and exploitation.
- 3D Visualization funded by ARO FY02 $86K
  - Further support for NTM data.
  - Immersive VR demonstration
- HART was a MERIT program with FY01 funding $498K FY00 $499K
  - Geo-Registration of EO,IR,SAR to within 2 pixels.
  - Fully automates the registration process

New imagery integrated with existing 3D NYC in minutes

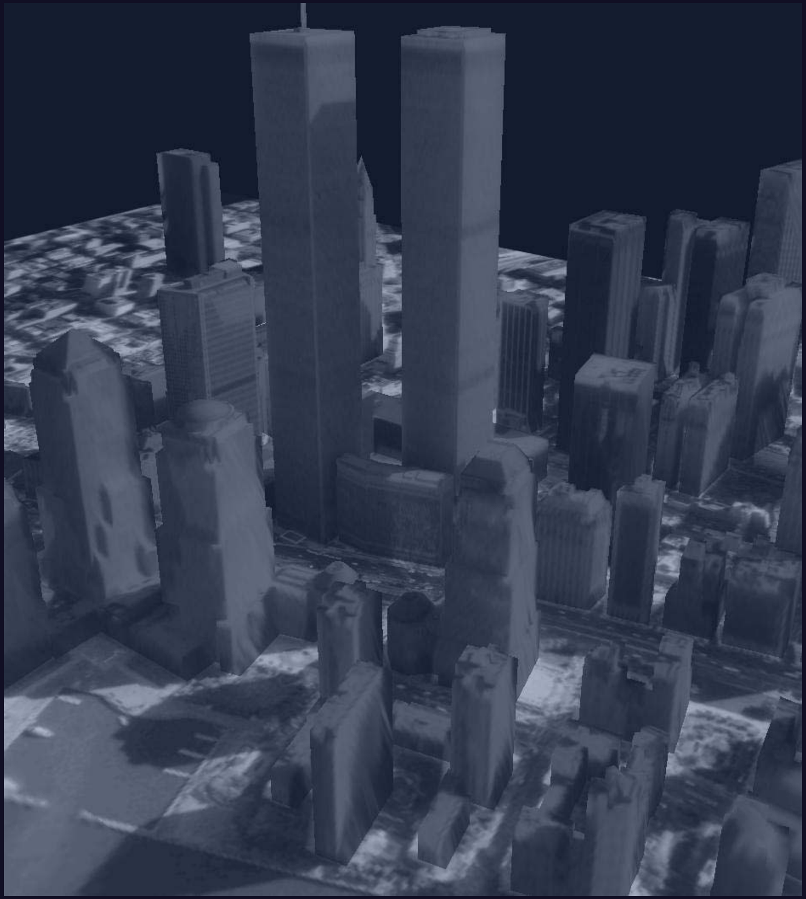

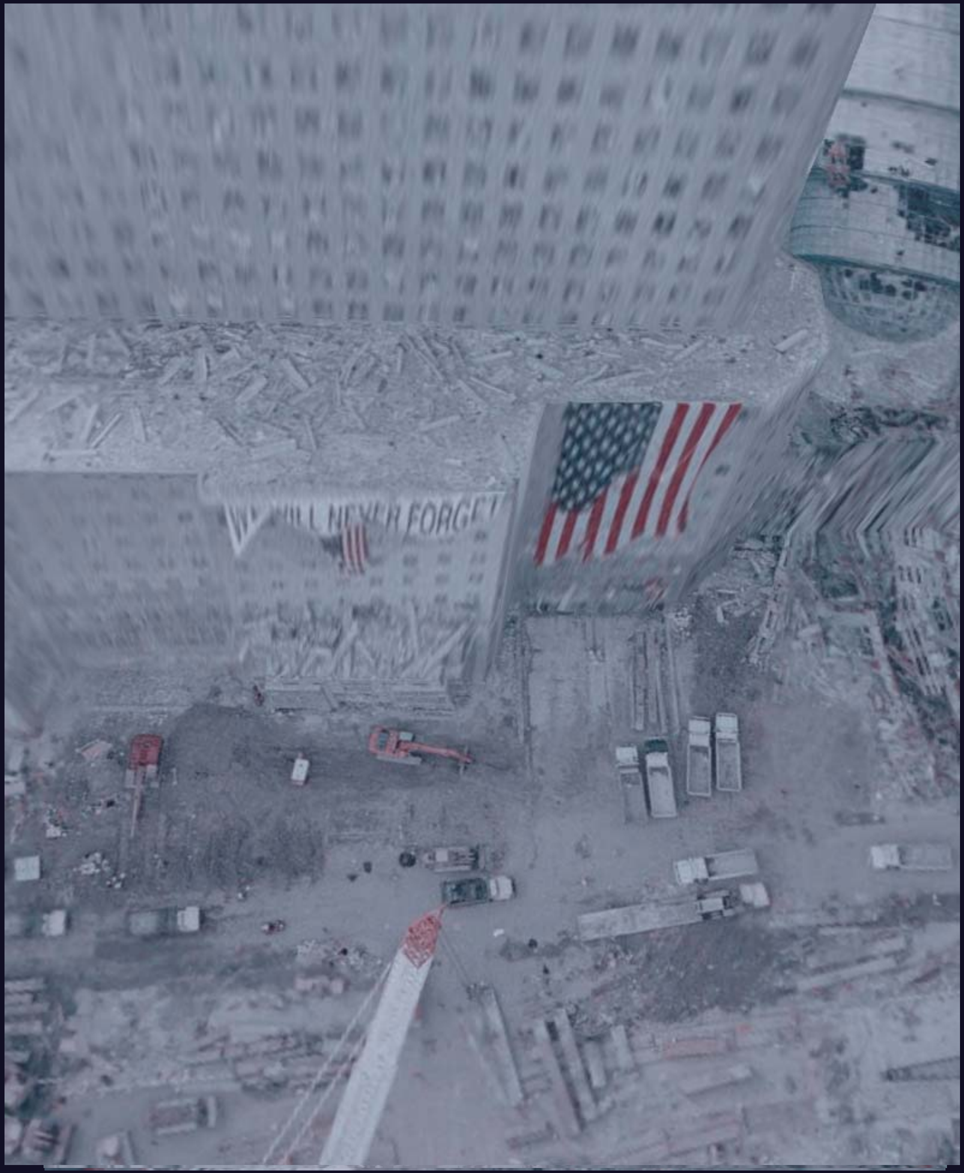

CNN Image Resection

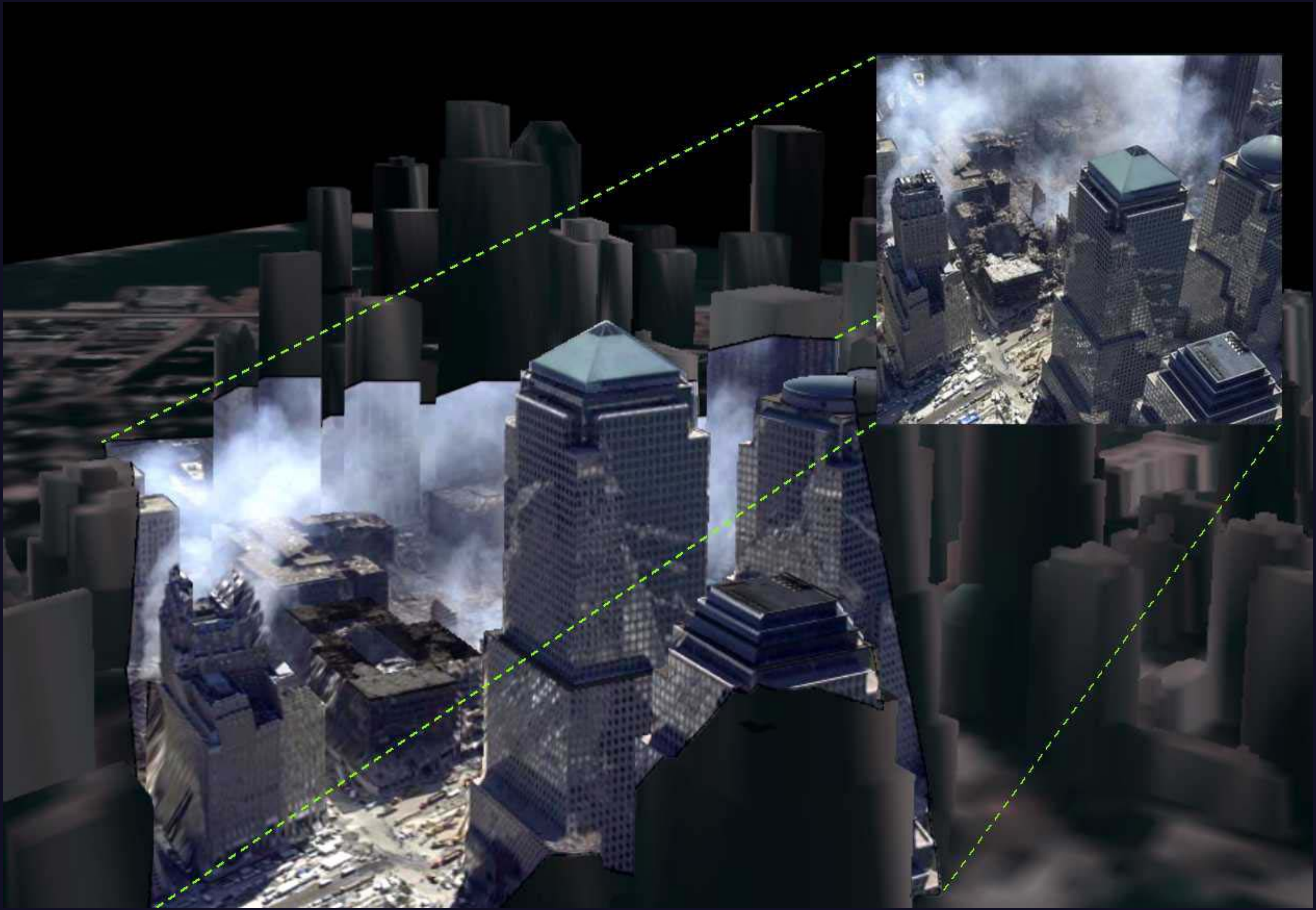

Visualization timelines for NYC

- The feature database was pre-existing from a 1995 ant-terrorism analysis of the WTC. If it hadn’t been, USGS DEM data would have been loaded for the terrain, a 5 minute download off the internet, and features would be either retrieved from other sources or modeled in VESPER using our Get3D modeling tool. Usually 2 minutes per building for moderate complexity. SocetSet to OpenFlight conversion took 10 min.

- The black and white aerial frame images over NYC were from the 1995 collection so they were precisely geo-registered previously. Imagery and support data had to be prepared for VESPER. ~5 minutes.

- The new image was off the internet without support data. An interactive resection was performed using 4 - 6 ground-to-image points. A 5 to 10 minute operation using a clumsy lab tool. This manual process can be reduced to 20 seconds with appropriate interfaces.

- The videos are real-time output from VESPER. NTSC is fed to a PC with an MPEG encoder card so time is length of video. Typically 1-3 minutes. Since it’s easy I often do 3 or 4 “takes” and pick the best.

Generic Object Placement

BAE SYSTEMS

Camera resection

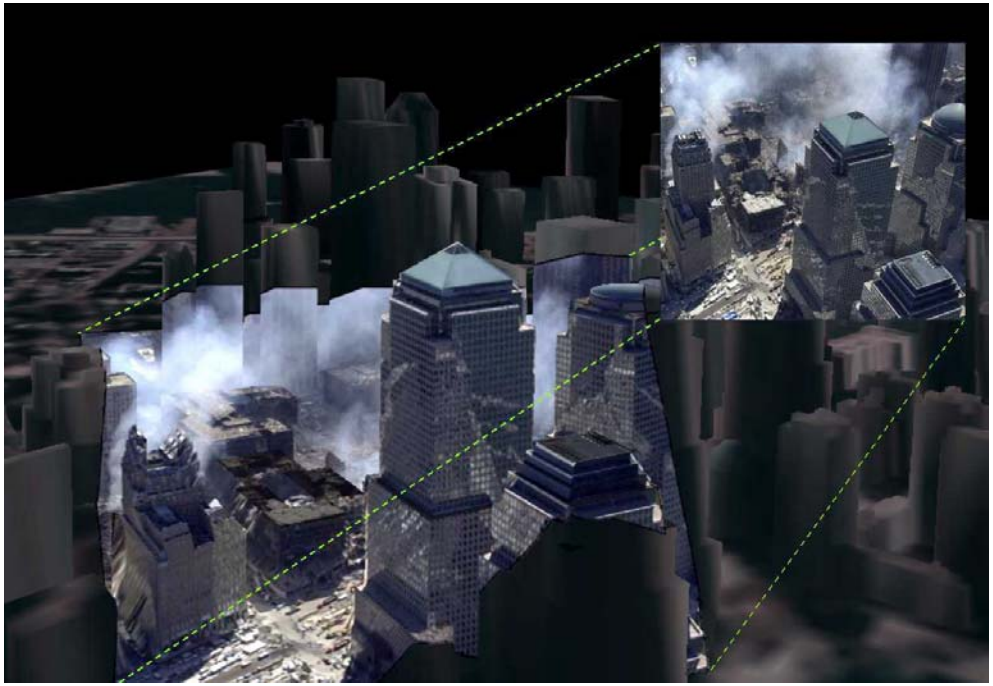

Presented by: ***Joseph Spann***

Nomination Details

- What is the nomination?

Dr. Taylor, Dr. Krinsky, and MS. Kaufman have developed and implemented camera resection algorithms that allow images from unknown sources to be managed with the same rigor as controlled imagery .

- Why was there a need for this activity?

There is a need to quickly understand image data from uncontrolled sources (CNN, NBC, Al Jazeera ..) in a precise geospatial context.

- How has the nominated activity been developed?

The initial resection algorithm was developed for customers in the intelligence community for processing Predator data and has been implemented on PTW and EPPIC. This work has been generalized for broader applicability and evaluated within the visual context of the Mission Solutions Advanced Programs Visualization activities.

Contribution from Nominees

- Originality/Novelty - how original is the idea / application / approach taken? *This was previously achievable only with controlled intelligence assets. Previous attempts at resection suffered from numerical instability. The strength of the this approach comes from the robustness of its solution.*
- Initiative - how much initiative did the nominee use in bringing the idea to fruition? This approach was initiated by the team to solve a basic image processing problem.
- Level of Effort - how much time and energy was applied by the nominee to develop and implement the innovation or in encouraging others to do so? This innovation was developed through many man months of concerted effort by the highly qualified team.

Business Benefit

- Has the innovation led to improved business performance?

This technology enables the exploitation of many new image sources.

It has been implemented in current products such as JTW and EPPIC and included in several new business proposals.

- What financial performance improvement or time savings have been realized?

It used to take 4 hours and required a skilled photogrammetrist to perform a resection. Now it can be done in under a minute with greater accuracy.

Technology

- Have any new innovations being generated as a result of this technology? The VESPER resection tool is based on this innovation. APY-6 risk mitigation applications.
- Has the innovation resulted in a competitive advantage for the company? This is a BAE Systems unique solution that is superior to the competition's rubber sheeting approach due to the sensor model rigor that is applied. This technology was included in new business proposals for "Situational Awareness for Field Units" (Homeland Defense) and "C3 Systems Discovery and Invention Program for Visualization" (ONR).
- How efficient was the application of this innovation in terms of cost, timescales, level of disruption etc.? Prior to this resection algorithm it usually took 4 hours and required a skilled photogrammetrist to perform a resection. Now it can be done in under a minute with greater accuracy.
- How does this product or service appeal to the customer? Data visualization in a common relevant operating picture (CROP) is a first order requirement to achieve Joint Vision 2020. Camera resection allows more data sources to be available for the CROP.

Applicability Across the Company

- What level of company support did the innovation have?

Mission Solutions Advanced Programs provided all the necessary resources and collaboration required to develop this innovation. This included funding under the Advanced Programs Visualization IRAD.

- What plans are there for sharing the innovation locally, within your business unit and across BAE SYSTEMS?

This camera resection work is being applied across business units already.

Impact on Company Values

- Furthering the Company Values - to what degree has the nominees action and behaviors impacted any or all of the Company values (People, Customers, Partners, Technology and Performance)?
- Customer: US ARMY Research Office, NIMA, Intelligence Community
- People: This team effort required imagination and deep understanding of sensor modelling, mathematics and visualization.
- Partnering: All users of geospatial and intelligence imagery can benefit from this innovation.
- Innovation and Technology: This multi disciplinary innovative technology was developed through interaction and sharing of expertise in mathematics, graphics, photogrammetry and sensor modelling. A collective capability unique to Mission Solutions.
- Performance: The resection algorithm allows imagery from unknown sources to be controlled and understood in a precision geospatial context within a few minutes.

Benefits Summary

- Top three benefits resulting from the innovation

- 1 *This innovation allows images from unknown sources to be managed with the same rigor as controlled imagery . This enables images from CNN or Al Jazeera to be understood in a precision geospatial context.*

- 2 *The algorithms are fast and easy to use. New images can be introduced in seconds instead of hours.*

- 3 *These algorithms make use of object oriented design technology, providing our business unit with capabilities applicable not just to the current systems but future systems as well.*

Supporting Information

The BAE SYSTEMS proprietary frame resection algorithm uses a set of at least four ground points and their corresponding image positions to find the position, attitude, and focal length of the camera. The interior orientation coefficients are assumed to be known. Suppose that a set of ground points (xGi, yGi, zGi) and the corresponding image points (li, si) are known. We assume that the focal plane coordinates (xFi, yFi) corresponding to the image coordinates (li, si) can be found.

The focal plane coordinates can be written explicitly in terms of the ground coordinates, the aperture position (xS, yS, zS), the effective focal length d, and the rotation matrix R that describes the camera attitude. Note that the focal plane coordinates are a linear rational transformation of the ground coordinates.

Precision Georegistration in seconds